Advancing the Hybrid Membrane Aerated Biofilm Reactor (MABR) Process for Sustainable Biological Nutrient Removal

by

Huanqi He

A dissertation submitted in partial fulfillment
of the requirements for the degree of
Doctor of Philosophy
(Environmental Engineering)
in the University of Michigan
2023

Doctoral Committee:

Professor Glen T. Daigger, Chair
Associate professor Vincent J. Denef
Professor Nancy G. Love
Assistant professor Aleksandra Szczuka

Huanqi He

huanqihe@umich.edu

ORCID ID: 0000-0003-2907-193X

Dedication

This dissertation is dedicated to my loving parents, Yuheng Xu and Xin He, for their boundless love, encouragement, and support throughout my education.

Acknowledgements

I would like to express my heartfelt gratitude and appreciation to the following people who have supported and contributed to the completion of this important milestone in my life.

First and foremost, I am deeply grateful to my advisor, Dr. Glen Daigger. Your support, guidance, and expertise have been invaluable throughout this entire research endeavor. My deepest gratitude to Glen for his life wisdoms - “You get there when you get there” and “Good engineers always have redundancy”. I would not be where I am without your encouragement and mentorship. Thank you for sharing your knowledge and insights with me. They have greatly broadened my scope and let me not be a narrowly-focused person. I extend my sincere thanks to Patty Daigger. I am profoundly grateful for her great food and encouragements to young water professionals. I truly appreciate that Patty graciously spent her time with me before my first-ever presentation at an international conference. That means a lot to me.

I would like to thank the members of my dissertation committee, Dr. Nancy Love, Dr. Vincent Denef, and Dr. Alex Szczuka. Your insightful feedback and dedication to my academic growth have played a pivotal role in shaping this dissertation. I would like to thank Dr. Love for her expertise and passion in instructing the course CEE592, which greatly advanced my knowledge and skills in wastewater treatment. I sincerely thank Dr. Vincent Denef for his timely feedback and willingness to share resources, which helped me address important questions especially in the microbial ecology chapter. I want to thank Dr. Alex Szczuka for her encouraging suggestions and discussions for my proposal and post-graduation plan.

I would like to extend my thanks to the colleagues and fellow researchers who offered their expertise, engaged in thought-provoking discussions, and provided invaluable assistance throughout my research. Thank you, all the amazing peers in the Daigger Research Group: Dr. Cheng Yang, Dr. Avery Carlson, Dr. Brett Wagner, Changyoon Jun, Yi Cao, Daehyun Ko, Ziheng Liang, Zihao Cui, Jiawei Liu, and Hongji Su. It has been such a wonderful experience to mutually learn from each other, and I am honored to have been part of you. I also want to thank the incredibly smart fellow researchers in the Environmental Biotechnology Group. Special thanks go to Delaney

Snead and Lucinda Li, for organizing the research and writing support groups which greatly helped with my progress. A huge thank you to the Civil and Environmental Engineering staff, Steve Donajkowski and Ethan Kennedy, for helping make my reactor systems.

I am extremely grateful to have my dissertation research supported by Zhidao Environment and the University of Michigan Rackham Predoctoral Fellowship. I gratefully acknowledge Dr. Chunyan Chai and incredible engineers in Nanjing, China along with this journal. I want to thank all the staff at Ann Arbor Wastewater Treatment Plant for being the host of my research project.

Last but least, to my families, loved ones, and all the friends. Your belief in my abilities, patience during the challenging times, and unwavering support have been my constant motivation throughout this doctoral journey. Thank you all for being so fantastic and supportive. I am so grateful to have you all by my side.

Table of Contents

List of Tables

List of Figures

List of Appendices

List of Abbreviations

ACN	Acetonitrile
AI	Artificial intelligence
AOA	Ammonia-oxidizing archaea
AOB	Ammonia-oxidizing bacteria
AS	Activated sludge
BNR	Biological nutrient removal
BOD	Biological oxygen demand
BOD_5	5-day biological oxygen demand
CH_4	Methane
COD	Chemical oxygen demand
Comammox	Complete ammonia oxidation
CoMANDR	Counter-diffusion membrane aerated nitrifying and denitrifying reactor
DNA	Deoxyribonucleic acid
DO	Dissolved oxygen

DOPA	L-3,4-dihydroxyphenylalanine
DPAO	Denitrifying polyphosphate-accumulating organism
EBPR	Enhanced biological phosphorus removal
EPS	Extracellular polymeric substance
FA	Free ammonia
FISH	Fluorescence *in situ* hybridization
GAO	Glycogen-accumulating organism
GHG	Greenhouse gas
GWP	Global warming potential
HRT	Hydraulic residence time
IWA	International Water Association
LCA	Life cycle analysis
MABR	Membrane aerated biofilm reactor
MAB	Membrane aerated biofilm
MBBR	Moving bed biofilm bioreactor
MBfR	Membrane biofilm reactor
MBR	Membrane bioreactor
MLSS	Mixed liquor suspended solids
MOB	Methane oxidation bacteria

MPC	Model predictive control
mRNA	Messenger ribonucleic acid
N	Nitrogen
N_2O	Nitrous oxide
NOB	Nitrite-oxidizing bacteria
NR	Nitrification rate
OCT	Optical coherence tomography
OHO	Ordinary heterotrophic organism
OTE	Oxygen transfer efficiency
ORP	Oxidation-reduction potential
OTR	Oxygen transfer rate
OUT	Operational taxonomic unit
P	Phosphorus
PAO	Polyphosphate-accumulating organism
PDMS	Polydimethylsiloxane
PHA	Polyhydroxy-alkanoates
PMP	Polymethylpentene
PN/A	Partial nitritation/anammox
PP	Polypropylene

PVDF	Polyvinylidene fluoride
qPCR	Quantitative polymerase chain reaction
rRNA	Ribosomal ribonucleic acid
SBR	Sequencing batch reactor
SI	Supporting information
SIP	Stable isotopic probing
SND	Simultaneous nitrification and denitrification
SOB	Sulfide-oxidizing bacteria
SOR	Sulfide-oxidizing rate
SRT	Solid residence time
SRR	Sulfate-reducing rate
TIN	Total inorganic nitrogen
TN	Total nitrogen
TOC	Total organic carbon
TP	Total phosphorus
TSS	Total suspended solid
TTR	Taxa-time relationship
VFA	Volatile fatty acid
VOC	Volatile organic compound

WRRF	Water resource recovery facility
WWTP	Wastewater treatment plant
1D	One-dimensional
2D	Two-dimensional

Abstract

Anthropogenic activities trigger high concentrations of nutrients in municipal wastewater. To prevent eutrophication in aquatic systems, nitrogen and phosphorous in municipal wastewater must be efficiently removed before the treated effluent re-enters receiving waters. Biological nutrient removal (BNR) via the suspended growth process (activated sludge) has been an effective tool for water pollution control, but nowadays it faces challenges associated with more stringent discharge limits, increasing energy costs, and carbon neutrality goals. The hybrid membrane aerated biofilm reactor (MABR) process, coupling the MABR biofilm and conventional suspended growth (the basis for the term "hybrid"), has a unique capacity to develop solutions for those challenges. This dissertation addresses practical and fundamental questions about the hybrid MABR process for sustainable BNR practice.

In recent years, commercial scale installations of hybrid MABRs are increasing along with process modeling. The resulting accumulated knowledge has greatly improved understanding, with new challenges and opportunities arising. Therefore, this dissertation commences with a literature review that outlined the fundamental principles of MABR technology and lessons-learned from recent commercial hybrid MABR systems. Performance and existing operational challenges were evaluated. Process control and optimization were identified as the future research needs to facilitate accelerated adaptation of the hybrid MABR process.

A fully anoxic suspended growth process is an appealing alternative to conventional suspended growth due to considerable aeration reduction and improved carbon processing efficiency. To investigate potentiaL of anoxic suspended growth operation, a physical anoxic system treating municipal wastewater was compared to a side-by-side aerobic system at the Ann Arbor Wastewater

Treatment Plant, Michigan, USA. We carried out microscopic examination and 16S rRNA gene-based microbial community profiling to determine how an anoxic suspended growth would differ from the conventional aerobic process in floc characteristics, microbial diversity, microbial

temporal dynamics, and community assembly pattern. Fewer filamentous populations were found in the anoxic mixed liquor, suggesting easily sheared flocs. Results show that the anoxic microbial community had a distinct composition and structure, but its diversity and temporal dynamics were similar to the conventional aerobic community. The anoxic microbial community assembly was more stochastic than the conventional aerobic community, but deterministic assembly was still significant with a large core microbiome adapted to the anoxic condition.

Finally, we used the plant-wide modelling approach with dynamic simulations to examine a novel hybrid MABR concept. The process implemented aeration controls to maximize the nitrification rate in the biofilm while the suspended growth remained anoxic for denitrification. Results show that the novel hybrid MABR process had resilient performance in response to diurnal loadings, achieving intensified nitrogen removal performance under both warm and cold temperature scenarios. Significant reductions in N_2O emissions, energy consumption, and physical footprint from the hybrid MABR were confirmed in comparison to the conventional suspended growth process. The model predicted higher CH_4 emissions from the hybrid MABR than the suspended growth process due to methanogen growth in the oxygen-depleted outer MABR biofilm layer. Future measurements for CH_4 emission are needed to obtain a holistic picture of the carbon footprint of the hybrid MABR process.

The results of this dissertation add knowledge about the performance and operation of the hybrid MABR process. The knowledge gained from this dissertation will expand our knowledge about the hybrid MABR process as well as our ability to accelerate translation of this beneficial process to sustainable BNR practice.

CHAPTER I

Introduction

Nitrogen and phosphorous are vital macronutrients for all life forms on earth, as they play fundamental roles in growth, development, metabolism, and production. In the aquatic environment, nitrogen and phosphorous can exist in a variety of inorganic forms like ammonium, nitrate, and nitrite for nitrogen, and ortho-phosphate for phosphorous. Organic nitrogen and phosphorous are also present in the complex matrix of amino acids, proteins, sugars, etc. The majority of water bodies have low thresholds for nitrogen and phosphorous concentrations, and inputs of a large amount of nutrients can pose great threats to the balance and bio-integrity of the ecosystem. However, anthropogenic activities trigger high concentrations of nitrogen and phosphorus in municipal wastewater, and if untreated, the discharge of such wastewater into natural waters can result in eutrophication. The most decipherable manifestation of eutrophication is algal blooms: the overgrowth and rapid accumulation of algae deplete oxygen that is needed for other aquatic organisms, and lead to water related impairments. Therefore, to prevent eutrophication in aquatic systems, nitrogen and phosphorous in the municipal wastewater must be efficiently removed before the treated effluent re-enters the receiving waters (Wang et al. 2019).

Today, planning of projects for biological nutrient removal (BNR) processes is significantly increasing in wastewater treatment plants (WWTPs). BNR has been an area of extensive research and practical development for the past several decades and is now mature and widely practiced on a global basis. The selected and widely implemented technology is the suspended growth (activated sludge) process. Ever since its discovery in the 20th century, the suspended growth process has played a dominant role in water pollution control with transformational results in terms of protecting the aquatic environment and enhancing human

health (Jenkins and Wanner, 2014). However, the question is whether the suspended growth process will meet future needs. Human society nowadays is facing both energy and water crises, due to population growth and urbanization. It is a very different situation than it was in the 19th and early 20th centuries. Significant energy consumption and large physical footprints of suspended growth plants result in continual increase in capital and operational costs, pushing the appropriateness of suspended growth to treat wastewater today under question.

In addition, greenhouse gas (GHG) emissions from wastewater treatment have become a significant concern relative to global climate change (Chen 2019). The key gas, carbon dioxide (CO_2), is produced directly via biological oxidation of organic matters as well as indirectly via electricity generation. Methane (CH_4), which has a global warming potential (GWP) of 25 CO_2-equavalents over a 100-year time horizon, also originates widely from the wastewater collection systems, primary sedimentation, biological treatment tanks, and sludge handling (Song et al. 2023). An increased awareness is related to nitrous oxide (N_2O) emissions from nitrification and denitrification processes. N_2O has a potent greenhouse effect (GWP_{N2O} = 298 GWP_{CO2}), and its emissions largely depend on process operation (Soares 2020). GHG mitigation is critical to address climate change. Combined with the growing wastewater volume and ever more stringent discharge limits, these factors push the process engineering of wastewater treatment to a critical level.

In recent years, WWTPs are being repurposed towards water resource recovery facilities (WRRFs) for water reuse, nutrient recovery and energy neutrality. Conventional BNR practices are confronted with challenges associated with the ever-increasing costs, stringent nutrient limits, and net zero emission goals. Therefore, new technologies that focus on low-energy, upgraded capacity, and reduced carbon footprint represent the next wave for nutrient management in WWTPs. The hybrid membrane aerated biofilm reactor (MABR) process, which combines elements of conventional activated sludge with an oxygen-permeable membrane, has a unique capacity to develop solutions for challenges confronting WWTPs. The membrane allows for oxygen transfer to the biofilm, enhancing nutrient removal efficiency and reducing energy consumption compared to traditional aeration. In comparison to the anammox process, which is another emerging technology for the main stream biological nitrogen removal, the hybrid MABR process is more versatile and can be applied to a broader range of wastewater types and temperature conditions. It primarily depends on the well-established mechanism of simultaneous nitrification denitrification, thereby providing simpler process control to manage fluctuations in wastewater

characteristics. Commercial applications world-wide have demonstrated many benefits of the hybrid MABR process, including robust treatment performance (Chang et al., 2022; Mei et al., 2019; Silveira et al., 2022; Sun et al., 2020), bioaugmentation (Corsino and Torregrossa, 2022; Houweling et al., 2018; Shechter et al., 2020), and energy savings (Guglielmi et al., 2020; Houweling et al., 2018; Peeters et al., 2017; Shechter et al., 2020).

This dissertation addresses practical and fundamental questions regarding a unique combination of the MABR biofilm and conventional suspended growth (the basis for the term "hybrid") for sustainable BNR practice. The knowledge gained from this research will expand our ability to accelerate translation of this beneficial process to practice.

1.1 Overview of dissertation

The overarching goal of this dissertation is to characterize the operation and performance of the hybrid MABR process treating municipal wastewater. We investigate a new hybrid MABR concept where the biofilm component nitrifies most of the influent ammonia and the majority of the suspended growth component remains unaerated for subsequent denitrification. Advanced analytical methods and mechanistic models, coupled with literature review are used to expand our "conventional wisdom" concerning the use of the biofilm and suspended growth components.

Chapter 2 is adapted from a review paper published in Water Science & Technology (He et al. 2021). It outlines the background and fundamental principles of MABR technology. Membrane materials, mass transfer mechanisms, and microbial community ecology in the biofilm are discussed. Commercial interest in MABRs has grown increasingly since the launch of the first generation of commercial MABR products in 2014, and contracted installations of MABR are now global. Chapter 2 incorporated valuable outcomes from the MABR workshop at the International Water Association (IWA) Biofilms 2020 conference, where we received significant inputs from researchers, practitioners, and MABR vendors. Practitioners and researchers have improved their understanding of the novel technology from the growing number of applications. Chapter 2 also reviews the performance and operational challenges from more recent pilot-, demonstration-, and full-scale hybrid MABRs. Performance and existing operational challenges are evaluated. Modeling efforts and emerging applications of MABR technology are also discussed.

Chapter 3 is adapted from a journal article published in Water Environment Research (He et al. 2022). This chapter explores the idea of incorporating a fully anoxic suspended growth into

the hybrid MABR for municipal wastewater. Anoxic suspended growth is beneficial for carbon and energy savings, but it has rarely been applied to treat municipal wastewater. The objective of this chapter is to better understand the process microbiology and associated tradeoffs in the suspended growth with the elimination of aeration. A physical anoxic suspended growth system treating municipal wastewater was compared to a side-by-side aerobic system at the Ann Arbor Wastewater Treatment Plant, Michigan, USA. Microscopic examination, molecular techniques, and statistical models were utilized to examine the floc characteristics, microbial diversity, and ecological succession mechanisms. The results are important to understand the microbial ecology and functioning of the anoxic suspended growth.

Chapter 4 uses dynamic modeling techniques to investigate a new hybrid MABR concept. Aeration controls were used to maximize the nitrification achieved in the biofilm component, and also "swinging" nitrification and denitrification capacities in the suspended growth component in response to varying loading conditions. This chapter represents a refined example that how the hybrid MABR process can be designed and operated. The plant-wide mechanistic model expanded conventional activated sludge models with components that have not been done before, thereby allowing an upgraded capacity to evaluate nitrogen removal performance along with process GHG emissions in the hybrid MABR.

Finally, Chapter 5 concludes this dissertation. This chapter summarizes the key research outcomes, highlights the engineering significance, and identifies future research needs.

Reference

Chang, M., Liang, B., Zhang, K., Wang, Y., Jin, D., Zhang, Q., Hao, L., and Zhu, T. (2022) Simultaneous shortcut nitrification and denitrification in a hybrid membrane aerated biofilms reactor (H-MBfR) for nitrogen removal from low COD/N wastewater. Water Research, **211**, 118027.

Chen, Y.-C. (2019) Estimation of greenhouse gas emissions from a wastewater treatment plant using membrane bioreactor technology. Water Environment Research, **91**(2), 111–118.

Corsino, S. F. and Torregrossa, M. (2022) Achieving complete nitrification below the washout SRT with hybrid membrane aerated biofilm reactor (MABR) treating municipal wastewater. Journal of Environmental Chemical Engineering, **10**(1), 106983.

Guglielmi, G., Coutts, D., Houweling, D., and Peeters, J. (2020) Full-scale application of MABR technology for upgrading and retrofitting an existing WWTP: performances and process modeling. Environmental Engineering and Management Journal, **19**(10), 1781–1789.

He, H., Carlson, A. L., Nielsen, P. H., Zhou, J., and Daigger, G. T. (2022) Comparative analysis of floc characteristics and microbial communities in anoxic and aerobic suspended growth processes. Water Environment Research, **94**(12). [online] https://onlinelibrary.wiley.com/doi/10.1002/wer.10822 (Accessed February 9, 2023).

He, H., Wagner, B. M., Carlson, A. L., Yang, C., and Daigger, G. T. (2021) Recent progress using membrane aerated biofilm reactors for wastewater treatment. Water Science and Technology, **84**(9), 2131–2157.

Houweling, D., Long, Z., Peeters, J., Adams, N., Côté, P., Daigger, G., and Snowling, S. (2018) Nitrifying below the "Washout" SRT: Experimental and Modelling Results for a Hybrid MABR / Activated Sludge Process. Proceedings of the Water Environment Federation, **2018**(16), 1250–1263.

Jenkins, D. and Wanner, J. (2014) *Activated Sludge - 100 Years and Counting*, IWA Publishing.

Mei, X., Liu, J., Guo, Z., Li, P., Bi, S., Wang, Yong, Yang, Y., Shen, W., Wang, Yihan, Xiao, Y., Yang, X., Zhou, B., Liu, H., and Wu, S. (2019) Simultaneous p-nitrophenol and nitrogen removal in PNP wastewater treatment: Comparison of two integrated membrane-aerated bioreactor systems. Journal of Hazardous Materials, **363**, 99–108.

Peeters, J., Adams, N., Long, Z., Côté, P., and Kunetz, T. (2017) Demonstration of innovative MABR low-energy nutrient removal technology at Chicago MWRD. Water Practice and Technology, **12**(4), 927–936.

Shechter, R., Downing, L., Gordon, K., and Nathan, N. (2020) "First Full-Scale Activated Sludge Retrofit Using a Spirally-Wound MABR: Results and Model Evaluation"

Silveira, I. T., Cadee, K., and Bagg, W. (2022) Startup and initial operation of an MLE-MABR treating municipal wastewater. Water Science and Technology, **85**(4), 1155–1166.

Soares, A. (2020) Wastewater treatment in 2050: Challenges ahead and future vision in a European context. Environmental Science and Ecotechnology, **2**, 100030.

Song, C., Zhu, J.-J., Willis, J. L., Moore, D. P., Zondlo, M. A., and Ren, Z. J. (2023) Methane Emissions from Municipal Wastewater Collection and Treatment Systems. Environmental Science & Technology, **57**(6), 2248–2261.

Sun, Z., Li, M., Wang, G., Yan, X., Li, Y., Lan, M., Liu, R., and Li, B. (2020) Enhanced carbon and nitrogen removal in an integrated anaerobic/anoxic/aerobic-membrane aerated biofilm reactor system. RSC Advances, **10**(48), 28838–28847.

Wang, X., Daigger, G., de Vries, W., Kroeze, C., Yang, M., Ren, N.-Q., Liu, J., and Butler, D. (2019) Impact hotspots of reduced nutrient discharge shift across the globe with population and dietary changes. Nature Communications, **10**(1), 2627.

CHAPTER II

Recent Progress Using Membrane Aerated Biofilm Reactors for Wastewater Treatment

Published as:

He, H., Wagner, B. M., Carlson, A. L., Yang, C., and Daigger, G. T. (2021) Recent progress using membrane aerated biofilm reactors for wastewater treatment. Water Science and Technology, **84**(9), 2131–2157.

2.1 Introduction

The membrane biofilm reactor (MBfR), based on the counter-diffusions of the electron donor and acceptor, is a promising technology for water and wastewater treatment (Martin and Nerenberg 2012; Aybar et al. 2012; Nerenberg 2016). An MBfR uses a gas-permeable membrane to support a counter-diffusional biofilm where gaseous substrates enter the biofilm opposite to substrates from the bulk liquid (Martin et al. 2013). As the constituents in the gas stream diffuse through the membrane while other substratesF(in the bulk liquid diffuse through the liquid boundary layer, biological activity is the highest in the center of the MBfR biofilm, where both gaseous and liquid substrates are sufficient. This counter-diffusion property of MBfRs ensures high functional

stability against shock loads and toxic inhibitors (Martin and Nerenberg 2012; Nerenberg 2016; Janczewski and Trusek-Holownia 2016).

The nature of the gaseous substrate is selected to enable the desired biochemical reactions in the MBfR. When air or oxygen is supplied in the lumen, MBfRs are often known as membrane aerated-biofilm reactors (MABRs). In MABRs, the oxygen supply in the lumen can be manipulated to create an inner oxygen-rich zone and outer oxygen-depleted zone in the biofilm, housing diverse ecological niches for a range of microbial functions in the same biofilm. The advantages of MABR technology include high effluent quality (Sunner et al. 2018; Sathyamoorthy et al. 2019), high carbon processing efficiency (Mehrabi et al. 2020; Houweling and Daigger 2019), up to 100% oxygen transfer efficiency (OTE) (Heffernan et al. 2017; Bicudo et al. 2019), and compact reactor footprints (Sunner et al. 2018). Compared to other biofilm reactors, like Moving Bed Biofilm Reactor (MBBR) with a typical designed nitrification rate (NR) of 0.5 g N/m^2-d, MABRs achieve greatly improved NRs of 1.0-3.0 g N/m^2-d (Côté et al. 2015; Kunetz et al. 2016; Peeters et al. 2017; Underwood et al. 2018; Nathan et al. 2020). The greatly improved NRs result from high oxygen transfer rates (OTRs) in MABRs. Moreover, the nitrification performance in MABRs is less susceptible to carbon loadings because the nitrifying population inhabits in the inner biofilm layer (Houweling and Daigger 2019).

Despite the recognized advantages, MABR technology is still in its early stage of commercialization, with developments ongoing to tackle unsolved issues. Lab-scale studies over the last several decades have explored the mass transfer mechanisms, biofilm characteristics, influencing factors, and treatment performance of MABRs, and several reviews have summarized the lessons learned from lab-scale investigations (Casey et al. 1999; Syron and Casey 2008a; Aybar et al. 2012; Martin and Nerenberg 2012; Nerenberg 2016). However, those early reviews did not cover pilot- to full-scale experiences because MABR technology has become commercially available only recently. Commercial interest in MABRs has also grown increasingly since the launch of the first generation of commercial MABR products (Martin et al. 2017; Underwood et

al. 2018; Guglielmi et al. 2020). With three commercial MABR products available, i.e. ZeeLung MABR by Suez Water Technologies & Solutions, OxyMem MABR by OxyMem Limited, and Fluence MABR by Fluence Corporation, global practitioners and researchers have significantly improved their understanding of the counter-diffusional biological process from the growing number of the pilot- to full-scale installations. Lu et al. 2020 reviewed several pilots and full-scale MABR applications for municipal and industrial wastewater treatment, but more commercial applications are occurring for different types of wastewater treatment, and long-term operation has been investigated (Guglielmi et al. 2020; Nathan et al. 2020; Uri-Carreno et al. 2021). This paper reviews the further accumulated knowledge and recent advances from the growing commercial installations. Moreover, current lab-scale research is moving towards a deeper understanding of membrane-aerated biofilms (MABs), including the metabolic pathways (Tian et al. 2019; Tian et al. 2020), MAB formation (Hu et al. 2020), predation activities (Aybar et al. 2019; Kim et al. 2020), and novel microbial compositions (Zhang et al. 2021). Process modeling is also improving to facilitate MABR design and operation (Chen et al. 2020; Carlson et al. 2021). However, active biofilm management is still a challenge, and fundamental knowledge is still limited regarding complex interactions between attached and suspended growth. Understanding their unique benefits and existing barriers to broader implementation is essential to set the stage for wider adoption of MABR technology. Future research directions need to be identified to accelerate MABR technology development. Accordingly, the objective of this review is to report and discuss the recent progress using MABRs for wastewater treatment, including:

1) Design and operational considerations, focusing the pilot and full-scale applications. This review also explicitly discussed differences and tradeoffs of hybrid and pure biofilm MABRs;

2) Microbial community ecology in MABRs;

3) Modeling efforts;

4) Performance assessment, including organic carbon, nitrogen (N), and phosphorus (P), removal, xenobiotics treatment, and sulfur recovery;

5) Current challenges and outlook.

This review is also supplemented by a workshop explicitly focusing on MABR technology held at the International Water Association (IWA) Biofilms Virtual Conference 2020, where the authors collected practice-based knowledge and integrated information from the three MABR vendors and a wide range of experts in the field.

2.2 Design and operational considerations

Design and operational conditions impact hydrodynamics and nutrient availability, which then influence mass transfer in MABRs. Design and operational conditions also influence biofilm characteristics, including thickness, density, microbial composition, and kinetics, which impact internal mass transfer and biodegradation rates within the biofilm. In hybrid MABRs, where MABRs are inserted into suspended growth bioreactors, operational conditions like solid retention time (SRT) also affect microbial activities in the suspended growth. The biochemical reaction rates at which target pollutants are consumed by microorganisms in both the attached and suspended growth define the overall performance of MABR processes (Syron and Casey 2008a). Membrane module configuration, membrane material selection, oxygen transfer and aeration mode, biofilm thickness control, and external mass transfer are among the most critical considerations for MABR design, startup and operation.

2.2.1 Membrane module configuration and process layout

Hollow-fiber and flat sheet are two common membrane configurations used in MABRs, and both are commercially available (Syron and Heffernan 2017; Shechter et al. 2020). In practice, hundreds of hollow-fiber membranes are potted to create a module, and modules are installed into cassettes for deployment in bioreactors (Figure 2-1A). ZeeLung MABR and OxyMem MABR have adopted membrane cassettes, while the Fluence MABR provides a flat sheet system in which a membrane sleeve is spiral wound around a core, and the liquid flow follows the pattern of an

airlift, rising through the spiral spacings and flowing downwards through the core (Figure 2-1C). In both designs, oxygen enters the biofilm from the lumen and is consumed. At the same time, liquid substrates diffuse into the biofilm from the boundary layer with their concentrations decreasing towards the inner biofilm (Figure 2-1B) (Pellicer-Nàcher et al. 2013; Tan et al. 2014; Janczewski and Trusek-Holownia 2016; Lu et al. 2020).

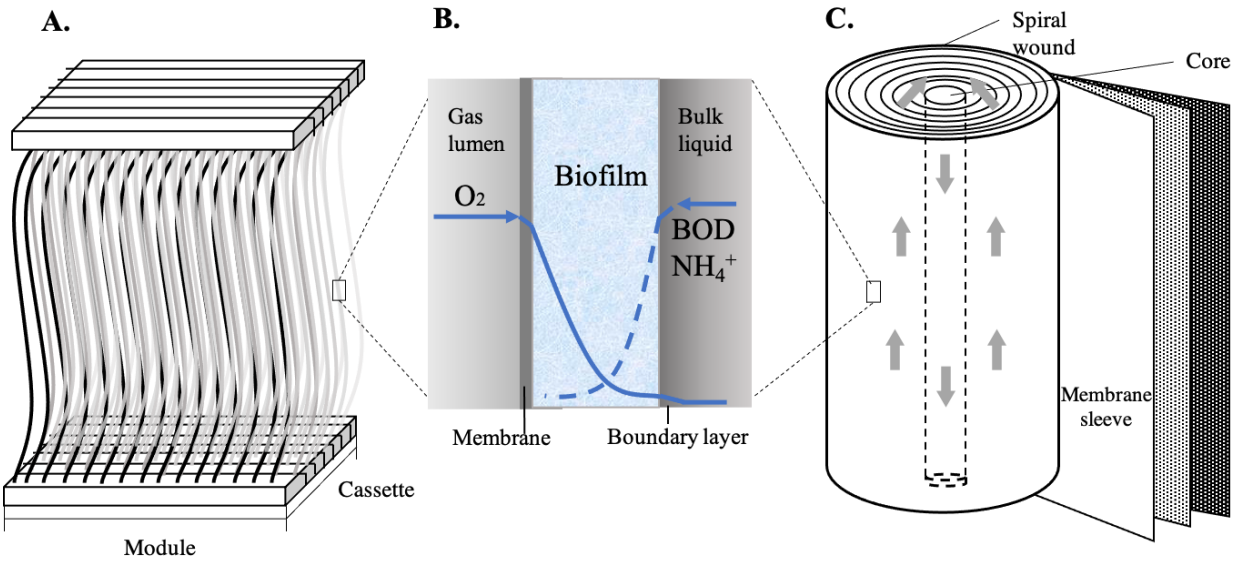

Figure 2-1 Schematic diagram of the MABR and concentration profiles of limiting substrates. A: Cassette and module of the hollow-fiber MABRs. B: Concentration profiles in MABRs. C: Spiral wound of the flat sheet MABRs. Grey arrows indicate the liquid flow pattern.

Liquid flow directions can be co-current (Pellicer-Nàcher et al. 2013; Castrillo et al. 2019), counter-current (Christenson et al. 2018), or cross-current (Kunetz et al. 2016) with respect to the inlet gas flow (Figure 2-2). A lab-scale study compared the oxygen transfer mechanism in co-current and counter-current MABRs (Perez-Calleja et al. 2017). A more significant oxygen partial pressure at the distal end was observed in the counter-current MABR rather than the co-current MABR. The effects of the oxygen partial pressure drop on the system performance will be discussed in the section 2.3 in more detail. However, for the pilot- to full-scale applications, due to the modest depletion of oxygen, greater flow velocity, and well-mixed conditions in bioreactors, impacts of liquid flow directions are generally modest at best.

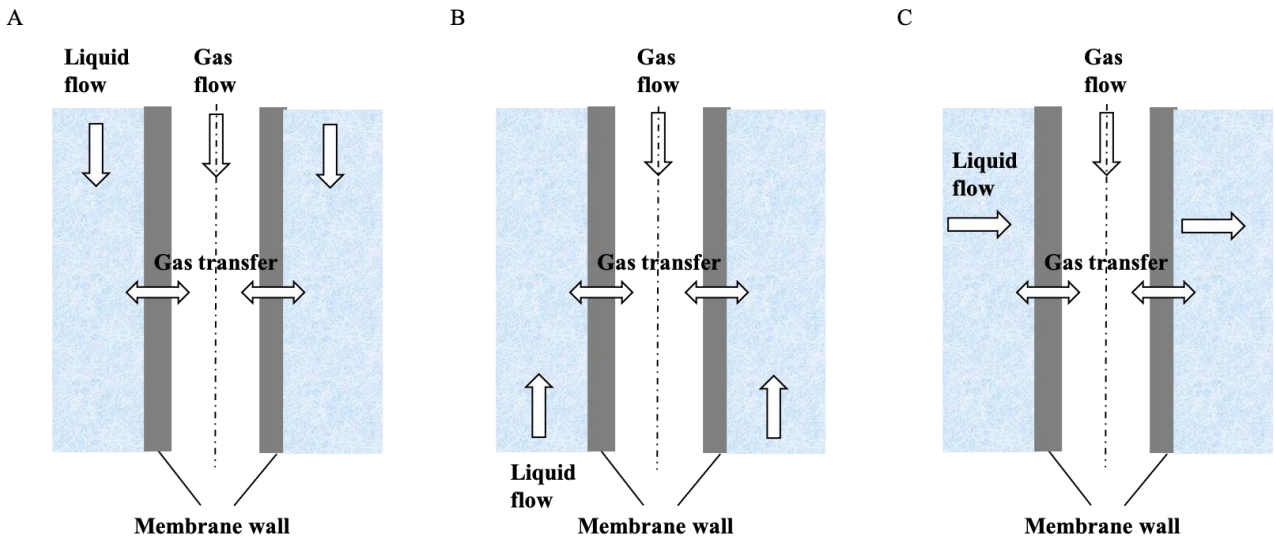

Figure 2-2 Flow configurations of MABRs. A: Co-current flow. B: Counter-current flow. C: Cross-current flow.

The MABR unit can either be operated as a pure biofilm process or coupled with conventional activated sludge (AS) as a hybrid biofilm process (Daigger 2020; Carlson et al. 2021). A fundamental difference between the two processes is the location where the organic carbon is metabolized (Carlson et al. 2021). In pure biofilm processes, organic carbon is utilized in the outer biofilm layer adjacent to the bulk liquid by heterotrophic organisms, and nitrification occurs in the inner portion of the MAB (Syron et al. 2015; Kunetz et al. 2016; Bicudo et al. 2019). In Hybrid MABR/AS processes, the organic carbon is mainly utilized by the suspended growth, and a nitrifying biofilm is developed in the attached growth for ammonia removal (Shechter and Dagai 2018; Houweling et al. 2018). The Hybrid MABR/AS process represents a full-scale solution for upgrading existing water resource recovery facilities. In practice, MABR units are commonly submerged in anoxic tanks to increase the biomass inventory, intensify the conventional AS process, and increase the facility's treatment capacity (**Error! Reference source not found.**A). W ith the aerobic MAB present in the anoxic zone, the Hybrid MABR/AS process can facilitate simultaneous nitrification and denitrification (SND) in a single tank and eliminate the internal nitrate recycling (Carlson et al. 2021). However, in such anoxic Hybrid MABR/AS system, a

modest amount of oxygen will be transferred into the anoxic zone when air scouring is applied for biofilm thickness control, which could affect denitrification activities.

Researchers also investigated the feasibility of incorporating MABR units into the aerobic zone with internal nitrate recycling (**Error! Reference source not found.**B) (Sun et al. 2020). With the a erobic MAB present in the aerobic zone, some bacteria capable of heterotrophic nitrification-aerobic denitrification, such as *Thauera* and *Paracoccus*, may facilitate the SND mechanism (Sun et al. 2020). For enhanced biological phosphorus removal (EBPR) systems, an initial anaerobic zone can be added upstream for hydrolysis of particulate and colloidal substrates and volatile fatty acids (VFAs) uptake by polyphosphate-accumulating organisms (PAOs). Incorporation of MABR units into an anaerobic zone can be problematic because membrane aeration introduces electron acceptors, i.e., dissolved oxygen (DO) directly and also nitrate if nitrification occurs, that reduces fermentation and allows other heterotrophs to compete with PAOs for VFAs that may be present. Placement of the MABR in the anoxic tank is an established practice for biological nitrogen removal (Houweling et al. 2017; Underwood et al. 2018; Guglielmi et al. 2020). More research and comparative studies are needed to analyze the ecological niches created and treatment performance achieved when MABRs are placed in anaerobic, anoxic, or aerobic zones in hybrid processes.

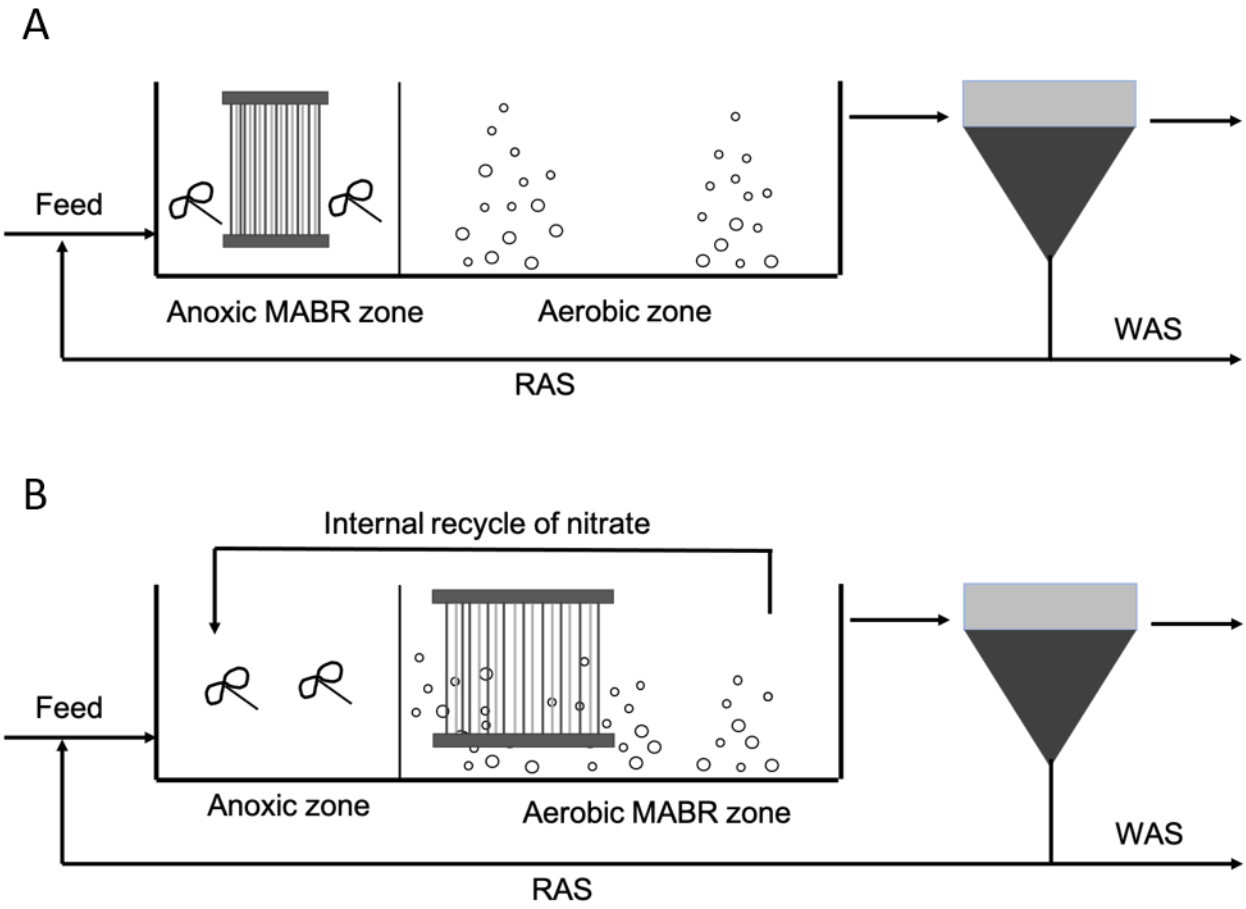

Figure 2-3 Hybrid MABR/AS process for intensifying the activated sludge. MABR unit submerged in the unaerated zone (A) or fine bubble aerated zone (B).

Packing density is a critical parameter to size the MABR zone in the hybrid process. While a high packing densities can provide a larger specific surface area to support biofilm attachment and consequently promote the pollutant removal rates, biofilm bridging can occur at high packing densities, resulting in a decrease in the effective surface area (Hou et al. 2019). Research and practice experiences are in need to investigate solutions to increase packing density while retaining efficient external mass transfer characteristics and avoiding solids build-up. This will lead to smaller units and further reductions in footprints and cost.

2.2.2 Membrane material selection

Membrane properties, including surface morphology, porosity, and permeability, have a significant impact on MABR performance as they affect microbial affinity for the membrane and oxygen transfer, which ultimately impact biofilm characteristics and biochemical reaction rates (Syron and Casey 2008a; Lu et al. 2020). Improper membrane materials can result in low oxygen transfer rates and poor biomass adhesion, hampering MABR performance with a longer startup phase. Membranes in MABRs are typically composed of hydrophobic materials such as polyvinylidene fluoride (PVDF) and polypropylene (PP) to enhance microbial attachment to form a functional biofilm (Lu et al. 2020; Hou et al. 2013; Xiao et al. 2021). A comparative study between PVDF and PP membranes showed that the PVDF membrane exhibited better resistance to pore blocking issues and improved biomass attachment to the MABR because of its higher hydrophilicity and surface roughness (Wu et al. 2019). Nylon silk was also used as the membrane material for surface water treatment (Zhong et al. 2019), but its long-term durability and impact on mass transfer and biofilm formation need further investigation. Overall, PVDF, PP, and nylon silk are classified as microporous membrane materials which have negligible mass transfer resistance (Janczewski and Trusek-Holownia 2016). These membrane materials are generally favored in lab-scale MABR studies because high oxygen transfer flux through pores promotes aerobic biochemical reaction rates (Syron and Casey 2008a; Nerenberg 2016; Lu et al. 2020). However, microporous membrane materials are not used in the pilot- or full-scale applications due to pore-clogging issues, low life span, and low air pressure requirements.

In contrast, dense membrane materials are used in commercial MABR units because of their increased strength, durability and decreased likelihood of membrane fouling (Syron and Casey 2008a; Nerenberg 2016; Lu et al. 2020). Examples of dense membrane materials include polymethylpentene (PMP) and silicone polydimethylsiloxane (PDMS). For instance, OxyMem uses PDMS membranes, with benefits including high oxygen permeability, chemical resistance, and resistance to mechanical stress (Bicudo et al. 2019).

A composite membrane combines a dense layer coated with a microporous layer. Hou et al. 2013 reported that a L-3,4-dihydroxyphenylalanine (DOPA) coated PVDF membrane increased the gas flux by two times and shortened the time required to achieve an optimal chemical oxygen demand (COD) removal rate from 6 hours to 0.5 hours. Overall, experience with composite membranes or surface modifications is still limited. Further research is needed to develop high-efficient and low-cost composite membrane materials for wastewater treatment using MABRs.

2.2.3 Oxygen transfer and aeration modes

OTRs and OTEs are two key performance indicators used to evaluate MABR processes (Houweling et al. 2017). The OTR across the membrane can be described as (Pellicer-Nàcher et al. 2013):

$$J_{O_2} = K(\frac{S_{O_2,g}}{H} - S_{O_2,bio}) \quad \text{(Eq. 1)}$$

where J_{O_2} is the OTR across the membrane (g/m^2-d), K is the mass transfer coefficient (m/d), $S_{O_2,g}$ and $S_{O_2,bio}$ are the oxygen concentrations in the gas phase and membrane-biofilm interface (g/m^3), and H represents the unitless Henry's Law constant. The OTE is characterized as (Houweling and Daigger 2019):

$$OTE = \frac{X_{O_2,in} - F_V X_{O_2,out}}{X_{O_2,in}} \quad \text{(Eq. 2)}$$

Where $X_{O_2,in}$ and $X_{O_2,out}$ are the mole fractions of oxygen in the air inlet and outlet (unitless); F_v is the unitless volumetric loss factor of oxygen:

$$F_V = \frac{1 - X_{O_2,in}}{1 - X_{O_2,out}} \quad \text{(Eq. 3)}$$

MABR aeration modes can be categorized as either flow-through or dead-end, according to the bulk gas flow. Higher average OTRs, which translate into higher average contaminant removal fluxes and treatment capacity, are usually achieved in the flow-through rather than dead-end operation (Syron and Casey 2008b). Therefore, the flow-through operation is preferred in commercial applications (Kunetz et al. 2016; Peeters et al. 2017; Underwood et al. 2018; Guglielmi

et al. 2020). The higher average OTRs in flow-through MABRs can be explained by the higher oxygen partial pressure, which allows uniform intra-membrane oxygen velocities in the membrane lumens and relatively constant biofilm thickness. For dead-end operation, all the supplied oxygen can be delivered into the biofilm, leading to a 100% OTE and much reduced aeration energy (Tian et al. 2020). However, the dead-end mode has relatively lower OTRs because of oxygen exhaustion and the back-diffusion of gases which cause significant oxygen partial pressure drop and consequently reduced biological reaction rates (Perez-Calleja et al. 2017). Therefore, it is important to consider the tradeoffs between the OTR vs. OTE and treatment capacity vs. aeration energy when selecting the aeration modes in practice. Innovative strategies are also available to balance such tradeoffs. For example, Perez-Calleja et al. 2017 explored the feasibility of operating MABRs in alternating flow-through and dead-end modes. Experimental and modeling results indicated that the transient behavior shifting between the two aeration modes could improve both OTE and OTR. More research is still needed to optimize the interval of switching and duration of each mode, and the optimization is likely to be unique in response to a range of factors, including oxygen partial pressure, oxygen flow rates, and treatment goals.

Table 2-1 Summary of operational parameters for aeration in selected MABR studies.

Wastewater type and application purpose	Scale	Air feed pressure (MPa)	Airflow rate (Normal L/m^2-h)	Feed gas	Aeration mode	OTR (g O_2/m^2-d)	OTE (%)	Aeration efficiency (kg O_2/kWh)	Reference
Municipal wastewater for nitrogen and phosphorus removal	Pilot	0.067	4.3	Process air	Continuous flow-through	8-12	NA	6.5-7.0	(Kunetz et al. 2016)
Municipal wastewater for N removal	Pilot	0.067	5.3	Process air	Continuous flow-through	8-15	30-40	6	(Côté et al. 2015)
Municipal wastewater for COD and nitrogen removal	Pilot	NA	NA	Process air	Continuous flow-through	NA	NA	4.0-4.9	(Sunner et al. 2018)
Municipal wastewater for COD and nitrogen removal	Full	0.048	4.8	Process air	Continuous flow-through	7.1-15.9	25, up to 50	NA	(Guglielmi et al. 2020)

Municipal wastewater for nitrogen and phosphorus removal	Pilot	0.025	NA	Process air	Continuous flow-through	Average: 1.5-4.5 Peak: 9	25-50	14	(Bicudo et al. 2019)
Industrial wastewater for COD and nitrogen removal	Pilot	0.041	1.8	Process air	Continuous flow-through	3	25	NA	(Stricker et al. 2011)
Industrial wastewater for COD and nitrogen removal	Pilot	0.041	1.4	Process air	Continuous flow-through	2.9	31	NA	(Stricker et al. 2011)
Landfill leachate for nitrification	Pilot	0.025	NA	Process air or pure oxygen	Continuous flow-through	8 with process air, 25 with pure oxygen	20-75 with process air; 50-80 with pure oxygen	4	(Syron et al. 2015)

It should be noted that aeration control via manipulating the oxygen partial pressure is often not practiced in commercial applications. Instead, oxygen is introduced into the MABR lumen at the design airflow rate, and oxygen partial pressure in the lumen changes as a result of oxygen transfer and microbial consumption (Côté et al. 2015; Bicudo et al. 2019). For Zeelung and OxyMem MABRs, this is done because exhaust gas from the MABR is used to create fluid flow through the MABR bundle to renew the fluid inside the bundle and to increase the mass transfer of substrates from the bulk liquid into the biofilm on the MABR membranes (Downing 2021). A summary of aeration parameters used in several commercial MABR applications is provided in Table 2-1. Reported OTEs were consistently higher than that of the conventional fine bubble aeration system (typically 10%) (Houweling and Daigger 2019). In mainstream commercial applications, a modest proportion of the oxygen in the feed gas (20-30%) is transferred into the biofilm, and the rest is exhausted. As a result, the oxygen partial pressure only declines slightly along the lumen, allowing high OTRs throughout the membrane. As discussed above, high OTRs support higher aerobic biological activities in the MAB, such as nitrification (Houweling and Daigger 2019). Such operations can maximize the ammonia removal fluxes and minimize the membranes needed, and therefore it is an economical choice to sacrifice aeration energy to achieve higher treatment capacity. However, even though the tradeoff between treatment capacity vs. aeration efficiency exists, reported aeration efficiencies of MABRs ranging from 4 - 14 kg O_2/kWh (Table 2-1) were consistently superior to that of conventional wastewater aeration systems of 1.0-1.5 kg O_2/kWh (Rosso et al. 2008). As aeration accounts for the most considerable energy cost in wastewater treatment plants (WWTPs) (Longo et al. 2016), the bubble-less aeration technology in MABRs, with demonstrated high aeration efficiency, can lead to significant energy savings.

Using pure oxygen instead of air in MABRs enhances OTRs and oxygen penetration depth (Brindle et al. 1998; Cole et al. 2004), enabling high COD and ammonia removal rates (Syron and Heffernan 2017). When operating with pure oxygen, the MABR process may require up to five times less membrane area than when operating with air, leading to capital investment reduction

and a smaller footprint (Syron et al. 2015). However, MABRs fed with pure oxygen tend to grow thicker biofilms and increased mass transfer resistance because of the enhanced growth of aerobes. Several studies also reported that air scouring could not effectively control biofilm thickness in this case, which can limit the overall removal performance of MABRs (Stricker et al. 2011; Syron et al. 2015). Moreover, excessive oxygen may create ecological niches that suppress *nirS* and *nirK* genes for denitrification (Cole et al. 2004). The choice of air or pure oxygen depends on the wastewater characteristics, treatment goal, and operational considerations. For example, feeding air may not be sufficient to treat wastewater with high organic carbon loadings, and in this case, pure oxygen may be beneficial to improve COD removal efficiency if the biofilm is not biomass limited. Ongoing research and practical experience are required to elucidate further the effects of pure oxygen on biofilm characteristics, including density, thickness, and microbial composition. Effective control strategies are needed to control the potentially thicker biofilms grown with pure oxygen feed.

Flow-through and dead-end aeration can both be operated in continuous or intermittent mode. While continuous aeration is typically applied for COD and nutrient removal processes, intermittent aeration is commonly selected when an oxygen limiting condition is desired to enrich ammonia-oxidizing bacteria (AOB) and suppress nitrite-oxidizing bacteria (NOB) for shortcut ammonia removal in MABR biofilms (Pellicer-Nàcher et al. 2014; Ma et al. 2017; Bunse et al. 2020). In a pilot-scale MABR operated for side-stream shortcut ammonia removal, i.e., the ZeeNAMMOX process, the vertical oxygen supply direction in the lumen was alternated periodically to switch the DO limited condition (oxygen < 2%) from top to bottom (Long et al. 2020). This study applied exhaust gas-based aeration control, which used oxygen sensors to measure the oxygen content in the off-gas. The measured oxygen content was then correlated to ammonia removal and residual ammonia concentrations, and therefore, the use of ammonia sensors was eliminated. Reliable suppression of NOB growth was achieved, limiting the ratio of nitrate generation to ammonia oxidation to 0.2. The alternation of oxygen feed direction also

exposed the biofilm to more uniform conditions along the length of the membranes. Gas from the outlet is usually not recycled due to 1) the depletion of oxygen in the lumen phase which, when recycled, would decrease the OTR (Uri-Carreno et al. 2021), and 2) back-diffusion can dilute the oxygen concentration in the lumen (Perez-Calleja et al. 2017).

It is also critical to consider the tradeoff between nitrification and total nitrogen (TN) removal under different aeration conditions. A higher oxygen availability can boost nitrification but also limit denitrification activity, reducing TN removal rates (Mehrabi et al. 2021). In contrast, operating at a lower air pressure or airflow rate can limit oxygen availability and promote TN removal in the MABR. In addition, the high availability of oxygen may lead to excessive growth of aerobes and thereby thick biofilms that are more prone to mass transfer limitations (Shanahan and Semmens 2015). Therefore, a tradeoff exists between nitrification and TN removal under different aeration conditions.

2.2.4 Biofilm thickness control

Biofilm thickness control is an important consideration for MABR operation, as excessive biofilm thickness, which is a frequently encountered problem in practice, raises concerns for increased mass transfer resistance and membrane clogging issues. In practice, biofilm thickness control is commonly accomplished by promoting biofilm detachment, which involves introducing scouring air bubbles onto the biofilm surface to remove the external layer of the biofilm (Heffernan et al. 2017). Commercial MABRs collect the exhaust gas for air scouring (Nathan et al. 2020; Downing 2021). Specifically, the OxyMem MABR has a unique scouring system that uses inert gas and a pressure decay test to measure the relative biofilm thickness, which controls a scouring system that intermittently creates air bubbles to encourage biofilm detachment (Casey et al. 2014).

For pure biofilm systems where both ammonia and organic carbon are metabolized in the attached growth, biofilm thickness control is critical to reduce mass transfer resistance. NRs in the MAB were doubled after air scouring because of the improved mass transfer rates of ammonia

(Supporting information (SI)). However, if too much biofilm is removed, the attached growth may not retain sufficient functional biomass, diminishing performance. Several studies have reported performance upsets following biofilm detachment events due to the reduced number of organisms in the MAB, and the unwanted performance lag can last up to several months before full efficiency was recovered (Shanahan et al. 2005; Bunse et al. 2020). More research is needed to investigate how a biofilm responds to scouring events, including detachment/reattachment rates, microbial composition shift, and changes to the physical properties of the biofilm. Practical experience is critical to identify the optimal air scouring frequency and intensity for biofilm detachment to help reduce the performance lag observed after air scouring events.

The MAB in hybrid systems behaves differently than that in pure biofilm systems. The MAB thickness in hybrid systems is often thinner, and less biofilm control is generally needed. This occurs because the suspended growth in the bulk liquid consumes soluble COD, thereby minimizing heterotrophic growth in the biofilm (Downing et al. 2010; Uri et al. 2018). Biofilm thickness does respond to temperature and operational conditions. For example, thicker biofilms tend to form during winter and short suspended growth SRT operations, while biofilms get thinner during summer and long SRT operations (SI). However, excessive biofilms can develop in Hybrid MABR/AS processes, raising clogging and mass transfer resistance issues because of the decreased effective biofilm surface area. They may also displace bioreactor volume for suspended growth and diminish the treatment performance contributed by the suspended growth (Houweling and Daigger 2019). Therefore, biofilm thickness control via air scouring is often applied in hybrid systems to ensure effective performance. Of course, overuse of air scouring in Hybrid MABR/AS systems must be avoided when the MABR unit is incorporated into the anoxic tank to prevent possible adverse impacts on denitrification. Therefore, understanding how a Hybrid MABR/AS process responds to scouring events is critical to control the biofilm as well as the suspended growth to maximize overall treatment performance.

2.2.5 External mass transfer

Bulk liquid hydrodynamic conditions affect external mass transfer from the bulk liquid to the biofilm in MABRs (Bicudo et al. 2019). The liquid flow produced by air bubbling renews the substrates in the bulk liquid within the membrane bundles so that continued substrate removal can occur (Daigger 2020). Liquid flow velocity, coupled with the introduction of air bubbles for scouring and promoting fluid flow, creates fluid shear on the biofilm surface. As a result, liquid flow velocity affects the thickness of the boundary layer at the liquid-biofilm interface and the biofilm detachment rate. Diffusion boundary layer thickness is reduced with increased liquid flow velocity, and biofilm detachment accelerates. As a result, the thinner diffusion boundary layer enhances the external mass transfer rate, providing higher overall removal rates (Shoji et al. 2020). However, in a previous tracer experiment (Castrillo et al. 2019), high flow velocities resulted in a non-optimal flow pattern, allowing no further enhancement of mass transfer. This lack of increase in mass transfer could be caused by flow channeling or short-circuiting, so the liquid flow velocity must be monitored to manage optimal reactor performance.

Liquid flow velocity also impacts MAB structure. Lab-scale studies reported a non-uniform biofilm density along the membrane of biofilms grown at a low fluid velocity (1.7 and 2 cm/s) (Shanahan et al. 2005; Pellicer-Nàcher et al. 2014). This resulted from the variation in the effective local diffusivity, which had a profound effect on biofilm stratification and microbial activities. However, such effects would not be observed for reactor configurations where flow recirculation is used to create the necessary fluid flow velocity, such is the case for some laboratory- and commercial-scale units. In commercial applications, gas sparging is often used to create flow through membrane bundles. The rate of gas sparging will control the liquid flow velocity independent of the organic and nitrogen loading on the membranes. Therefore, the biofilms in commercial MABRs are exposed to relatively constant diffusivity and liquid substrates. The representative vendor should be able to provide information on the effects of liquid flow velocity

on performance for their respective units, which depend on the MABR configuration and method for creating liquid flow velocity.

2.3 Microbial community ecology

Activities of the complex microbial communities that form are the foundation for the biological transformations that occur in MABR systems. Important elements in the microbial community ecology include taxonomic diversity, functional pathways, and interactions between microbial groups (Konopka 2009). A meaningfully defined microbial community ecology is crucial in developing an operational strategy that affects system performance, energy consumption, and costs. To date, taxonomic diversity and functional pathways in MABRs have been studied using a range of technologies. However, knowledge is still limited to systematically understand microbial interactions in the MABR and their shifts in response to operational conditions.

2.3.1 Taxonomic diversity

The counter-diffusional property of MABs results in distinct microbial community structures and behaviors. In most studies, Proteobacteria is the most abundant phylum present in MABRs (Cole et al. 2004; Tian et al. 2017; Kinh et al. 2017; Li and Liu 2019; Sathyamoorthy et al. 2019). Specifically, sub-Proteobacteria, Alphaproteobacteria, and Gammaproteobacteria, prefer anaerobic environments and inhabit the outer biofilm layers or suspended growth, while Betaproteobacteria and Deltaproteobacteria tend to inhabit the aerated portions within the biofilm (Sathyamoorthy et al. 2019; Lan et al. 2018). Proteobacteria is expected to be a key player responsible for nitrogen removal, and both AOB and NOB guilds have been observed in this phylum (Lan et al. 2018; Baskaran et al. 2020). Excessive growth of the filamentous Alphaproteobacteria (‘Nostocoida’-like) and Gammaproteobacteria (Thiothrix and type 021N) are commonly associated with sludge bulking and foaming (Nielsen et al. 2009).

Abundant Flavobacteria of Bacteroidetes phylum in the MAB were also observed in the lab- and pilot-scale investigations (Aybar et al. 2019; Sathyamoorthy et al. 2019). Bacteroidetes organisms are reported to be responsible for phosphorus removal (Xu et al. 2018). In a pilot-scale MABR system, considerable relative abundances of Actinobacteria in both biofilm (7%) and mixed liquor (14%) were identified (Sathyamoorthy et al. 2019). An early study suggested that Actinobacteria may play an important role in the EBPR process but can also lead to operational problems of bulking and foaming (Seviour et al. 2008). Overall, researchers have identified key categories of organisms performing a variety of functions within the microbial community in MABRs. However, this field still needs more research to fully understand microbial interactions between the microbial groups, e.g., symbiosis, competition, or predation, during the wastewater treatment process. This is critical to translate the observed biodiversity to the operation and management of MABRs.

Higher life forms like eukaryotes are also part of the microbial community in MABs. At the genus level, Aybar et al. 2019 reported a substantial abundance of amoeba and flagellated protozoa in MABs. MAB images showed internal voids due to protozoa predation (Kim et al. 2020). Such voids can alter biofilm properties like porosity, density, and mechanical strength, mass transfer of substrates, and microbial community ecology, all of which ultimately affect the net reaction rate in MABRs (Syron and Casey 2008a). More research is needed to fully characterize the conditions affecting the type and activity of eukaryotes and the effects of predation on biofilm formation, detachment, and microbial dynamics in MABRs.

2.3.2 Functional pathways for biological nutrient removal (BNR)

MABRs enable SND for novel nitrogen removal and carbon degradation compared to the various conventional nitrogen removal schemes. Nitrification, predominantly carried out by AOBs and NOBs, occurs in the inner-most aerobic MAB layer, while denitrification occurs in the anoxic layer and/or suspended growth as heterotrophic denitrifiers occupy the outer layer or bulk liquid

(Zhao et al. 2021; Landes et al. 2021). Early MABR studies identified dominant nitrifying populations such as *Nitrosomonas* and *Nitrosospira* in the AOB guild as well as *Nitrospira* and *Nitrobacter* in the NOB guild (Liu et al. 2010; Gilmore et al. 2013). Ammonia-oxidizing archaea (AOA), e.g., *Candidatus Nitrososphaera*, was also identified in the MAB as a functional group for nitrification under low oxygen supply (Liu et al. 2016; Tian et al. 2017).

The denitrifying population was more diverse than the nitrifying population, and the relative dominance varied according to the COD loadings and pH (Tian et al. 2015). Some commonly expressed genes throughout the SND process include ammonia monooxygenase gene (*amoA*) for ammonia oxidation and nitrite reductase genes (*nirK* and *nirS*) for nitrite reduction. Several lab-scale studies have confirmed the coexistence of *amoA*, *nirK*, and *nirS* in the MAB, which validates the SND pathway at the genetic level (Cole et al. 2004; Liu et al. 2015).

Anaerobic ammonia oxidation, or anammox, is another innovative pathway that has been intensively studied in MABRs for nitrogen removal (Gong et al. 2007; Cema et al. 2011; Gilmore et al. 2013; Bunse et al. 2020). Anammox is usually combined with partial nitritation, where ammonia is partially oxidized to nitrite by AOBs, and the remaining ammonia is oxidized to nitrogen gas anaerobically via nitrite reduction by anammox bacteria. NOBs, which compete for nitrite with anammox bacteria, are undesirable in partial nitritation/anammox (PN/A) MABRs, and an oxygen-limited condition is employed to out-select NOBs (Gong et al. 2007; Cema et al. 2011; Cho et al. 2019). Compared to traditional nitrogen removal via nitrification and denitrification, the PN/A process reduces both oxygen and carbon requirements (Kuenen 2008; Cho et al. 2019). Core genes for hydrazine metabolism (*hzs* and *hdh*) and the gene cluster for nitrite reduction (*nirK* and *nirS*) are all essential for anammox (Speth et al. 2016). A previous study detected the anammox species *Candidatus Jettenia*, *Ca. Brocadia*, and *Ca. Anammoxoglobus* in an MABR (Zhao et al. 2021). As strict anaerobic organisms, anammox bacteria grow in the anaerobic outer layer of the MAB or suspended growth, and AOBs grow in the inner aerobic biofilm layer (Gong et al. 2007; Bunse et al. 2020). Proliferation of *R*-strategist AOBs (e.g., *Nitrosomonas*) in the inner MAB layer

can quickly consume DO and mitigate the inhibitory effect of oxygen on anammox growth (Terada et al. 2010). Overall, the successful application of the anammox process for nitrogen removal in MABRs relies on the symbiosis between AOBs and anammox bacteria, which is still challenged by the low growth rate of anammox bacteria and microbial competition by NOBs for the nitrite formed by AOBs.

In terms of phosphorus removal, the same metabolic pathways exist in MABRs as conventional AS approaches. PAOs incorporate VFAs in the anaerobic zone for the production of a stored fat reserve, polyhydroxy-alkanoate (PHA), while intercellular supplies of glycogen and polyphosphate are exhausted for energy. In the subsequent aerobic phase, the stored reserve is oxidized back to glycogen, and PAOs uptake excess phosphate from the mixed liquor to regenerate stored polyphosphate (Arun et al. 1988). Some commonly expressed genes throughout the metabolic processing of phosphorus code for key enzymes including: polyphosphate kinase (*ppk*) which facilitates phosphorylation of the polyphosphate chain, exophosphatase (*ppx*) that catalyzes polyphosphate hydrolysis, and adenylate kinase (*adk*) that regulates energy levels in the cell (Akiyama et al. 1993; Shiba et al. 2000; Kristiansen et al. 2013). These annotated functional gene sequences have been valuable to understand the shared metabolic pathways among different PAO taxonomies, such as *Accumulibacter* and *Tetrasphaera* (Kristiansen et al. 2013), and used as marker genes for fine-scale phylogenetic distribution (Gao et al. 2017).

Phosphate uptake can also be coupled with nitrate or nitrite reduction in the anoxic environment via the denitrifying PAOs (DPAOs) (Díez-Montero et al. 2016). The ability to use nitrate and nitrite as the terminal electron instead of oxygen has been demonstrated for selected *Accumulibacter* lineages (Carvalho et al. 2007; Flowers et al. 2009). In the Hybrid MABR/AS process, the nitrate and nitrite produced by the aerobic MAB could diffuse into the anoxic bulk liquid and serve as the electron acceptor for the DPAO metabolism (Carlson et al. 2021). This can lead to significant energy saving for aeration. However, identification of PAOs and DPAOs and

the functional mechanism of phosphorus removal remain understudied areas regarding pure MABRs or Hybrid MABR/AS systems.

2.3.3 Microbial community characterization tools

Three main approaches have been applied to obtain a holistic view of the functioning microbial world in the MABR process: physical analysis, microscopic imaging, and "omic" techniques. Microsensors are commonly used for physical analysis to measure the concentration of key substrates such as DO, pH, ammonia, nitrite, and nitrate in increments as low as 10 μm within the biofilm (Gilmore et al. 2009). Profiles of these substrates allow observation of the microbial stratification into aerobic, anoxic, and anaerobic regions of an MAB, and the abundance of bacterial guilds and substrate uptake rates in each region can be calculated (Tan et al. 2014). A comparative study examined emissions of the strong greenhouse gas nitrous oxide (N_2O) in MABs and co-current biofilms by measuring DO and N_2O throughout the depth of the biofilm via microsensors (Kinh et al. 2017). The results showed for the first time that the MABR can mitigate N_2O emissions because the N_2O produced by AOBs in the aerobic biofilm layers can be uptake in the adjacent anoxic layers by heterotrophs. Microsensors have been used in a variety of MABR studies for *in situ* monitoring of ammonia removal (Underwood et al. 2018), SND (Underwood et al. 2018), the occurrence of sulfate reduction (Tan et al. 2014), and DO profiles (Aybar et al. 2019). The application of microsensors has revealed that exposure to sublethal concentrations of toxins caused a significant increase in oxygen and hydrogen ion flux from the bulk liquid to the MAB (McLamore et al. 2010). This result linked cellular stress response to bulk liquid water quality, which is critical to establishing effective monitoring and control strategies in MABRs.

Microscopic methods can be extremely helpful in visualizing the mesoscale structure and volumetric features of biofilms. Fluorescence *in situ* hybridization (FISH) uses a fluorescent-labeled probe that attaches to specific genomic regions of a microorganism, with fluorescence observed under a confocal laser scanning microscope to see the microorganism's location within

the biofilm. FISH is frequently applied on MABR biofilms to identify the presence and spatial distribution of bacterial groups. *Nitrosospira* and *Nitrosomonas* have been revealed by FISH as the dominant AOBs in the inner portion of a nitrifying MAB (Liu et al. 2010; Gilmore et al. 2013). *Nitrosomonas*, known as an *R*-strategist which favors higher DO concentration than *Nitrosospira*, was located in the inner-most layer near the membrane surface (Terada et al. 2010). The same studies also observed *Nitrospira* and *Nitrobacter* as the dominant NOBs adjacent to the AOB layer.

A separate microscopic technique, optical coherence tomography (OCT), can show the presence of microbial predators within an MAB (Aybar et al. 2019; Kim et al. 2020). However, a major hurdle for the use of microscopic methods in MABRs is sampling, which is invasive and involves cutting the membrane so that the biofilm sample and stratification can be preserved. In addition, due to the variations in the biofilm along the MABR fiber, multiple samples need to be analyzed to account for the biofilm heterogeneity. Other microscopic analysis techniques involving Confocal Raman micro-spectroscopy have been used to monitor the live bacterial biofilm as a function of space and time (Sandt et al. 2007). Though very few studies have applied Confocal Raman micro-spectroscopy for biofilm analysis in MABRs, it is a promising non-invasive technique for future studies for the *in situ* mapping, tracking, and identification of microbes in MABs.

Omics methods, such as deoxyribonucleic acid (DNA) sequencing technologies, provide unprecedented insights into the biodiversity and genetic information of the microbial community in MABRs. This is extremely important to understand the biological transformations of pollutants and behaviors of functional microorganisms in the MABR process. In particular, 16S ribosomal ribonucleic acid (rRNA) gene sequencing, which targets the widely conserved 16S rRNA gene, continues to be one of the most commonly applied methods for taxonomy identification and quantification in both lab-scale MABs and pilot hybrid systems (Kinh et al. 2017; Sathyamoorthy et al. 2019). Quantitative polymerase chain reaction (qPCR) has also been widely used in MABR studies to quantify the presence of a targeted gene and its relative or absolute abundance (Cole et

al. 2004). In a recent full-scale Hybrid MABR/AS system, *amoA*, anammox 16S, *Nitrospira* 16S, and *Nitrobacter* 16S rRNA genes were targeted to analyze the nitrifying populations via qPCR analysis (Underwood et al. 2018). Results of the same study indicated a large imbalanced abundance of NOBs and low abundance of AOBs, suggesting the possible existence of the complete ammonia oxidation (comammox) bacteria fully nitrifying ammonia to nitrate.

The downsides of 16S rRNA sequencing and qPCR-based analysis are that they cannot describe the metabolic pathways (Dick 2018). In addition, as the so-called "universal" PCR primers target the 16S rRNA gene of highly conserved sequence and length that can be reliably amplified and compared to a database, 16S rRNA sequencing may miss novel organisms that have genes of unknown sequences. Shotgun metagenomics improves upon the sequencing of targeted genes and provides a means of assessing the total genetic material in a microbial community (Dick 2018). Delgado et al. 2020 examined nitrogen metabolism in an MABR with the presence of sulfide using metagenomic approaches. Results indicated that sulfide could disrupt nitrification by decreasing nitrite oxidation rates but increasing ammonia oxidation rates and N_2O production. Hu et al. 2020 used metagenomic sequencing to investigate MAB formation in a phenolic wastewater treatment process. Their results suggested the formation and performance of the biofilm were potentially regulated by quorum sensing systems which can be highly impacted by influent phenolic loadings. Therefore, an optimized phenolic loading rate can be critical to foster MAB formation and shorten the startup time of the system. The metagenomic analysis is also powerful in discovering novel genes and organisms. One of the most recent examples is shown in the discovery of comammox bacteria, which has the full suite of nitrification genes to oxidize ammonia to nitrate (Daims et al. 2015). Such metagenomic analysis could be used on MABRs in future studies to validate the presence of comammox bacteria and other novel organisms, which, if present, could impact the performance of nitrogen removal.

While metagenomic sequencing provides information on the abundance and metabolic potential of organisms within an MABR, it does not describe whether those processes are active

across time or space. In contrast, quantifying messenger ribonucleic acid (mRNA) and proteins with metatranscriptomics and metaproteomics, respectively, can show which genes are actively being expressed and translated into proteins. In addition, stable isotopic probing (SIP) is very powerful to identify cross-feeding, which is the phenomenon of one species living off the metabolic products of another species in complex microbial communities (Mooshammer et al. 2021). Applying those advanced microbial tools in further MABR studies can help quantify the relative contributions of different microbial groups to nutrient removal and microbial interactions between the attached and suspended growth. These omics approaches can be costly and time-intensive, however, and therefore have not been applied to MABR studies to date. The selection of methods should, of course, be based on the scientific questions of interest and research objectives.

2.4 Modeling

Mathematical modeling is essential to understand and develop biofilm reactors. Given the complex biological treatment configurations of MABRs, mathematical models are frequently used to assist with system design and operation. The ability of models to capture the integrated behavior of complex systems makes them useful research tools, often used in combination with other research techniques, such as molecular approaches discussed in the previous section and wet chemistry analysis.

Conventional biofilm modeling practice (Wanner et al. 2006) and the framework for good biofilm reactor modeling practice (Rittmann et al. 2018) are fully applicable to MABR modeling. However, a unique aspect of MABR modeling is the need to expressly re-formulate oxygen transfer. In conventional co-current biofilms, oxygen is first transferred into the liquid through the gas-liquid interface and then acts like other substrates that diffuse into the biofilm from the liquid (Wanner et al. 2006). As a result, an oxygen-rich zone of active growth develops adjacent to the biofilm-liquid boundary layer. In contrast, in an MABR, oxygen is transferred to the inner surface

of the MABR membrane, diffuses through the membrane, and then enters the biofilm. The MAB layer adjacent to the membrane is an oxygen-rich zone of active growth. Given the different mass transfer schemes and distribution of biomass growth, MABs respond to operational and kinetic parameters differently from conventional biofilms (Syron and Casey 2008b). Martin et al. 2017 reported that the diffusivity of ammonia nitrogen, biofilm thickness, and liquid-biofilm boundary layer thickness mostly impacted the NRs in MABs. In contrast, NRs in conventional biofilms are mostly influenced by the liquid-biomass boundary layer thickness, maximum AOB growth rate, and half-saturation constant of oxygen for AOBs. Therefore, MABR models will have to be calibrated differently than traditional biofilm models for a specific application.

MABR modules that account for the unique mass transfer scheme are available in several commercial simulators. This availability allows researchers and practitioners to use models to investigate the impact of process conditions, including bulk biological oxygen demand (BOD) concentrations (Downing and Nerenberg 2008), DO gradients (Downing and Nerenberg 2008), intra-membrane gas pressure (Syron and Casey 2008; Amadi et al. 2008), pH and alkalinity (Shanahan and Semmens 2015), COD/N ratio (Carlson et al. 2021), and mixing intensity (Schraa et al. 2018). The mass transport of substrates, detachment processes of MABR biofilms, and attachment of suspended solids (Brannock et al. 2010; Qi et al. 2013; Plascencia-Jatomea et al. 2015) have also been modeled. Downing et al. 2017 investigated the impacts of adding an MABR in an unaerated zone in the Ejby Molle facility in Odense, Denmark. Their results revealed the feasibility of achieving shortcut nitrogen removal in the biofilm by manipulating the intramembrane air pressure. The process model also predicted more than a 50% reduction in energy and a 40% increase in peak flow capacity with the incorporation of MABRs. A recent study investigated the possibility of using MABRs to produce nitrate coupled with heterotrophic denitrification from suspended biomass in a largely anoxic suspended growth bioreactor (Carlson et al. 2021). This study provided a proof of concept in sizing the MABR to accomplish a substantial

proportion of the ammonia removal via nitrification, which significantly reduced or even eliminated aerated zones while still achieving effective BNR performance.

The unique oxygen transfer scheme in MABRs can also be modeled explicitly. Houweling and Daigger 2019 described two methods: (1) the pressure-based model and (2) the exhaust oxygen-based model. (Peeters et al. 2017) used a version of the pressure-based model to account for variations in the oxygen partial pressure along the length of the MABR fiber. Guglielmi et al. 2020 developed an exhaust oxygen-based model to monitor the key performance indicator OTR, which correlated with the ammonia removal rate in the biofilm. Even though both modeling methods have been used in commercial MABR applications, each is associated with biases. For the pressure-based model, the oxygen concentration at the base MAB significantly influences the oxygen transfer fluxes through the membrane into the biofilm, but the measurement of the oxygen concentration in the base layer can be difficult in practical applications (Houweling and Daigger 2019). On the other hand, current exhaust oxygen-based models ignore nitrogen gas diffusion across the membrane into the biofilm, and because of that, the predicted OTEs may be underestimated (Houweling and Daigger 2019). More detailed oxygen transfer models can undoubtedly be formulated and developed. Still, the benefits of the resulting more complex models need assessments relative to the needs for various modeling objectives.

To date, most MABR models are one-dimensional (1D), which has limitations to reflect the biological processes in MABs accurately. Non-uniform distribution of the DO concentration, microbial composition, and biofilm characteristics along the membrane fibers of the MABR poses a significant challenge for accurately modeling MABRs. An MABR model excluding the longitudinal heterogeneity of the biofilm may lead to biased evaluation of N_2O production (Chen et al. 2020) and nitrogen removal (Acevedo and Lackner 2019). To account for the longitudinal heterogeneity of the MAB, dynamic and multi-dimensional models are needed. Schraa et al. 2018 developed a dynamic MABR model that predicted the performance of a pilot-scale MABR system for 220 days under dynamic operational conditions. The dynamic MABR model allowed

non-uniform biofilm geometries so that a fixed thickness did not constrain the predicted biofilm thickness. In addition, a two-dimensional (2D) model was developed to simulate autotrophic denitrification in a spiral wound MBfR (Martin et al. 2013). The results highlighted the importance of using multi-dimensional models to capture the uneven biofilm thickness and density along the membrane. However, dynamic and multi-dimensional models increase modeling complexity, resulting in outstanding computational efforts (Wanner et al. 2006). Thus, it is essential to consider if a complex multi-dimensional model is necessary or whether a simplified model could answer the same question.

Extracellular polymeric substances (EPS) are fundamental constituents of the biofilm structure (Kreft and Wimpenny 2001). To date, few models have explicitly defined the role played by the EPS matrix in MABs (Boltz et al. 2017). Hu et al. 2020 reported that EPS production in a pure biofilm MABR system for phenol degradation was mediated by quorum-sensing systems. Production of EPS in Hybrid MABR/AS processes might be different from that in pure biofilm systems, but a systematic understanding is still lacking (SI). Further research needs to characterize EPS production in pure biofilm and hybrid MABR applications examining factors such as gene expression, impacting factors, and production rates.

Another knowledge gap is the need to implement dynamic detachment to predict the effects of air scouring in layered MABR models. Biofilm detachment typically is modeled by detaching the outermost biofilm layer, but in reality, not just the outer layer leaves from the biofilm (Petrova and Sauer 2016). A relevant question is the movement of microbial species within the biofilm, which affects their net retention in the process. Aerobes enriched in the inner layers are likely to move to outer layers, and in this case, air scouring can lead to detachment of nitrifiers. In addition, inner layers of the biofilm can also slough off due to structural weaknesses resulting from voids and cell dispersion (Petrova and Sauer 2016; Aybar et al. 2019; Kim et al. 2020). Considering these factors during model development is important to improve accuracy and reduce biases, but they also

increase model complexity and runtimes. Research questions also remain concerning how to model microbial behaviors and how to validate such models.

2.5 Performance assessment

2.5.1 Biological carbon and nutrient removal

MABRs are a competitive alternative for process intensification in water resource recovery facilities (WRRFs) to treat greater substrate loads and achieve higher effluent qualities without additional footprint (Kunetz et al. 2016). **Error! Reference source not found.** summarizes the r eported NRs and carbon removal rates from the selected pilot- to full-scale studies. MABRs enable high NRs in the biofilm, which is beneficial for plants to achieve effective ammonia removal. A pilot plant in Ontario, Canada using the Zeelung Hybrid MABR/AS process reported an NR of 2.6 g N/m^2-d in the biofilm (Peeters et al. 2017). Similarly, the full-scale spirally-wound hybrid MABR achieved an average NR of 3.1 g N/m^2-d in the biofilm (Nathan et al. 2020). In fact, NRs in Hybrid MABR/AS systems were generally within the range of 1-3 g NH_4^+-N/m^2-d (**Error! Reference source not found.**). In comparison, a typical NR in Hybrid MBBR/AS system is 0.5 g N/m^2-d (Houweling and Daigger 2019).

A tradeoff also exists between TN and ammonia removal, and higher COD/N ratios in the influent favor TN removal but reduce NRs. Nitrification products in the hybrid MAB are exported to the bulk liquid where nitrate and nitrite are consumed together with the biodegradable organic matter by the suspended heterotrophic biomass (Downing et al. 2008). As discussed in section 2, the hybrid process represents an effective approach to reduce the competition between heterotrophs and nitrifiers, which can explain the consistent and stable nitrification performance observed in various hybrid systems (Downing and Nerenberg 2008). NRs in pure biofilm systems (e.g., one-stage MABRs) can vary significantly depending on influent wastewater characteristics. As ammonia and biological organic carbon are metabolized together in the biofilm, it is commonly

observed that the NRs in pure biofilm systems are more susceptible to the influent COD/N. At high COD/N ratios, AOBs can be outcompeted by heterotrophic bacteria, while at low COD/N ratios, nitrification would proceed but the availability of electron donors can limit denitrification. Therefore, the relative concentrations of ammonia and biodegradable organic carbon are critical for SND in pure biofilm systems. A former study reported that a COD/N ratio of 4 was optimal for SND in an one-stage MABR (LaPara et al. 2006), but COD/N ratios and biodegradability of the given carbon source in different applications vary greatly. In this case, more elaborated biofilm and oxygen control strategies are needed to develop the desired stratification in pure biofilm systems.

The Hybrid MABR/AS process is a typical configuration to intensify biological carbon and nutrient removal in plants. Incorporating MABRs in the unaerated zones creates an aerobic condition in the biofilm for nitrification, and the produced nitrate is released into the anoxic bulk liquid where the suspended biomass performs denitrification for complete nitrogen removal (Houweling et al. 2017). The SND pathway has been well-demonstrated in pilot-scale testing (Kunetz et al. 2016; Peeters et al. 2017) and full-scale applications (Houweling et al. 2017; Underwood et al. 2018; Nathan et al. 2020). Nathan et al. 2020 reported that 97% of the ammonia removed in the MABR zone was denitrified in the same tank. In 2017, an Oxymem MABR was installed on-site to expand the capacity of its aerobic lagoons (Heffernan et al. 2017). The hybrid MABR system facilitated SND in a single bioreactor, removing of 85% for total COD, 88% for ammonia, and 68% for TN (effluent quality: 44mg/L total COD and 16 mg/L TN). The SND facilitated by hybrid MABRs increases treatment capacity within a given tank volume, which, combined with significant energy savings, makes the hybrid MABR a promising alternative for process intensification.

Table 2-2 Process intensification performance in MABR applications.

Configuration	Wastewater type	Membrane type	Influent wastewater	MABR unit HRT (hrs)	NR (g N/m^2-d)	Carbon removal (%)	Suspended growth SRT (d)	Reference
One-stage MABR	Municipal landfill leachate, Ireland	Dense polydimethylsiloxane (PDMS) membrane	sCOD: 1000-3000 mg/L, NH_4^+-N: 500-2500 mg/L	108-156	1.0-1.59	Effluent sCOD: 200-500 mg/L	NA	(Syron et al. 2015)
One-stage MABR	Municipal wastewater with industrial loads, Ontario, Canada	OxyMem MABR PDMS membrane	sCOD/NH_4^+-N: 9.2-21.5	5.2-18	0.24-0.60	26-64 % sCOD removal	NA	(Bicudo et al. 2019)
One-stage MABR	Municipal wastewater PE+RAS, North America*	ZeeLung MABR dense membrane	NA	0.38	2.2	NA	NA	(Houweling et al. 2017)
One-stage MABR	Municipal wastewater sidestream, Israel	Fluence MABR membrane	NH_4^+-N: 250 mg/L	NA	6-7	NA	NA	(Shechter et al. 2020)

Hybrid MABR in the anoxic zone in the A^2O process	Municipal wastewater, Israel	Fluence MABR membrane	sCOD/NH_4^+-N: 10.1	NA	1.3-5.5, average: 3.1	NA	NA	(Nathan et al. 2020)
Hybrid MABR in the anoxic zone in the A^2O process	Municipal wastewater, Ontario, Canada	ZeeLung dense MABR membrane	sCOD/NH_4^+-N: 0.96-5	7.5	1.2-2.6	77.5 % sCOD removal	4-8	(Peeters et al. 2017)
Hybrid MABR in the anoxic zone in the A^2O process	Municipal wastewater, USA	ZeeLung MABR dense membrane	BOD_5/ NH_4^+-N:5.6	NA	Average: 1.6 Peak: 3	42% filtered BOD_5 removal	10	(Kunetz et al. 2016)
Hybrid MABR in the anoxic zone in the A^2O process	Municipal wastewater, USA	ZeeLung MABR dense membrane	BOD/ NH_4^+-N:9.3	0.32	2.36	Not reported	10-12	(Underwood et al. 2018)
Hybrid MABR in the anoxic zone in the A^2O process	Municipal wastewater, USA	ZeeLung MABR dense membrane	BOD_5/ NH_4^+-N:8.4	0.32	2.1, up to 3.1	Not reported	12	(Guglielmi et al. 2020)

Hybrid MABR in the anoxic zone in the MLE process	Municipal wastewater, Sweden	ZeeLung MABR dense membrane	sCOD: 30-120 mg/L, NH_4^+-N: 10-22 mg/L	2.4-3.6	0.37-5.93	56.66 % sCOD removed	12-14	(Li 2018)
3-stage Hybrid MABRs in the anoxic zone in the MLE process	Municipal wastewater, Canada	ZeeLung MABR dense membrane	sCOD/NH_4^+-N: 0.23-1.35	7.5	1-3	NA	7.5	(Côté et al. 2015)

Hybrid MABR/AS processes can be operated at a lower suspended growth SRT than conventional AS systems, which translates into potentially lower footprints and reduced construction costs (Houweling and Daigger 2019; Carlson et al. 2021). A pilot Hybrid MABR/AS system at the Hayward Water Pollution Control Facility achieved 25%-30% TN removal at a low SRT of 1.5 days, typically too short for nitrogen removal in conventional AS systems (Sathyamoorthy et al. 2019). Researchers hypothesized that the ability to nitrify at a low SRT (usually below the washout SRT of nitrifiers) in the Hybrid MABR/AS system was due to the seeding effect from the MABR media, which supplemented nitrifying populations in the suspended biomass (Sunner et al. 2018). This theory has been validated in a comparative study where the downstream bioreactor, seeded by the MABR, fully nitrified at an SRT below the washout SRT of nitrifiers (Houweling et al. 2018). Process modeling in the same study further identified that the fraction of ammonia removed in the biofilm and the sloughed yield of nitrifiers from the biofilm were the most significant influencing factors for the seeding effect. Similarly, Houweling et al. 2017 demonstrated the robustness of the hybrid process at an SRT less than five days under diurnal loading variations: with a peak loading factor of 1.9 and an influent ammonia concentration of 5-30 mg/L, the effluent ammonia was less than 1 mg/L 45% of the time and less than 2 mg/L 94% of the time.

Biological nitrogen removal processes can be a significant source of the potent greenhouse gas N_2O (Conthe 2019; Duan et al. 2021). In MABRs where ammonia and oxygen diffuse into the biofilms from opposite directions, N_2O formation mainly occurs in the inner biofilm portion by AOBs via the hydroxylamine oxidation pathway (Kinh et al. 2017; Sabba 2018). In addition, heterotrophic denitrifiers via the incomplete denitrification pathway may also contribute N_2O production in the transition zone from aerobic to anoxic within the MAB (Pellicer-Nàcher et al. 2010). This occurs because the NOS enzyme that reduces N_2O to N_2 can be selectively inhibited by oxygen (Morley et al. 2008). However, compared to co-diffusional biofilm reactors, significantly less N_2O emissions and accumulation in the biofilm-liquid interface have been

observed in MABRs, due to the adjacent positions of the N_2O formation and degradation zones (Kinh et al. 2017). A former study indicated that heterotrophic bacteria, e.g., *Thauera* and *Rhizobium*, could reduce the N_2O produced in the inner biofilm layers (Kinh et al. 2017).

To date, several conditions are known to promote N_2O formation in the biological nitrogen removal process: 1) low or fluctuating DO concentrations, which leads to nitrite reduction by AOBs, 2) high nitrogen loadings that lead to the greater formation of intermediates (e.g., hydroxylamine and nitrite); or 3) limited carbon sources which lead to incomplete denitrification (Sabba 2018). Even though MABRs can mitigate N_2O emissions compared to conventional biofilm reactors, some N_2O produced in the MAB can still be stripped into the gas lumen and release into the air if operated in the flow-through aeration mode (Kinh et al. 2017). A question is whether the exhaust gas stream can be practically captured and the N_2O contained in it can be controlled.

EBPR occurs in Hybrid MABR/AS systems where an additional anaerobic zone is added prior to the anoxic MABR zones (Sathyamoorthy et al. 2019). A benefit of performing EBPR in a Hybrid MABR/AS system is that the SND in the MABR zone can decrease nitrate return to the anaerobic zone and reduce its interference with PAO activities. Robust EBPR activity was observed in a full-scale Hybrid MABR/AS process in Yorkville, IL with an average effluent total phosphorus (TP) concentration of 0.49 mg/L (Underwood et al. 2018). The same study reported that the SND in the MABR decreased the nitrate return to the anaerobic zone and reduced its interference with EBPR. Similarly, the pilot Hybrid MABR/AS in the O'Brien Water Reclamation Plant showed that a TP limit of 1 mg-P/L could be sustained with existing plant infrastructure (Kunetz et al. 2016). In addition, a pilot plant study at the Ekeby WWTP (Eskilstuna, Sweden) recorded a >65% removal of TP without the use of coagulants or a well-defined anaerobic zone, despite phosphorus removal being an auxiliary design objective (Li 2018). Overall, phosphorus removal has been observed in MABRs, but it is still an underdeveloped topic in MABR systems. More research needs to investigate the conditions under which optimal EBPR can occur and the effects of MABRs on both PAO and DPAO activities.

2.5.2 Autotrophic nitrogen removal

Autotrophic nitrogen removal via anammox microorganisms is an emerging application of MABRs. Lab-scale studies using synthetic feed have demonstrated the feasibility to achieve PN/A via an one-stage MABR where AOB are abundant in oxygen-rich layers close to the lumen while anammox bacteria are located in the anoxic zone closer to the bulk liquid (Gong et al. 2007; Augusto et al. 2018; Pellicer-Nàcher et al. 2014). In a recent lab-scale study, an one-stage MABR was used to treat municipal wastewater under mainstream conditions (Bunse et al. 2020). Under low ammonia and COD concentrations (31-120 mg N/L, 7-230 mg sCOD/L), the MABR achieved an average ammonia removal rate of 2.3-3.6 g N/m^2-d and a TN removal rate of 1.2 g N/m^2-d. Excellent nitrogen removal by MABRs performing PN/A was also observed in a recent pilot treating digestate from the side stream of a WRRF (Coutts et al. 2020). This pilot achieved an ammonia removal rate of 5.5 g N/m^2-d and a TN removal rate of 4.4 g N/m^2-d. Overall, MABRs performing PN/A show good performance and considerable energy savings (energy consumption of 0.4 kWh/kgN (Coutts et al. 2020). However, excessive growth of NOBs and nitrate build-up are challenges for PN/A (Lackner et al. 2014). Online monitoring and control will be critical to ensuring process resilience and optimization of MABRs performing PN/A.

Previous studies confirmed the coexistence of anammox bacteria, AOB, NOB, and heterotrophic bacteria in PN/A MABRs (Gong et al. 2007; Ma et al. 2017; Zhao et al. 2021). Because of the complex microbial community and competing reactions, the manipulation of operational parameters is critical to creating an environment for the anammox bacteria's optimal growth. For instance, anammox bacteria are sensitive to DO levels, and the presence of oxygen also promotes NOB growth and competition for nitrite, hampering PN/A performance (Strous et al. 1997; Kuenen 2008). Too little oxygen, on the other hand, limits AOB growth, leading to insufficient nitrite production (Cema et al. 2011). Therefore, oxygen mass transfer is a key factor that determines the success of PN/A.

In MABRs, transmembrane gas pressure is often manipulated to control oxygen transfer (Gong et al. 2007; Zhao et al. 2021). Wang et al. 2016 reported that an increase in transmembrane gas pressure from 2 to 5 kPa increased nitrite accumulation from 2.8 to 7.4 mg/L, indicating successful suppression of NOBs. However, a further increase to 20 kPa resulted in excessive oxygen supply and unwanted full nitrification. Nevertheless, control of the transmembrane gas pressure may not be suitable to sustain nitritation in long-term operation because of the accumulation of *K*-strategist NOBs, such as *Nitrospira*, under continuous low DO conditions (Gilmore et al. 2013; Gilbert et al. 2014). Therefore, intermittent aeration is commonly used in MABRs as a long-term solution to suppress NOBs (Pellicer-Nàcher et al. 2014; Ma et al. 2017). Pellicer-Nàcher et al. 2014 observed a considerable decrease in NOB-related 16S rRNA gene abundance and a considerable increase in anammox 16S rRNA gene abundance, when intermittent aeration was implemented in a one-stage MABR. Additionally, the ZeeNAMMOX process reversed the vertical oxygen supply direction in the MABR lumen periodically to switch the DO limited condition from top to bottom, suppressing NOB growth by periodic exposure to anoxic conditions (Long et al. 2020). As was indicated by the ratio of nitrate generation to ammonia oxidation of 0.2, which is relatively close to the stoichiometric ratio for PN/A (0.11) (Strous et al. 1998), the pilot ZeeNAMMOX process achieved excellent NOB suppression, and the specific total inorganic nitrogen (TIN) removal rates reached 6-10 g N/m^2-d. Overall, management of oxygen in the MABR lumen is critical to enrich AOBs and anammox while selectively suppressing NOBs. Achieving stable nitritation by manipulating the oxygen availability in long-term operation is still challenging, and further research needs to optimize the aeration intermittency and duration.

Ammonia loading is another critical factor that affects PN/A in MABRs. Although free ammonia (FA) and nitrite are essential substrates for anammox processes, high concentrations of FA and nitrite can be toxic and inhibitory to anammox activity (Cho et al. 2019). Lackner et al. 2014 reported that a higher availability of nitrite (higher than 0.07 g N/L) at the startup stage can interrupt anammox growth. Increased ammonia loadings have also been shown to complicate

process operation and control, as the oxygen flux is typically increased proportionally to the increase in ammonia loading to ensure sufficient ammonia oxidation, which may pose problems to the microbial community. For example, in a one-stage MABR system fed with synthetic wastewater, increasing the ammonia loading rate from 50 to 100 g N/m^3d under the same DO condition resulted in a drop in the TN removal efficiency from 84% to 69% (Augusto et al. 2018). Decreased removal performance was attributed to the increased airflow with DO spikes under the increased nitrogen loading, which might have allowed NOBs to proliferate. Although it may be advantageous to perform PN/A in counter-diffusional MABs because of the independent control of oxygen and ammonia availability, advanced monitoring and control strategies must be applied to keep the balance.

Low DO concentrations favored by the PN/A process are also conducive to the unwanted formation of N_2O (Ma et al. 2017). Compared to SND MABRs, more N_2O can be potentially produced in PN/A MABRs where DO limiting conditions are intentionally created to suppress NOB growth. However, as discussed in section 5.1, MABRs emit and accumulate less N_2O at the biofilm-liquid interface, which is likely due to the adjacent positions of the N_2O formation and degradation zones (Wang et al. 2016; Kinh et al. 2017). Similar to biological nitrogen removal via SND, N_2O in PN/A MABRs may derive predominantly from AOBs in the inner MAB (Pellicer-Nàcher et al. 2010; Gilmore et al. 2013). Besides hydroxylamine oxidation via AOBs, N_2O may also be produced by nitrite reduction during denitrification (Khalil et al. 2004). Overall, avoiding simultaneous low DO and high nitrogen loadings in PN/A MABRs is vital for minimizing N_2O formation (Sabba 2018). In this case, one-stage MABRs with continuous nitrite consumption under low DO conditions should have a lower N_2O footprint than two-stage MABRs, which requires a significant nitrite residual conveyed to the separate anammox reactor. However, N_2O formation is a complex process that involves multiple microbial groups, and factors that influence the N_2O formation in PN/A MABRs are not always intuitive. Future investigations need to characterize the production and mitigation mechanisms in MABRs performing the PN/A process.

2.5.3 Space-based wastewater treatment

Federal programs have assessed MABR technology into low or no-gravity wastewater treatment applications over the last two decades at both pilot- and full-scale (Morse et al. 2004; Chen et al. 2008; Christenson et al. 2018). It is envisioned that MABRs could provide unique benefits to the closed-loop recycling of wastewater to potable water in missions outside of Earth, including the upcoming Artemis program destined for Earth's moon. At a fundamental level, the mechanism of oxygen delivery used by MABRs avoids one of the significant pitfalls of conventional aeration in an environment without gravity: bubbles. Since oxygen transfer from the membrane is driven by a concentration gradient, microbial growth can occur in both micro-gravity (e.g., Lunar or Martian) or reduced gravity conditions (Jackson et al. 2009; Landes et al. 2021).

MABR design and operation can enhance health and safety, logistics, and functionality in non-terrestrial systems. The integration of MABRs would minimize the use of toxic chemicals, which are typically used to pretreat the high concentrations of urea and ammonia in space-based wastewater. Historical pilot studies conducted by Chen et al. 2008 and Jackson et al. 2009, using a carbon limited and nitrogen dominant wastewater at small loading rates that reflect the characteristics of a space mission, suggested promising SND with ammonia and COD removal efficiencies up to 90%. When a full-scale MABR (the Counter-diffusion Membrane Aerated Nitrifying and Denitrifying Reactor or CoMANDR) was designed for integration with critical water recovery systems, the unit achieved 90% carbon oxidation and 60% nitrification efficiencies at a hydraulic residence time of approximately 3 days (Christenson et al. 2018). Furthermore, the system was tested during a separate "hibernation" phase and rapid startup to regular operation, where necessary systems were shut off for nearly a month and then returned to normal system feed, which are typical during space missions. Christenson et al. 2018 found that the CoMANDR system could recover quickly after hibernating for almost a month and was well-suited as an upstream treatment step in a water recovery scheme. In a most recent lab-scale study, the MABR was designed to treat synthetic space-based wastewater with limited total organic carbon (TOC) and

concentrated ammonia (TOC/N<1) (Landes et al. 2021). Successful SND was observed in this study with a TN removal efficiency of 36.5% and removal rate of 0.24 g N/ m^2-d.

The uniqueness of this application of MABR technology creates an opportunity for continuing research. The small number of crew on space missions limits the hydraulic loading on the system, allowing for batch systems to be a possibility. However, in contrast to municipal wastewater, the low COD/N ratio (<2) in space-based wastewater hampers denitrification, as stoichiometric limitations are shown to be major obstacles in MABR application (Landes et al. 2021). Finally, the effluent produced from an MABR used in a non-terrestrial application must be of the highest quality and readily compatible with downstream treatment processes for potable water generation.

2.5.4 High-strength industrial wastewater and xenobiotics biotreatment

MABRs are advantageous to treat high-strength, industrial wastewater due to their high OTEs and OTRs, tolerance of high salinity, ability to degrade intermediates in multiple redox gradient zones, and minimized stripping of volatile organic compounds (VOCs) (Quan et al. 2018; Tian et al. 2020; Hu et al. 2020). A lab-scale MABR system treating synthetic high-strength swine wastewater (4500 mg COD/L,4000 mg TN/L) achieved 96% COD removal and 83% TN removal at removal rates of 5.8 g COD/m^2-d and 4.5 g N/m^2-d (Terada et al. 2003). A similar COD removal rate (6 g COD/m^2-d) was reported in a pilot-scale MABR system treating a synthetic high-strength industrial wastewater (4700 mg COD/L, 145 mg TKN/L). Even though a low NR of 0.04-0.09 g N/ m^2-d was reported in this pilot due to the high COD/N ratio, 76%-85% of the nitrite and nitrate produced were immediately denitrified, with an overall denitrification efficiency of 94%.

MABRs are beneficial to treat xenobiotics because that MABs can sustain substrate degradation rates from industrial wastewater loads, as the microbes embedded in the biofilm are protected by the outer EPS matrix (Abdelfattah et al. 2020). Specifically, McLamore et al. 2010 analyzed the cellular stress response of a counter-diffusional MAB under increasing loadings of

toxins. The study found that exposure to higher concentrations of toxins led to increased oxygen and proton flux into the biofilm, which might be a defense mechanism for survival.

A number of laboratory studies have investigated the degradation of xenobiotics with MABRs, including fluorinated organics (Heffernan et al. 2009; Misiak et al. 2011), phenolic compounds (Tian et al. 2019; Mei et al. 2019; Tian et al. 2020), dyes (Wang et al. 2012), and organonitrile compounds (Li and Liu 2019). Figure 2-4 illustrated the treatment performance of those MABR studies. Tian et al. 2019 used a two-stage MABR system for *o*-aminophenol and nitrogen removal. The effective removal of *o*-aminophenol in the first MABR (removal rate of 17.6 g/m^2-d) mitigated the inhibitory effect of xenobiotics on the nitrifiers, and therefore good nitrogen removal efficiency of 90% was achieved in the second MABR. A single MABR used to treat multiple phenolic compounds achieved a removal rate of 8.9 g/m^2-d for total phenolics (Tian et al. 2020). In a separate study, an acetonitrile (ACN) removal efficiency of 98% was achieved in an one-stage MABR with an hydraulic residence time (HRT) of 6 h, which corresponded to an ACN removal rate of 3.63 g/m^2-d (Kunlasubpreedee and Visvanathan 2020). Besides the application for single contaminant removal, another research team reported the capability of an MABR system to treat a complex pharmaceutical wastewater mixture with 90% COD removal and 98% ammonia removal (Wei et al. 2012). Overall, both one- and two-stage MABR applications achieved good removal efficiencies of industrial pollutants. Their demonstrated resilient performance opens the possibility of applying MABRs to treat more emerging pollutants, and such potential applications need further investigation.

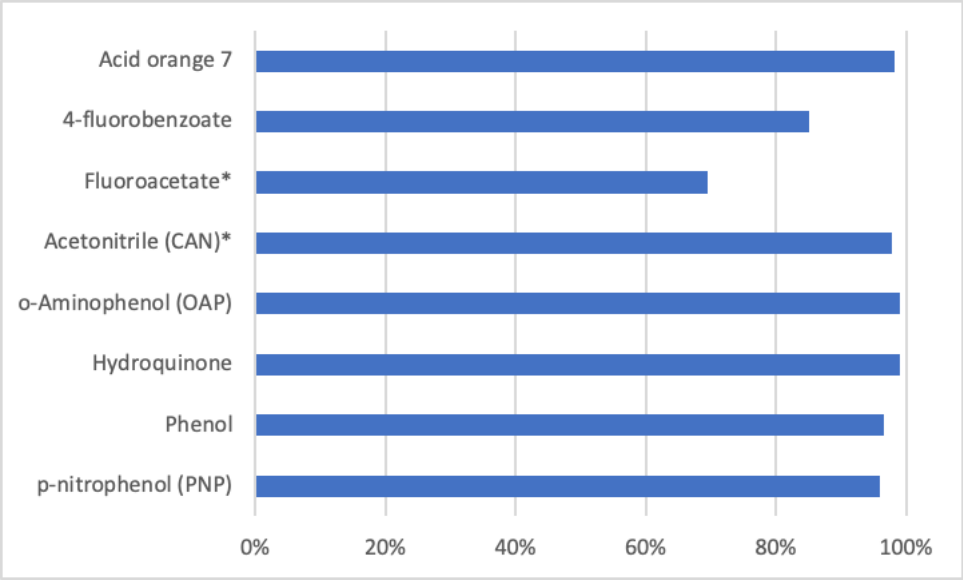

Figure 2-4 Average removal efficiency of MABRs for xenobiotics bioremediation. * indicated optimal removal efficiency rather than average removal efficiency

A long SRT operation is usually necessary to develop sufficient biomass for industrial compounds removal because of their low biodegradability and inhibitory effects. As a result of the long SRT, a thicker biofilm is likely to develop (SI). In addition, the high-strength industrial wastewater is associated with high organic carbon loading rates, and thereby supplying pure oxygen into MABRs may be beneficial to improve COD removal efficiency. As was discussed in section 2.3, thicker biofilms also grow under high loadings and pure oxygen feed. All these factors may lead to an excessively biofilm accumulation that is prone to mass transfer resistance issues that decrease the activity of the biofilm. Stricker et al. 2011 reported that intermittent air sparging failed to control the biofilm thickness in an MABR treating high-strength industrial wastewater, leading to performance upset. An explanation was that, after air scouring events, the promoted mass transfer in the thinner biofilm resulted in faster diffusion of the highly concentrated substrates and quick accumulation of biomass. Therefore, more aggressive and continuous air scouring may be needed for biofilm thickness control in MABRs for high-strength industrial wastewater treatment. Still, investigations are required to understand biofilm responses to such events.

2.5.5 Sulfur recovery

MABR technology represents an efficient aerobic method to deliver oxygen directly into the biofilm formed by sulfide-oxidizing bacteria (SOB) (Sun et al. 2017). The complete oxidation of sulfide to sulfate is a favored metabolism for SOB as the process yields more energy compared to the partial oxidation of sulfide to elemental sulfur, and thereby the successful operation of biological elemental sulfur recovery relies on a delicate balance between oxygen and sulfide availabilities to SOB to stop biological sulfide oxidation at elemental sulfur (Cai et al. 2017). The counter-diffusional geometry in MABRs is an efficient means of controlling the oxygen supply independent of sulfide availability which creates an oxygen-limiting condition that favors elemental sulfur production. A good sulfur recovery rate (> 75 %) in MABRs has been successfully demonstrated in both experimental studies and mathematical modeling by controlling the combination of membrane oxygen pressure, HRT, and sulfide loading rate (Sahinkaya et al. 2011; Sun et al. 2017).

A previous study analyzed the competition between aerobic heterotrophs and SOB for oxygen in MABRs, and the results suggested that SOB were better scavengers for low DO concentrations than heterotrophs (Sahinkaya et al. 2011). This finding was consistent with a multispecies modeling study, where SOBs outcompeted heterotrophs under low oxygen flux conditions (Jiang et al. 2019). Camiloti et al. 2019 reported that *Geovibrio*, *Flexispira*, and *Sulfurospirillum* were key functional sulfide oxidation genera in the MAB.

To summarize, MABRs are promising for sulfur recovery from wastewaters. Nevertheless, this research topic is still at its early stage, and more studies need to analyze different impacting factors, e.g. presence of VFAs and nitrate, and different aeration strategies. In addition, as the produced elemental sulfur is colloidal and hydrophilic (Cai et al. 2017), solutions are needed to efficiently separate and recover the sulfur from MABs.

2.6 Current challenges and outlook

Investigations of the first generation of commercial MABR products show that MABR processes are capable of efficient treatment of a range of pollutants (COD, N, P, xenobiotics), advantageous for resource recovery (e.g., sulfur), capable of mitigating N_2O emissions, and beneficial for carbon and energy savings. The compact size of the MABR unit makes it easy to be installed in existing facilities and intensifies treatment performance without additional footprints. The demonstrated benefits provide incentives to enhance the performance capabilities further and lower the cost of subsequent generations of commercial products. Researchers have also investigated novel combinations of MABRs with other technologies, including microbial electrolysis cells (Paepe et al. 2020) and membrane bioreactors (MBRs) (Daigger 2020). Novel bacterial-algae biofilms have also been developed in MABRs to treat wastewater of wider COD/N ratios (Zhang et al. 2021). It is foreseeable that the expanded use of MABRs and novel treatment processes will result in new research questions to be pursued, such as adequate mass transfer models, dynamic biofilm attachment/detachment, resilience design, and life cycle analysis (LCA).

Several existing challenges need ongoing research to improve future applications of MABRs. Firstly, solutions are needed to increase packing density while retaining efficient external mass transfer characteristics and avoiding solids build-up. This will lead to more compact units and further reductions in system size and cost. Secondly, a systematic understanding of functional pathways, particle attachment/detachment mechanisms, and correlation between ecology niches and operating conditions is likely to improve biofilm control and treatment performance. In addition, microbial interactions between the attached and suspended growth, including cross-feeding, competition, and biomass exchange, occur dynamically under different conditions. A holistic view of the whole community requires comparative analyses across multiple information levels (biological, chemical, physical, and mechanical) to diagnose system states and predict system performance. Thirdly, process optimization is vital to fulfilling the design objectives but remains a challenge. As MABRs have the potential to achieve simultaneous COD and nutrient removal, fundamental understanding of their mechanisms needs to be improved for operations and

configuration design compared to the conventional AS processes. Site-specific issues and treatment tradeoffs must be also considered to optimize the operational conditions.

Process control is critical to assist in the automation of MABR operation and decision-making. For this to occur, MABR models must be improved to account for dynamic spatial and physiological heterogeneity in the MAB of reasonable computational intensity. Moreover, it is challenging to decouple the interactions between biofilm and suspended biomass; therefore, the biofilm and suspended biomass in MABRs cannot be controlled independently. More advanced control approaches, such as model predictive control (MPC) (Zeng and Liu 2015) and data-driven control (Newhart et al. 2019), may be applied in future MABR studies to address the issues brought by complex interactions between biofilm and suspended biomass. In addition, artificial intelligence (AI) algorithms represent a robust alternative to control and optimize wastewater treatment processes (Zhao et al. 2020). New research in the utilization of AI in MABRs may increase the understanding of MABR operation, which could be used to improve process control.

2.7 Conclusions

MABR technology, whether operating in a pure biofilm or a hybrid process, is a promising technology for wastewater treatment. The bubble-less aeration enables higher oxygen transfer rates and efficiencies, leading to significantly reduced aeration costs. Due to the unique oxygen mass transfer scheme and microbial population stratification developed in the MAB, biomass inventory and removal fluxes are promoted within the compact MABR cassettes, intensifying the treatment capacity of existing facilities in a given reactor volume.

Studies in microbial community ecology and process models for MABRs have improved our understanding of the counter-diffusional biological process. Increased applications of MABR at pilot- and full-scales have proven that this technology is beneficial for removing a range of pollutants (COD, N, P, xenobiotics) and advantageous for resource recovery (e.g., sulfur). The unique microbial stratification can also mitigate N_2O emissions, which is an emerging issue of

concern for the BNR process. As MABR technology is rapidly evolving for wastewater treatment, conclusions at this stage are preliminary. Further research is needed to characterize microbial interactions between the biofilm and suspended growth in hybrid systems, address existing assumptions for improved MABR biofilm modeling and process control, and optimize the operational conditions that govern MABR performance.

Reference

Abdelfattah, A., Hossain, M. I., and Cheng, L. 2020 High-strength wastewater treatment using microbial biofilm reactor: a critical review. *World Journal of Microbiology and Biotechnology*, **36**5, 75.

Acevedo Alonso, V. and Lackner, S. 2019 Membrane Aerated Biofilm Reactors – How longitudinal gradients influence nitrogen removal – A conceptual study. *Water Research*, **166**, 115060.

Ahmadi Motlagh, A. R., LaPara, T. M., and Semmens, M. J. 2008 Ammonium removal in advective-flow membrane-aerated biofilm reactors (AF-MABRs). *Journal of Membrane Science*, **319**1–2, 76–81.

Akiyama, M., Crooke, E., and Kornberg, A. 1993 An exopolyphosphatase of Escherichia coli. The enzyme and its ppx gene in a polyphosphate operon. *Journal of Biological Chemistry*, **268**1, 633–639.

Arun, V., Mino™, T., and Matsuo™, T. 1988 Biological mechanism of acetate uptake mediated by carbohydrate consumption in excess phosphorus removal systems. *Water Research*, **22**5, 565–570.

Augusto, M. R., Camiloti, P. R., and Souza, T. S. O. de 2018 Fast start-up of the single-stage nitrogen removal using anammox and partial nitritation (SNAP) from conventional activated sludge in a membrane-aerated biofilm reactor. *Bioresource Technology*, **266**, 151–157.

Aybar, M., Perez-Calleja, P., Li, M., Pavissich, J. P., and Nerenberg, R. 2019 Predation creates unique void layer in membrane-aerated biofilms. *Water Research*, **149**, 232–242.

Aybar, M., Pizarro, G., Martin, K., Boltz, J., Downing, L., and Nerenberg, R. 2012 The Air-based Membrane Biofilm Reactor (MBfR) For Energy Efficient Wastewater Treatment. *Proceedings of the Water Environment Federation*, **2012**10, 5458–5485.

Baskaran, V., Patil, P. K., Antony, M. L., Avunje, S., Nagaraju, V. T., Ghate, S. D., Nathamuni, S., Dineshkumar, N., Alavandi, S. V., and Vijayan, K. K. 2020 Microbial community profiling of ammonia and nitrite oxidizing bacterial enrichments from brackishwater ecosystems for mitigating nitrogen species. *Scientific Reports*, **10**1, 5201.

Bicudo, J. R., Heffernan, B., Klassen, A., Rao, M., McConomy, J., Syron, E., and McDermott, L. 2019 "A one-year demonstration of nutrient removal with membrane aerated biofilm reactor" in WEF NNutrient Removal and Recovery Symposium 2019., 89–103.

Boltz, J. P., Smets, B. F., Rittmann, B. E., Van Loosdrecht, M. C. M., Morgenroth, E., and Daigger, G. T. 2017 From biofilm ecology to reactors: A focused review. *Water Science and Technology*, **75**8, 1753–1760.

Brannock, M., Wang, Y., and Leslie, G. 2010 Mixing characterisation of full-scale membrane bioreactors: CFD modelling with experimental validation. *Water Research*, **44**10, 3181–3191.

Brindle, K., Stephenson, T., and Semmens, M. J. 1998 Nitrification and oxygen utilisation in a membrane aeration bioreactor. *Journal of Membrane Science*.

Bunse, P., Orschler, L., Agrawal, S., and Lackner, S. 2020 Membrane aerated biofilm reactors for mainstream partial nitritation/anammox: Experiences using real municipal wastewater. *Water Research X*, **9**, 100066.

Cai, J., Zheng, P., Qaisar, M., and Zhang, J. 2017 Elemental sulfur recovery of biological sulfide removal process from wastewater: A review. *Critical Reviews in Environmental Science and Technology*, **47**21, 2079–2099.

Camiloti, P. R., Valdés, F., Delforno, T. P., Zaiat, M., and Jeison, D. 2019 A membrane aerated biofilm reactor for sulfide control from anaerobically treated wastewater. , **3330**.

Carlson, A. L., He, H., Yang, C., and Daigger, G. T. 2021 Comparison of hybrid membrane aerated biofilm reactor (MABR)/suspended growth and conventional biological nutrient removal processes. *Water Science and Technology*, wst2021062.

Carvalho, G., Lemos, P. C., Oehmen, A., and Reis, M. A. M. 2007 Denitrifying phosphorus removal: Linking the process performance with the microbial community structure. *Water Research*, **41**19, 4383–4396.

Casey, E., Glennon, B., and Hamer, G. 1999 Review of membrane aerated biofilm reactors. *Resources, Conservation and Recycling*, **27**1–2, 203–215.

Casey, E., Syron, E., and Heffernan, B. 2014 Determining biofilm thickness in a membrane supported biofilm reactor.

Castrillo, M., Díez-Montero, R., Esteban-García, A. L., and Tejero, I. 2019 Mass transfer enhancement and improved nitrification in MABR through specific membrane configuration. *Water Research*, **152**, 1–11.

Cema, G., Płaza, E., Trela, J., and Surmacz-Górska, J. 2011 Dissolved oxygen as a factor influencing nitrogen removal rates in a one-stage system with partial nitritation and Anammox process. *Water Science and Technology*, **64**5, 1009–1015.

Chen, R. D., Semmens, M. J., and LaPara, T. M. 2008 Biological treatment of a synthetic space mission wastewater using a membrane-aerated, membrane-coupled bioreactor (M2BR). *Journal of Industrial Microbiology & Biotechnology*, **35**6, 465–473.

Chen, X., Yang, L., Sun, J., Wei, W., Liu, Y., and Ni, B.-J. 2020 Influences of Longitudinal Heterogeneity on Nitrous Oxide Production from Membrane-Aerated Biofilm Reactor: A Modeling Perspective. *Environmental Science & Technology*, **54**17, 10964–10973.

Cho, S., Kambey, C., and Nguyen, V. 2019 Performance of Anammox Processes for Wastewater Treatment: A Critical Review on Effects of Operational Conditions and Environmental Stresses. *Water*, **12**1, 20.

Christenson, D., Sevanthi, R., Morse, A., and Jackson, A. 2018 Assessment of Membrane-Aerated Biological Reactors (MABRs) for Integration into Space-Based Water Recycling System Architectures. *Gravitational and Space Research*, **6**2, 12–27.

Cole, A. C., Semmens, M. J., and LaPara, T. M. 2004 Stratification of Activity and Bacterial Community Structure in Biofilms Grown on Membranes Transferring Oxygen. *Applied and Environmental Microbiology*, **70**4, 1982–1989.

Conthe, M. 2019 Denitrification as an N2O sink. *Water Research*, 7.

Côté, P., Peeters, J., Adams, N., Hong, Y., Long, Z., and Ireland, J. 2015 A new membrane-aerated biofilm reactor for low energy wastewater treatment: Pilot results. *88th Annual Water Environment Federation Technical Exhibition and Conference, WEFTEC 2015*, **6**2014, 4226–4239.

Coutts, D., Di Pofi, M., Baumgarten, S., Guglielmi, G., Peeters, J., and Houweling, D. 2020 “Side-Stream treatment with Membrane Aerated Biofilm Reactors – the Simple, Robust and Energy Efficient Path” in Helsinkin, Finland.

Daigger, G. 2020 MABR Workshop: Current Status and Emerging Applications. *IWA Biofilms 2020 Virtual Conference*.

Daims, H., Lebedeva, E. V., Pjevac, P., Han, P., Herbold, C., Albertsen, M., Jehmlich, N., Palatinszky, M., Vierheilig, J., Bulaev, A., Kirkegaard, R. H., von Bergen, M., Rattei, T., Bendinger, B., Nielsen, P. H., and Wagner, M. 2015 Complete nitrification by Nitrospira bacteria. *Nature*, **528**7583, 504–509.

Delgado Vela, J., Bristow, L. A., Marchant, H. K., Love, N. G., and Dick, G. J. 2020 Sulfide alters microbial functional potential in a methane and nitrogen cycling biofilm reactor. *Environmental Microbiology*, 1462-2920.15352.

Dick, G. 2018 *Genomic approaches in Earth and environmental sciences*, Wiley Blackwell.

Díez-Montero, R., De Florio, L., González-Viar, M., Herrero, M., and Tejero, I. 2016 Performance evaluation of a novel anaerobic–anoxic sludge blanket reactor for biological nutrient removal treating municipal wastewater. *Bioresource Technology*, **209**, 195–204.

Downing, Bibby, K. J., Fascianella, T., Esposito, K., and Nerenberg, R. 2008 The hybrid membrane biofilm process for TN removal from wastewater: Bench and pilot scale studies. *World Environmental and Water Resources Congress 2008: Ahupua'a - Proceedings of the World Environmental and Water Resources Congress 2008*, **316**, 1–10.

Downing, L. 2021 Next Generation Biofilms. *The Water Research Foundation*. https://www.waterrf.org/resource/emerging-technologies-nutrient-optimization (accessed 27 May 2021)

Downing, L. S., Bibby, K. J., Esposito, K., Fascianella, T., Tsuchihashi, R., and Nerenberg, R. 2010 Nitrogen Removal from Wastewater Using a Hybrid Membrane-Biofilm Process: Pilot-Scale Studies. *Water Environment Research*, **82**3, 195–201.

Downing, L. S. and Nerenberg, R. 2008 Effect of oxygen gradients on the activity and microbial community structure of a nitrifying, membrane-aerated biofilm. *Biotechnology and Bioengineering*, **101**6, 1193–1204.

Downing, L. S., Willoughby, A., Constantine, T., Sandino, J., Uri, N., and Nielsen, P. 2017 Applying a Disruptive Technology: Practical Considerations for the MABR at the Ejby Molle facility in Odense, Denmark. *Proceedings of the Water Environment Federation*, **2017**16, 266–271.

Downing and Nerenberg, R. 2008 Effect of bulk liquid BOD concentration on activity and microbial community structure of a nitrifying, membrane-aerated biofilm. *Applied Microbiology and Biotechnology*, **81**1, 153–162.

Duan, H., Zhao, Y., Koch, K., Wells, G. F., Zheng, M., Yuan, Z., and Ye, L. 2021 Insights into Nitrous Oxide Mitigation Strategies in Wastewater Treatment and Challenges for Wider Implementation. *Environmental Science & Technology*, **55**11, 7208–7224.

Flowers, J. J., He, S., Yilmaz, S., Noguera, D. R., and McMahon, K. D. 2009 Denitrification capabilities of two biological phosphorus removal sludges dominated by different 'Candidatus Accumulibacter' clades. *Environmental Microbiology Reports*, **1**6, 583–588.

Gao, H., Liu, M., Griffin, J. S., Xu, L., Xiang, D., Scherson, Y. D., Liu, W.-T., and Wells, G. F. 2017 Complete Nutrient Removal Coupled to Nitrous Oxide Production as a Bioenergy Source by Denitrifying Polyphosphate-Accumulating Organisms. *Environmental Science & Technology*, **51**8, 4531–4540.

Gilbert, E. M., Agrawal, S., Brunner, F., Schwartz, T., Horn, H., and Lackner, S. 2014 Response of Different *Nitrospira* Species To Anoxic Periods Depends on Operational DO. *Environmental Science & Technology*, **48**5, 2934–2941.

Gilmore, K. R., Little, J. C., Smets, B. F., and Love, N. G. 2009 Oxygen Transfer Model for a Flow-Through Hollow-Fiber Membrane Biofilm Reactor. *Journal of Environmental Engineering*, **135**9, 806–814.

Gilmore, K. R., Terada, A., Smets, B. F., Love, N. G., and Garland, J. L. 2013 Autotrophic Nitrogen Removal in a Membrane-Aerated Biofilm Reactor Under Continuous Aeration: A Demonstration. *Environmental Engineering Science*, **30**1, 38–45.

Gong, Z., Yang, F., Liu, S., Bao, H., Hu, S., and Furukawa, K. 2007 Feasibility of a membrane-aerated biofilm reactor to achieve single-stage autotrophic nitrogen removal based on Anammox. *Chemosphere*, **69**5, 776–784.

Guglielmi, G., Coutts, D., Houweling, D., and Peeters, J. 2020 FULL-SCALE APPLICATION OF MABR TECHNOLOGY FOR UPGRADING AND RETROFITTING AN EXISTING WWTP: PERFORMANCES AND PROCESS MODELLING. *Environmental Engineering and Management Journal*, **19**10, 1781–1789.

Heffernan, B., Murphy, C. D., Syron, E., and Casey, E. 2009 Treatment of Fluoroacetate by a *Pseudomonas fluorescens* Biofilm Grown in Membrane Aerated Biofilm Reactor. *Environmental Science & Technology*, **43**17, 6776–6785.

Heffernan, B., Shrivastava, A., Toniolo, D., Semmens, M., and Syron, E. 2017 Operation of a Large Scale Membrane Aerated Biofilm Reactor for the treatment of Municipal Wastewater. *Proceedings of the Water Environment Federation*, **2017**16, 285–297.

Hou, D., Jassby, D., Nerenberg, R., and Ren, Z. J. 2019 Hydrophobic Gas Transfer Membranes for Wastewater Treatment and Resource Recovery. *Environmental Science & Technology*, **53**20, 11618–11635.

Hou, F., Li, B., Xing, M., Wang, Q., Hu, L., and Wang, S. 2013 Surface modification of PVDF hollow fiber membrane and its application in membrane aerated biofilm reactor (MABR). *Bioresource Technology*, **140**, 1–9.

Houweling, D. and Daigger, G. T. 2019 *Intensifying Activated Sludge Using Media-Supported Biofilms*, CRC Press.https://www.taylorfrancis.com/books/9780429522420 (accessed 2 March 2021).

Houweling, D., Long, Z., Peeters, J., Adams, N., Côté, P., Daigger, G., and Snowling, S. 2018 Nitrifying below the "Washout" SRT: Experimental and Modelling Results for a Hybrid MABR / Activated Sludge Process. *Proceedings of the Water Envirnment Federation*, **2018**16, 1250–1263.

Houweling, D., Peeters, J., Cote, P., Long, Z., and Adams, N. 2017 Proving membrane aerated biofilm reactor (mabr) performance and reliability: Results from four pilots and a full-scale plant. *Water Environment Federation Technical Exhibition and Conference 2017, WEFTEC 2017*, **5**, 3420–3432.

Hu, Yanzhuo, Hu, Yuansen, Li, Y., Hui, M., Lu, Z., Li, H., and Tian, H. 2020 Metagenomic insights into quorum sensing in membrane-aerated biofilm reactors for phenolic wastewater treatment. *Environmental Technology*, 1–10.

Jackson, W. A., Morse, A., McLamore, E., Wiesner, T., and Xia, S. 2009 Nitrification-Denitrification Biological Treatment of a High-Nitrogen Waste Stream for Water-Reuse Applications. *Water Environment Research*, **81**4, 423–431.

Janczewski, L. and Trusek-Holownia, A. 2016 Biofilm-based membrane reactors – selected aspects of the application and microbial layer control. *Desalination and Water Treatment*, **57**48–49, 22909–22916.

Jiang, X., Xu, B., and Wu, J. 2019 Sulfur recovery in the sulfide-oxidizing membrane aerated biofilm reactor: experimental investigation and model simulation. *Environmental Technology*, **40**12, 1557–1567.

Khalil, K., Mary, B., and Renault, P. 2004 Nitrous oxide production by nitrification and denitrification in soil aggregates as affected by O2 concentration. *Soil Biology and Biochemistry*, **36**4, 687–699.

Kim, B., Perez-Calleja, P, and Nerenberg, R. 2020 Effect of predation on the mechanical properties and detachment of MABR biofilms. *Water Research*, **186**, 9.

Kinh, C. T., Riya, S., Hosomi, M., and Terada, A. 2017 Identification of hotspots for NO and N2O production and consumption in counter- and co-diffusion biofilms for simultaneous nitrification and denitrification. *Bioresource Technology*, **245**August, 318–324.

Kinh, C. T., Suenaga, T., Hori, T., Riya, S., Hosomi, M., Smets, B. F., and Terada, A. 2017 Counter-diffusion biofilms have lower N2O emissions than co-diffusion biofilms during simultaneous nitrification and denitrification: Insights from depth-profile analysis. *Water Research*, **124**, 363–371.

Konopka, A. 2009 What is microbial community ecology? *The ISME Journal*, **3**11, 1223–1230.

Kreft, J.-U. and Wimpenny, J. W. 2001 Effect of EPS on biofilm structure and function as revealed by an individual-based model of biofilm growth. *Water Science and Technology*, **43**6, 135–135.

Kristiansen, R., Nguyen, H. T. T., Saunders, A. M., Nielsen, J. L., Wimmer, R., Le, V. Q., McIlroy, S. J., Petrovski, S., Seviour, R. J., Calteau, A., Nielsen, K. L., and Nielsen, P. H. 2013 A metabolic model for members of the genus Tetrasphaera involved in enhanced biological phosphorus removal. *The ISME Journal*, **7**3, 543–554.

Kuenen, J. G. 2008 Anammox bacteria: from discovery to application. *Nature Reviews Microbiology*, **6**4, 320–326.

Kunetz, T. E., Oskouie, A., Poonsapaya, A., Peeters, J., Adams, N., Long, Z., and Côté, P. 2016 Innovative Membrane-Aerated Biofilm Reactor Pilot Test to Achieve Low-energy Nutrient Removal at the Chicago MWRD. *Proceedings of the Water Environment Federation*, **2016**14, 2973–2987.

Kunlasubpreedee, P. and Visvanathan, C. 2020 Performance Evaluation of Membrane-Aerated Biofilm Reactor for Acetonitrile Wastewater Treatment. *Journal of Environmental Engineering*, **146**7, 04020055.

Lackner, S., Gilbert, E. M., Vlaeminck, S. E., Joss, A., Horn, H., and van Loosdrecht, M. C. M. 2014 Full-scale partial nitritation/anammox experiences – An application survey. *Water Research*, **55**, 292–303.

Lan, M., Li, M., Liu, J., Quan, X., Li, Y., and Li, B. 2018 Coal chemical reverse osmosis concentrate treatment by membrane-aerated biofilm reactor system. *Bioresource Technology*, **270**, 120–128.

Landes, N., Rahman, A., Morse, A., and Jackson, W. A. 2021 Performance of a lab-scale membrane aerated biofilm reactor treating nitrogen dominant space-based wastewater through simultaneous nitrification-denitrification. *Journal of Environmental Chemical Engineering*, **9**1, 104644.

LaPara, T. M., Cole, A. C., Shanahan, J. W., and Semmens, M. J. 2006 The effects of organic carbon, ammoniacal-nitrogen, and oxygen partial pressure on the stratification of membrane-aerated biofilms. *Journal of Industrial Microbiology & Biotechnology*, **33**4, 315–323.

Li, Q. 2018 *Pilot-scale plant application of membrane aerated biofilm reactor (MABR) technology in wastewater treatment*. Master thesis, School of Architecture and The Built Environment, KTH Royal Institute of Technology, Stockholm, Sweden.

Li, T. and Liu, J. 2019 Factors affecting performance and functional stratification of membrane-aerated biofilms with a counter-diffusion configuration. *RSC Advances*, **9**50, 29337–29346.

Liu, H., Tan, S., Sheng, Z., Yu, T., and Liu, Y. 2015 Impact of oxygen on the coexistence of nitrification, denitrification, and sulfate reduction in oxygen-based membrane aerated biofilm. *Canadian Journal of Microbiology*, **61**3, 237–242.

Liu, H., Yang, F., Shi, S., and Liu, X. 2010 Effect of substrate COD/N ratio on performance and microbial community structure of a membrane aerated biofilm reactor. *Journal of Environmental Sciences*, **22**4, 540–546.

Liu, Y., Ngo, H. H., Guo, W., Peng, L., Pan, Y., Guo, J., Chen, X., and Ni, B.-J. 2016 Autotrophic nitrogen removal in membrane-aerated biofilms: Archaeal ammonia oxidation versus bacterial ammonia oxidation. *Chemical Engineering Journal*, **302**, 535–544.

Long, Z., Houweling, D., Ireland, J., Peeters, J., Coutts, D., and Reeve 2020 "ZeeNAMMOX^{TM}: Cracking the Code on Resilient and Cost-effective Side-stream Nitrogen Removal" in Innovations in process engineering 2021. Virtual.

Longo, S., d'Antoni, B. M., Bongards, M., Chaparro, A., Cronrath, A., Fatone, F., Lema, J. M., Mauricio-Iglesias, M., Soares, A., and Hospido, A. 2016 Monitoring and diagnosis of

energy consumption in wastewater treatment plants. A state of the art and proposals for improvement. *Applied Energy*, **179**, 1251–1268.

Lu, D., Bai, H., Kong, F., Liss, S. N., and Liao, B. 2020 Recent advances in membrane aerated biofilm reactors. *Critical Reviews in Environmental Science and Technology*.

Ma, C., Jensen, M. M., Smets, B. F., and Thamdrup, B. 2017 Pathways and Controls of N2O Production in Nitritation–Anammox Biomass. *Environmental Science & Technology*, **51**16, 8981–8991.

Ma, Y., Domingo-Félez, C., Plósz, B. Gy., and Smets, B. F. 2017 Intermittent Aeration Suppresses Nitrite-Oxidizing Bacteria in Membrane-Aerated Biofilms: A Model-Based Explanation. *Environmental Science & Technology*, **51**11, 6146–6155.

Martin, K. J. and Nerenberg, R. 2012 The membrane biofilm reactor (MBfR) for water and wastewater treatment: Principles, applications, and recent developments. *Bioresource Technology*, **122**, 83–94.

Martin, K. J., Picioreanu, C., and Nerenberg, R. 2013 Multidimensional modeling of biofilm development and fluid dynamics in a hydrogen-based, membrane biofilm reactor (MBfR). *Water Research*, **47**13, 4739–4751.

Martin, K., Sathyamoorthy, S., Houweling, D., Long, Z., Peeters, J., and Snowling, S. 2017 A Sensitivity Analysis of Model Parameters Influencing the Biofilm Nitrification Rate: Comparison between the Aerated Biofilm Reactor (MABR) and Integrated Fixed Film Activated Sludge (IFAS) Process. *Proceedings of the Water Environment Federation*, **2017**16, 257–265.

McLamore, E. S., Zhang, W., Porterfield, D. M., and Banks, M. K. 2010 Membrane-Aerated Biofilm Proton and Oxygen Flux during Chemical Toxin Exposure. *Environmental Science & Technology*, **44**18, 7050–7057.

Mehrabi, S., Houweling, D., and Dagnew, M. 2020 Establishing mainstream nitrite shunt process in membrane aerated biofilm reactors: Impact of organic carbon and biofilm scouring intensity. *Journal of Water Process Engineering*, **37**, 101460.

Mehrabi, S., Houweling, D., and Dagnew, M. 2021 *Single-Stage Biofilm-Based Total Nitrogen Removal in a Membrane Aerated Biofilm Reactor: Impact of Aeration Mode, HRT and Scouring Intensity*, In Review. [online] https://www.researchsquare.com/article/rs-400202/v1 (Accessed May 25, 2021).

Mei, X., Liu, J., Guo, Z., Li, P., Bi, S., Wang, Yong, Yang, Y., Shen, W., Wang, Yihan, Xiao, Y., Yang, X., Zhou, B., Liu, H., and Wu, S. 2019 Simultaneous p-nitrophenol and nitrogen removal in PNP wastewater treatment: Comparison of two integrated membrane-aerated bioreactor systems. *Journal of Hazardous Materials*, **363**September 2018, 99–108.

Misiak, K., Casey, E., and Murphy, C. D. 2011 Factors influencing 4-fluorobenzoate degradation in biofilm cultures of Pseudomonas knackmussii B13. *Water Research*, **45**11, 3512–3520.

Mooshammer, M., Kitzinger, K., Schintlmeister, A., Ahmerkamp, S., Nielsen, J. L., Nielsen, P. H., and Wagner, M. 2021 Flow-through stable isotope probing (Flow-SIP) minimizes cross-feeding in complex microbial communities. *The ISME Journal*, **15**1, 348–353.

Morley, N., Baggs, E. M., DÃ¶rsch, P., and Bakken, L. 2008 Production of NO, N2O and N2 by extracted soil bacteria, regulation by NO2− and O2 concentrations: Production of NO, N2O and N2 by extracted soil bacteria. *FEMS Microbiology Ecology*, **65**1, 102–112.

Morse, A., Jackson, W. A., and Kaparthi, S. 2004 “Biological Treatment of a Urine-Humidity Condensate Waste Stream”

Nathan, N., Shefer, I., Shechter, R., Sisso, Y., and Gordon, K. J. 2020 Start-up of a Full-Scale Activated Sludge Retrofit Using a Spirally-Wound MABR – Results and Model Evaluation.

Nerenberg, R. 2016 The membrane-biofilm reactor (MBfR) as a counter-diffusional biofilm process. *Current Opinion in Biotechnology*, **38**, 131–136.

Newhart, K. B., Holloway, R. W., Hering, A. S., and Cath, T. Y. 2019 Data-driven performance analyses of wastewater treatment plants: A review. *Water Research*, **157**, 498–513.

Nielsen, P. H., Kragelund, C., Seviour, R. J., and Nielsen, J. L. 2009 Identity and ecophysiology of filamentous bacteria in activated sludge. *FEMS Microbiology Reviews*, **33**6, 969–998.

Paepe, J. De, Paepe, K. De, Gòdia, F., and Rabaey, K. 2020 Bio-electrochemical COD removal for energy-efficient , maximum and robust nitrogen recovery from urine through membrane aerated nitrification. *Water Research*, **185**, 116223.

Peeters, J., Adams, N., Long, Z., Côté, P., and Kunetz, T. 2017 Demonstration of innovative MABR low-energy nutrient removal technology at Chicago MWRD. *Water Practice and Technology*, **12**4, 927–936.

Peeters, Jeff, Long, Z., Houweling, D., Côté, P., Daigger, G. T., and Snowling, S. 2017 Nutrient Removal Intensification with MABR – Developing a Process Model Supported by Piloting. *Proceedings of the Water Environment Federation*, **2017**3, 657–669.

Pellicer-Nàcher, C., Domingo-Félez, C., Lackner, S., and Smets, B. F. 2013 Microbial activity catalyzes oxygen transfer in membrane-aerated nitritating biofilm reactors. *Journal of Membrane Science*, **446**, 465–471.

Pellicer-Nàcher, C., Franck, S., Gülay, A., Ruscalleda, M., Terada, A., Al-Soud, W. A., Hansen, M. A., Sørensen, S. J., and Smets, B. F. 2014 Sequentially aerated membrane biofilm reactors for autotrophic nitrogen removal: Microbial community composition and dynamics. *Microbial Biotechnology*, **7**1, 32–43.

Pellicer-Nàcher, C., Sun, S., Lackner, S., Terada, A., Schreiber, F., Zhou, Q., and Smets, B. F. 2010 Sequential Aeration of Membrane-Aerated Biofilm Reactors for High-Rate Autotrophic Nitrogen Removal: Experimental Demonstration. *Environmental Science & Technology*, **44**19, 7628–7634.

Perez-Calleja, P., Aybar, M., Picioreanu, C., Esteban-Garcia, A. L., Martin, K. J., and Nerenberg, R. 2017 Periodic venting of MABR lumen allows high removal rates and high gas-transfer efficiencies. *Water Research*, **121**, 349–360.

Petrova, O. E. and Sauer, K. 2016 Escaping the biofilm in more than one way: desorption, detachment or dispersion. *Current Opinion in Microbiology*, **30**, 67–78.

Plascencia-Jatomea, R., Almazán-Ruiz, F. J., Gómez, J., Rivero, E. P., Monroy, O., and González, I. 2015 Hydrodynamic study of a novel membrane aerated biofilm reactor (MABR): Tracer experiments and CFD simulation. *Chemical Engineering Science*, **138**, 324–332.

Qi, W. K., Guo, Y. L., Xue, M., and Li, Y. Y. 2013 Hydraulic analysis of an upflow sand filter: Tracer experiments, mathematical model and CFD computation. *Chemical Engineering Science*, **104**, 460–472.

Quan, X., Huang, K., Li, M., Lan, M., and Li, B. 2018 Nitrogen removal performance of municipal reverse osmosis concentrate with low C/N ratio by membrane-aerated biofilm reactor. *Frontiers of Environmental Science & Engineering*, **12**6, 5.

Rittmann, B. E., Boltz, J. P., Brockmann, D., Daigger, G. T., Morgenroth, E., Sørensen, K. H., Takács, I., Van Loosdrecht, M., and Vanrolleghem, P. A. 2018 A framework for good biofilm reactor modeling practice (GBRMP). *Water Science and Technology*, **77**5, 1149–1164.

Rosso, D., Larson, L. E., and Stenstrom, M. K. 2008 Aeration of large-scale municipal wastewater treatment plants: state of the art. *Water Science and Technology*, **57**7, 973–978.

Sabba, F. 2018 Nitrous oxide emissions from biofilm processes for wastewater treatment. *Appl Microbiol Biotechnol*, 15.

Sahinkaya, E., Hasar, H., Kaksonen, A. H., and Rittmann, B. E. 2011 Performance of a Sulfide-Oxidizing , Sulfur-Producing Membrane Biofilm Reactor Treating Sulfide-Containing Bioreactor Effluent. , 4080–4087.

Sandt, C., Smith-Palmer, T., Pink, J., Brennan, L., and Pink, D. 2007 Confocal Raman microspectroscopy as a tool for studying the chemical heterogeneities of biofilms in situ. *Journal of Applied Microbiology*, **103**5, 1808–1820.

Sathyamoorthy, S., Tse, Y., Gordon, K., Houwelling, D., and Coutts, Daniel. 2019 “BNR Process Intensification using Membrane Aerated Biofilm Reactors” in WEF Nutrient Removal and Recovery Symposium., 527–535.

Schraa, O., Alex, J., Rieger, L., and Miletic, I. 2018 Dynamic Modeling of Membrane-Aerated Biofilm Reactors. *Proceedings of the Water Environment Federation*, **2018**16, 1297–1312.

Seviour, R. J., Kragelund, C., Kong, Y., Eales, K., Nielsen, J. L., and Nielsen, P. H. 2008 Ecophysiology of the Actinobacteria in activated sludge systems. *Antonie van Leeuwenhoek*, **94**1, 21–33.

Shanahan, J. W., Cole, A. C., Semmens, M. J., and LaPara, T. M. 2005 Acetate and ammonium diffusivity in membrane-aerated biofilms: Improving model predictions using experimental results. *Water Science and Technology*, **52**7, 121–126.

Shanahan and Semmens, M. 2015 Alkalinity and pH effects on nitrification in a membrane aerated bioreactor: An experimental and model analysis. *Water Research*, **74**, 10–22.

Shechter, R. and Dagai, L. 2018 Simultaneous Nitrification, Denitrification and Bio-P Removal in Staged Membrane Aerated Biofilm Reactors. *Proceedings of the Water Environment Federation*, **2018**16, 1321–1327.

Shechter, R., Downing, L., Gordon, K., and Nathan, N. 2020 “First Full-Scale Activated Sludge Retrofit Using a Spirally-Wound MABR: Results and Model Evaluation”

Shechter, R., Szczupak, A., and Stein, D. 2020 “High rate ammonia removal in side stream treatment with MABR: lab and pilot results” in Proceedings of the Water Environment Federation., 8.

Shiba, T., Tsutsumi, K., Ishige, K., and Noguchi, T. 2000 Inorganic Polyphosphate and Polyphosphate Kinase: Their Novel Biological Functions and Applications. , **65**3, 10.

Shoji, T., Itoh, R., Nittami, T., Kageyama, T., Noguchi, M., and Yamasaki, A. 2020 Influence of the flow velocity on membrane-aerated biofilm reactors: Application of a rotating disk for local flow control. *Biochemical Engineering Journal*, **164**, 107771.

Speth, D. R., in ’t Zandt, M. H., Guerrero-Cruz, S., Dutilh, B. E., and Jetten, M. S. M. 2016 Genome-based microbial ecology of anammox granules in a full-scale wastewater treatment system. *Nature Communications*, **7**1, 11172.

Stricker, A.-E., Lossing, H., Gibson, J. H., Hong, Y., and Urbanic, J. C. 2011 Pilot Scale Testing of A New Configuration of The Membrane Aerated Biofilm Reactor (MABR) to Treat High-Strength Industrial Sewage. *Water Environment Research*, **83**1, 3–14.

Strous, M., Heijnen, J. J., Kuenen, J. G., and Jetten, M. S. M. 1998 The sequencing batch reactor as a powerful tool for the study of slowly growing anaerobic ammonium-oxidizing microorganisms. *Applied Microbiology and Biotechnology*, **50**5, 589–596.

Strous, M., Van Gerven, E., Kuenen, J. G., and Jetten, M. 1997 Effects of aerobic and microaerobic conditions on anaerobic ammonium-oxidizing (anammox) sludge. *Applied and Environmental Microbiology*, **63**6, 2446–2448.

Sun, J., Dai, X., Liu, Y., Peng, L., and Ni, B. J. 2017 Sulfide removal and sulfur production in a membrane aerated biofilm reactor: Model evaluation. *Chemical Engineering Journal*, **309**, 454–462.

Sun, Z., Li, M., Wang, G., Yan, X., Li, Y., Lan, M., Liu, R., and Li, B. 2020 Enhanced carbon and nitrogen removal in an integrated anaerobic/anoxic/aerobic-membrane aerated biofilm reactor system. *RSC Advances*, **10**48, 28838–28847.

Sunner, N., Long, Z., Houweling, D., Monti, A., and Peeters, J. 2018 MABR as a low-energy compact solution for nutrient removal upgrades — results from a demonstration in the UK. *Proceedings of the Water Environment Federation*, **2018**16, 1264–1281.

Syron, E. and Casey, E. 2008a Membrane-Aerated Biofilms for High Rate Biotreatment: Performance Appraisal, Engineering Principles, Scale-up, and Development Requirements. *Environmental Science & Technology*, **42**6, 1833–1844.

Syron, E. and Casey, E. 2008b Model-based comparative performance analysis of membrane aerated biofilm reactor configurations. *Biotechnology and Bioengineering*, **99**6, 1361–1373.

Syron, E. and Heffernan, B. 2017 OxyMem, The Flexiable MABR. *Proceedings of the Water Environment Federation*, **2017**3, 650–656.

Syron, E., Semmens, M. J., and Casey, E. 2015 Performance analysis of a pilot-scale membrane aerated biofilm reactor for the treatment of landfill leachate. *CHEMICAL ENGINEERING JOURNAL*, **273**, 120–129.

Tan, S., Yu, T., and Shi, H. 2014 Microsensor determination of multiple microbial processes in an oxygen-based membrane aerated biofilm. *Water Science and Technology*, **69**5, 909–914.

Terada, A., Hibiya, K., Nagai, J., Tsuneda, S., and Hirata, A. 2003 Nitrogen Removal Characteristics and Biofilm Analysis of a Membrane-Aerated Biofilm Reactor Applicable to High-Strength Nitrogenous Wastewater Treatment. *Journal of Bioscience and Bioengineering*, **95**2, 170–178.

Terada, A., Lackner, S., Kristensen, K., and Smets, B. F. 2010 Inoculum effects on community composition and nitritation performance of autotrophic nitrifying biofilm reactors with counter-diffusion geometry. *Environmental Microbiology*, **12**10, 2858–2872.

Tian, H., Hu, Yanzhuo, Xu, X., Hui, M., Hu, Yuansen, Qi, W., Xu, H., and Li, B. 2019 Enhanced wastewater treatment with high o-aminophenol concentration by two-stage MABR and its biodegradation mechanism. *Bioresource Technology*, **289**June, 121649.

Tian, H., Liu, J., Feng, T., Li, H., Wu, X., and Li, B. 2017 Assessing the performance and microbial structure of biofilms adhering on aerated membranes for domestic saline sewage treatment. *RSC Advances*, **7**44, 27198–27205.

Tian, H., Xu, X., Qu, J., Li, H., Hu, Y., Huang, L., He, W., and Li, B. 2020 Biodegradation of phenolic compounds in high saline wastewater by biofilms adhering on aerated membranes. *Journal of Hazardous Materials*, **392**, 122463.

Tian, H., Zhao, J., Zhang, H., Chi, C., Li, B., and Wu, X. 2015 Bacterial community shift along with the changes in operational conditions in a membrane-aerated biofilm reactor. *Applied Microbiology and Biotechnology*, **99**7, 3279–3290.

Underwood, A., McMains, C., Coutts, D., Peeters, J., Ireland, J., and Houweling, D. 2018 Design and Startup of the First Full-Scale Membrane Aerated Biofilm Reactor in the United States. *Proceedings of the Water Environment Federation*, **2018**16, 1282–1296.

Uri, N., Constantine, T., Sandino, J., Willoughby, A., and Nielsen, P. H. 2018 Membrane-Aerated Biofilm Reactor (MABR) Demonstration at Ejby Mølle WRRF. *Proceedings of the Water Environment Federation*, **2018**5, 201–207.

Uri-Carreno, N., Nielsen, P. H., Gernaey, K., and Flores-Alsina, X. 2021 Long-term operation assessment of a full-scale membrane-aerated biofilm reactor under Nordic conditions. , **779**.

Wang, J., Liu, G. F., Lu, H., Jin, R. F., Zhou, J. T., and Lei, T. M. 2012 Biodegradation of Acid Orange 7 and its auto-oxidative decolorization product in membrane-aerated biofilm reactor. *International Biodeterioration and Biodegradation*, **67**, 73–77.

Wang, R., Xiao, F., Wang, Y., and Lewandowski, Z. 2016 Determining the optimal transmembrane gas pressure for nitrification in membrane-aerated biofilm reactors based on oxygen profile analysis. *Applied Microbiology and Biotechnology*, **100**17, 7699–7711.

Wanner, O., Eberl, H. J., Morgenroth, B., Noguera, D. R., Picioreanu, C., Rittmann, B. E., and Loosdrecht, M. C. M. 2006 *Mathematical Modeling of Biofilms*,

Wei, X., Li, B., Zhao, S., Wang, L., Zhang, H., Li, C., and Wang, S. 2012 Mixed pharmaceutical wastewater treatment by integrated membrane-aerated biofilm reactor (MABR) system - A pilot-scale study. *Bioresource Technology*, **122**, 189–195.

Wu, Y., Wu, Z., Chu, H., Li, J., Hao, H., Guo, W., Zhang, N., and Zhang, H. 2019 Comparison study on the performance of two different gas-permeable membranes used in a membrane-aerated bio fi lm reactor. *Science of the Total Environment*, **658**, 1219–1227.

Xiao, P., Zhou, J., Luo, X., Kang, B., Guo, L., Yuan, G., Zhang, L., and Zhao, T. 2021 Enhanced nitrogen removal from high-strength ammonium wastewater by improving heterotrophic nitrification-aerobic denitrification process: Insight into the influence of dissolved oxygen in the outer layer of the biofilm. *Journal of Cleaner Production*, **297**, 126658.

Xu, F., Cao, F., Kong, Q., Zhou, L., Yuan, Q., Zhu, Y., Wang, Q., Du, Y., and Wang, Z. 2018 Electricity production and evolution of microbial community in the constructed wetland-microbial fuel cell. *Chemical Engineering Journal*, **339**, 479–486.

Zeng, J. and Liu, J. 2015 Economic Model Predictive Control of Wastewater Treatment Processes. *Industrial & Engineering Chemistry Research*, **54**21, 5710–5721.

Zhang, H., Gong, W., Zeng, W., Chen, R., Lin, D., Li, G., and Liang, H. 2021 Bacterial-algae biofilm enhance MABR adapting a wider COD/N ratios wastewater: Performance and mechanism. *Science of The Total Environment*, **781**, 146663.

Zhao, B., Ma, X., Xie, F., Cui, Y., Zhang, X., and Yue, X. 2021 Development of simultaneous nitrification-denitrification and anammox and in-situ analysis of microbial structure in a novel plug-flow membrane-aerated sludge blanket. *Science of The Total Environment*, **750**, 142296.

Zhao, L., Dai, T., Qiao, Z., Sun, P., Hao, J., and Yang, Y. 2020 Application of artificial intelligence to wastewater treatment: A bibliometric analysis and systematic review of technology, economy, management, and wastewater reuse. *Process Safety and Environmental Protection*, **133**, 169–182.

Zhong, H., Wang, H., Tian, Y., Liu, X., Yang, Y., Zhu, L., Yan, S., and Liu, G. 2019 Treatment of polluted surface water with nylon silk carrier-aerated biofilm reactor (CABR). *Bioresource Technology*, **289**, 121617.

CHAPTER III

Comparative Analysis of Floc Characteristics and Microbial Communities in Anoxic and Aerobic Suspended Growth Processes

Published as:

He, H., Carlson, A. L., Nielsen, P. H., Zhou, J., and Daigger, G. T. (2022) Comparative analysis of floc characteristics and microbial communities in anoxic and aerobic suspended growth processes. Water Environment Research, **94**(12). DOI: 10.1002/wer.10822.

3.1 Introduction

Anoxic conditions (zones) are routinely incorporated in suspended growth processes for biological nutrient removal (BNR). Nitrogen removal occurs through the denitrification pathway in the anoxic zones of these processes by a mix of heterotrophic bacteria that metabolize organic carbon using nitrate, nitrite, and intermediates as electron acceptors. Fully anoxic suspended growth systems have been used to degrade xenobiotics in industrial wastewater (Bajaj et al., 2010,

Moussavi et al., 2014), and nitrate-enriched marine recirculating aquaculture wastewater (Y. Gao et al., 2020, Letelier-Gordo and Martin Herreros, 2019). These results suggested that heterotrophic denitrification can be an economically and environmentally sustainable wastewater treatment strategy compared to aerobic carbon oxidation, as it produces less biomass to be handled and eliminates aeration energy.

Although separate stage anoxic suspended growth processes exist treating a nitrified secondary effluent, fully anoxic suspended growth systems directly treating municipal wastewater are very rare. Essentially, all conventional BNR facilities incorporate aerobic zones for nitrification. Due to the slow growth rates of nitrifying bacteria, the aerobic zone usually accounts for the largest portion of the bioreactor volume in municipal wastewater treatment plants. Maintaining a large aerobic zone is not desirable, however, because it increases the extent to which influent carbon is oxidized. In fact, adding a supplemental carbon source is a common practice to maintain sufficient denitrifying activity and meet low effluent total nitrogen (TN) limits. Elimination of the aerobic zone in a suspended growth BNR process can significantly reduce the influent carbon required to meet a specified effluent TN limit, thereby reducing or eliminating the need for supplemental carbon and allowing an increased proportion of the carbon entering the wastewater treatment plant to be captured for other purposes, such as energy production (Carlson, et al., 2021, Daigger et al. 2019). More complex BNR strategies, such as biological phosphorus removal, could also benefit from aeration reduction. The activities of denitrifying polyphosphate-accumulating organisms (PAOs) under anoxic conditions have also been documented (Carvalho et al., 2007, Díez-Montero et al., 2016, Filipe and Daigger, 1999, H. Gao et al., 2017), indicating that biological phosphorus removal can also be achieved in a fully anoxic suspended growth process.

The development of hybrid membrane aerated biofilm reactor (MABR) technology in recent years provides a practical alternative to an aerated suspended growth bioreactor for nitrification. It is well demonstrated that incorporation of an appropriately sized MABR in the unaerated

suspended growth zone of activated sludge can provide additional surface area for a nitrifying biofilm to produce nitrate for subsequent denitrification in the bulk mixed liquor (He et al. 2021; Lu et al. 2020). In a computer model simulation of the hybrid BNR/MABR process treating wastewater characteristic of domestic sewage, high-quality effluents were achieved despite 98% of the total bioreactor volume being unaerated (anaerobic zone of 12%, anoxic zone of 86%), leaving a 2% aerobic zone for final polishing (Carlson et al., 2021). Energy requirements were also reduced substantially as less carbon was needed for BNR, and the oxygen needed for nitrification was transferred much more efficiently with MABR than with conventional suspended growth oxygen transfer systems.

While modeling exercises can provide proof of concept that anoxic suspended growth processes can provide significant advantages, today's state-of-the-art activated sludge mathematical models do not incorporate information on microbial composition, structure, and dynamics. These models describe the microbial community based on principal metabolisms (e.g., nitrification, denitrification), and "lump" the microorganisms into functional groups, namely ordinary heterotrophs, autotrophs, PAOs, and glycogen-accumulating organisms (GAOs) (Henze et al., 2000). Overall treatment performance is then linked to these metabolisms using mathematical equations. As biological activities of the microbial communities are the foundation for the biological transformations in suspended growth processes and directly link to the BNR performance, efforts to understand microbial composition, structure, and dynamics are critical to improving treatment processes.

Consequently, the characteristics of anoxic suspended growth biomass require further investigation to demonstrate that a viable suspended growth mixed liquor can be produced. It is unclear how the elimination of aeration would impact growth of the filamentous backbone and mixed liquor bio-flocculation. The population of filamentous organisms is often reduced in low dissolved oxygen (DO) environments (Chudoba, 1985, Gabb et al., 1991). Although some filamentous bacteria can use nitrate as the electron acceptor (B. Wang et al., 2016), it is unclear if

their growth in a fully anoxic process will be sustainable. With rare examples of fully anoxic suspended growth systems for municipal wastewater treatment, the knowledge gap must be addressed.

On-going research comparing biological phosphorus removal under aerobic versus anoxic conditions provided the opportunity to better understand the process microbiology of an anoxic suspended growth system. We combined microscopic examination, molecular techniques, and ecological models to address questions on how an anoxic alternative would differ from an aerobic counterpart in floc characteristics, microbial diversity, temporal dynamics, and community assembly processes. We hypothesized that, while a distinct microbial community structure would develop under the anoxic condition, and the anoxic suspended growth will have more heterotrophic denitrifiers, the functional structures of the anoxic and aerobic systems may be similar. We also hypothesized that the anoxic community would be less diverse and less stochastic. Our results are important to understanding the biodiversity, functioning, and management of anoxic suspended growth, which may help to facilitate wider adoption of the anoxic suspended growth process.

3.2 Materials and methods

3.2.1 Bioreactor description and operating conditions

This study was carried out in two bench-scale suspended growth sequencing batch reactors (SBRs) constructed at Ann Arbor Wastewater Treatment Plant (AAWWTP), USA. The working volume of each SBR was 6.5 L. The SBRs were inoculated with biomass from the full-scale plant and fed with the primary effluent from the plant. One SBR, identified as the anoxic bioreactor, was operated in anaerobic-anoxic cycles with external nitrate dosed in the anoxic reaction phase. DO concentrations in the anoxic bioreactor were not detected (WTW Multi 3420, WTW GmbH, Germany), and the closed mass balance of chemical oxygen demand (COD) to nitrate indicated negligible interference with oxygen in the anoxic bioreactor (data not shown). The other SBR,

identified as the control aerobic bioreactor, was operated in parallel with conventional anaerobic-aerobic cycles. Oxygen was the electron acceptor and was delivered in the aerobic reaction phase via a fine bubble air diffuser. In general, the SBR cycles included feed (5 min, 4 L of the working volume), anaerobic reaction (36.7 min), anoxic or aerobic reaction (167.8 min), waste (5 min), settle (20 min), decant (5 min, 4 L of the supernatant), and idle (0.5 min). Each SBR was provided with a stirrer (Xin Da Motor Co., LTD) with a variable speed to ensure good mixing conditions.

Monthly average SRTs of the bioreactors from December 2020 to April 2022 were illustrated in Figure B 1. SRTs were varied in the same manner as Carlson et al., 2021, to establish critical operating parameters for biological phosphorus removal. During this operational period, the mixed liquor suspended solid (MLSS) concentrations were 1,434 ± 153 mg TSS/L for the aerobic bioreactor and 1,263 ± 380 mg TSS/L for the anoxic bioreactor. The bioreactor temperature was stable at 18^{o}C.

3.2.2 Floc morphology and filaments examination

Multiple mixed liquor samples from the bioreactors were collected from March to September 2021. Following proper sample handling and staining methods (Jenkins et al., 2003), observations were made using light microscopy under direct illumination (Zeiss Axioplan EL-Einsatz, White plains, NY, USA). General floc properties (e.g., size, shape, and structure) and filament index were recorded following the protocols by Eikelboom, 2000. The circumscribing diameter was used to define the floc size (Jarvis et al., 2005), and the measurement was performed in Carl Zeiss AxioVision Rel. 4.7. Filaments which protrude from the floc were not included when establishing the circumscribing diameter. 10 flocs of each sample were randomly selected and measured to calculate the average floc size. Filamentous bacteria identification was based on both morphotypes and 16S rRNA gene sequencing data.

3.2.3 DNA extraction, PCR amplification and Illumina sequencing

A total of 42 mixed liquor samples were collected from February 2021 to April 2022 for 16S rRNA gene sequencing. All samples were stored in -80^{o}C before sequencing. DNA was extracted with the Maxwell 16 LEV blood DNA kit (Promega Corporation, WI, USA) following the modified protocol developed by Pinto et al., 2012. The prepared extractions were submitted to the University of Michigan Microbiome Core for 16S rRNA gene sequencing. Sequencing was performed on the Illumina MiSeq platform (Illumina Inc., San Diego, CA, USA) in a 500v2 Full Flow Cell. 515F/806R primers were used to target the V4 region of 16S rRNA genes (Walters et al., 2016).

3.2.4 Statistical analysis

3.2.4.1 Community composition, structure, and diversity analysis

Sequence processing and analysis were performed using Mothur (version 1.45.3) (Schloss et al., 2009), following the protocol outlined in Kozich et al. 2013. Sequences were aligned to the customized Silva database of V4 region, and sequences that did not align to the correct region were culled. A pseudo-single linkage algorithm was used to further de-noised the sequences by allowing for up to 2 differences between sequences. In the resulting sequences, chimeras were removed via the VSEARCH algorithm in Mothur (Rognes et al., 2016). The remaining quality sequences were classified with the MiDAS 4 reference database (Dueholm et al., 2022), with a threshold confidence level of 80% (Q. Wang et al., 2007). Sequences with unknown domain level of taxonomy were not included, and the rest were clustered into operational taxonomic units (OTUs) with a similarity threshold of 97%.

Statistical comparison between the anoxic and aerobic communities was performed in R (version 4.0.5). Alpha diversity indices focusing on both evenness and richness, i.e., Shannon and Simpson indices, were used to quantify microbial taxonomic diversity. Indices focusing solely on

species richness were not used in this study due to their intrinsic estimation uncertainty (Haegeman et al., 2013). The Shapiro-Wilk test revealed that the Alpha diversity indices had a non-normal distribution.

Beta-diversity analyses were performed to measure the compositional dissimilarities between samples. Two-dimensional Principle Coordinate Analysis (PCoA) plots based on the Bray-Curtis metric was created to visualize the compositional dissimilarity between communities in the two bioreactors (Schloss et al., 2009). Non-parametric analysis of molecular variance (AMOVA) was employed to determine whether the clustering within the ordinations was statistically significant ($p < 0.05$ was determined to be significant a priori) (Schloss, 2008).

3.2.4.2 Community temporal dynamics analysis

The taxa-time relationship (TTR) and core microbiome were explored to assess microbial temporal dynamics in the overall bacterial assemblage in the aerobic and anoxic suspended growth communities. TTR describes the accumulation of new taxa over time via a power law model ($S = cT^w$) and was used to assess species turnover in the microbial community. In the TTR model, S is the cumulative observed taxa, c is a constant, T is the time of observation, and w is the temporal scaling exponent which measures the relative species turnover rate (Guo et al., 2019, Meerburg et al., 2016, Wells et al., 2011). The core microbiome was determined based on the relative abundance and occurrence frequency of OTUs (Saunders et al., 2016). Three frequency thresholds were used for core members with > 0.1% relative abundance in 80% (strict core), 50% (general core), and 20% (loose core) of all samples from each bioreactor (Dueholm et al., 2022).

3.2.4.3 Community temporal assembly analysis

Two types of null model analysis were employed to disentangle the stochastic and deterministic assembly. The first one was based on the method proposed by Ning et al., 2019. Normalized stochastic ratios (NSTs) and standardized effect sizes (SESs) based on the Bray-Curtis dissimilarity metric were calculated for both the anoxic and aerobic communities. NST reflects the

contribution of stochastic processes to the community assembly relative to deterministic processes, based on magnitude rather than significance, and SES measures the significance of deterministic factors on community assembly. In the second null model analysis, a modified Raup-Crick (RC) metric was calculated using the pipeline proposed by Chase et al., 2011. Non-metric Multi-dimensional Scaling (NDMA) plots based on the modified RC metric were created to visualize the dissimilarity between samples

3.2.5 Wet chemistry analysis

Colloidal COD (cCOD) was measured as the difference between COD of the filtrates from 1.2 and 0.45 μm filters. The measurement steps followed Method 5220 A and C of Standard Methods for the Examination of Water and Wastewater, 22nd Edition (2012) (APHA, 2012). Phosphorus measurements used the ascorbic acid colorimetric method derived from Method 4500-P-E of Standard Methods for the Examination of Water and Wastewater, 21nd Edition (2005) (APHA, 2005)

3.3 Results and discussion

3.3.1 Floc morphology and potential link to cCOD removal

Microscopic examinations showed that the aerobic flocs were larger in size, stronger and more compact in structure, while anoxic flocs were smaller, less firm with internal voids, and had less filaments (Figure B 2). The discrepancy was consistent throughout the operational period at different SRTs (Table 3-1). The weaker strength was likely associated with anoxic flocs that were more susceptible to shear force, resulting in increased dispersed cells in the mixed liquor (Figure B 3). Compared to the aerobic bioreactor, the anoxic bioreactor consistently had elevated concentrations of cCOD in the effluents (Figure 3-1a). cCOD generally represents non-settleable particulate matter such as the dispersed solids noted microscopically. Those dispersed solids also

include single cells. Furthermore, incomplete flocculation of cCOD contained in the influent wastewater is often observed for systems operating at lower SRT but is more complete as the SRT increases (Grady et al., 2011, Jimenez et al., 2005), a trend which is observed for both bioreactors (Figure 3-1b).

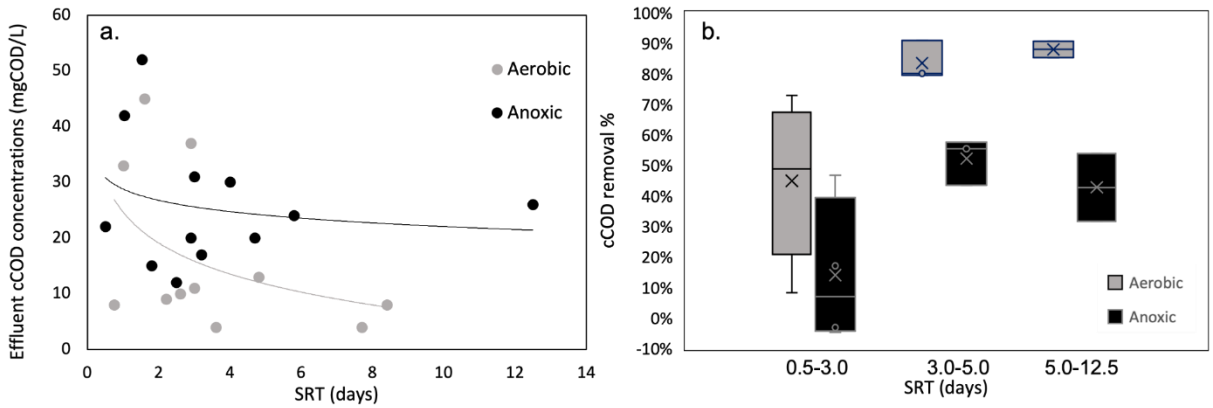

Figure 3-1 Comparison of the colloidal COD removal performance between the aerobic and anoxic bioreactors. a: cCOD concentrations in the effluents at different SRTs. b: cCOD percentage removal at different SRT ranges.

Table 3-1 Floc sizes and filamentous index of mixed liquor samples at different SRTs based on the microscopy examination

Sample type	SRT (days)	Average floc size (μm)	Filamentous index
Aerobic	3.6	240.7 ± 40.9	2.5
	4.6	241.1 ± 97.4	2.5
	10.1	265.3 ± 112.2	2
Anoxic	3.2	155.4 ± 42.7	1.5
	4.7	166.2 ± 93.5	1.5
	11.2	185.8 ± 79.6	1

3.3.2 Filamentous bacteria identification

Filamentous bacteria are essential backbones to form strong flocs needed for optimal performance. In this study, over 20 genera known to contain filamentous species were screened in the 16S rRNA gene sequencing data for both bioreactors at different SRTs (Figure 3-2). Consistent with microscopic observations, the anoxic suspended growth contained fewer filaments than the aerobic one throughout the operational period. Mean relative abundances with standard deviation (SD) of the identified filaments were 4.23 ± 2.19% in the aerobic community and 1.53 ± 0.54% in the anoxic community.

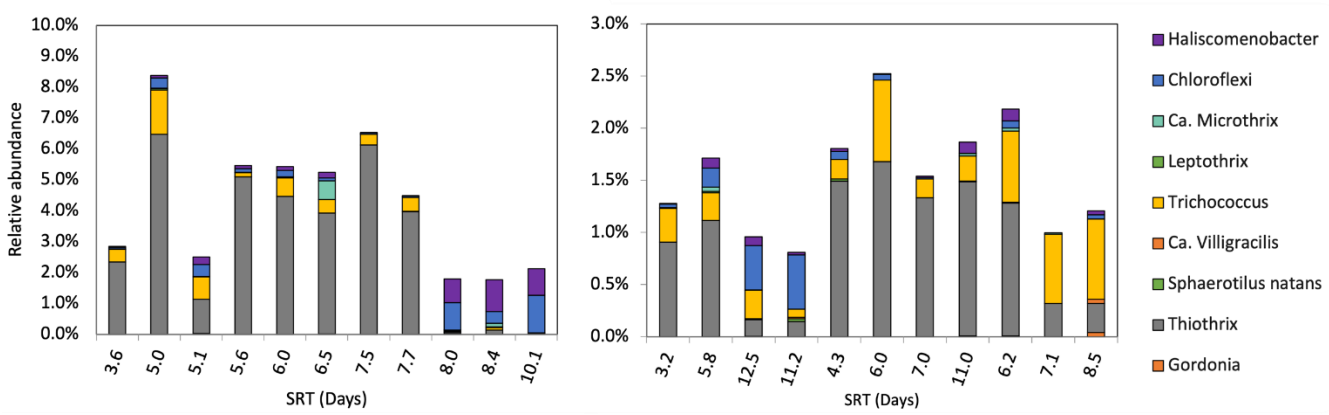

Figure 3-2 Relative abundances of known filamentous organisms in aerobic and anoxic suspended growth communities at different SRTs.

Thiothrix were predominant in both aerobic and anoxic bioreactors. *Thiothrix* are mixotrophs and can use organic acids as well as H_2S as electron donors (Ravin et al., 2021). The filamentous *Trichococcus*, possibly corresponding to the frequently observed Nostocoida limicola morphotype (Nielsen et al., 2009), were also abundant in anoxic samples. Previous study reported that *Trichococcus* were very common in the influent wastewater (Dottorini et al., 2021), which may have contributed to their high abundances in the anoxic bioreactor. *Haliscomenobacter* filament type was abundant in the aerobic samples (mean ± SD = 0.31 ± 0.38%) but less represented in the

anoxic samples (0.05 ± 0.04 %). *Haliscomenobacter* are strictly aerobic heterotrophs and their low abundance in the anoxic samples might be attributed to the immigration via the source community in the influent wastewater (Gonzalez-Martinez et al., 2016, van Veen et al., 1973).

Successful operation of AS systems requires a balanced composition of filamentous bacteria to ensure a good bio-flocculation and strong flocs. With the well-studied growth kinetics and habitats of filamentous bacteria (Chudoba, 1985, Jenkins et al., 2003, Nittami and Batinovic, 2022), identifying which filamentous bacteria can sustainably grow under anoxic conditions helps develop control strategies for anoxic suspended growth applications. For example, the Nostocoida filament type, which may translate to *Trichococcus* in this study (Nielsen et al., 2009), favors moderate to long SRTs; therefore, if excessive growth occurred, one approaching for controlling its growth is to reduce the SRT (Grady et al. 2011). However, unlike conventional AS processes where bulking and foaming are major operational problems (Eikelboom, 2000, Jenkins et al., 2003, Nittami and Batinovic, 2022), the anoxic suspended growth may face the issue of insufficient filaments and thereby easily sheared flocs. One standard approach applied in BNR systems when insufficient filaments are present is to provide a modest level of aeration in the anoxic zone to encourage the controlled growth of a modest fraction of low-DO filaments (Jenkins et al., 2003). Such a strategy could be pursued in a largely anoxic system.

3.3.3 Microbial community structure and recurring seasonal pattern

PCoA analysis showed a clear clustering of aerobic and anoxic bioreactor samples (Figure 3-3), suggesting that the anoxic and aerobic suspended growth developed distinct microbial structures (AMOVA test $p < 0.001$). Both anoxic and aerobic suspended growth communities exhibited clear seasonal cycling and potential annual reproducibility in the microbial structure. Specifically, samples collected in seasons from the first year clustered with the samples from corresponding seasons of the following year. In addition, compared to the clusters of samples collected in cold seasons, the clusters of warm season samples from one bioreactor were more distant from the

clusters of the other bioreactor, indicating that the two communities became more distinct in the warm season. Seasonal patterns have been observed in many full-scale WWTPs, and process tank temperature was generally believed to be an important factor driving community dynamics (Flowers et al., 2013, Peces et al., 2022, Roy et al., 2017). Process tank temperature was unlikely a key factor in this study, however, as both bioreactors were operated at a constant temperature year-round. Considering the suspended growth community and influent wastewater community as a unique entity, we hypothesize that the yearly variation and seasonal occurring pattern observed in the bioreactors were due to seasonal variations in wastewater characteristics and immigration via the influent microbial community, which was indeed affected by seasonal temperatures. It was likely that certain obligate aerobes and anaerobes had a narrow temperature range for their optimal growth, and their abundances in the influent peaked during warm seasons. After they were transported into the bioreactors, they thrived as a result of species sorting carried out by aerobic or anoxic operations, thereby resulting in different compositions and structure between the aerobic and anoxic communities. The observed ordination pattern may also result from alternating wet and dry seasons during the cold and warm months (Wágner et al., 2022). Seasonal rainfall events may change the strength of organic loads and nutrient levels of the influent wastewater which affected the microbial compositions. In addition, variations in the influent wastewater's composition, such as the presence of specific industrial or agricultural waste, can introduce different types of carbon and nutrients, leading to shifts in the microbial community structure and function. A detailed investigation of seasonality was not performed in this study, and future research is in need to explore the linkages between environmental variables, influent communities, wastewater characteristics, and microbial seasonal dynamic patterns.

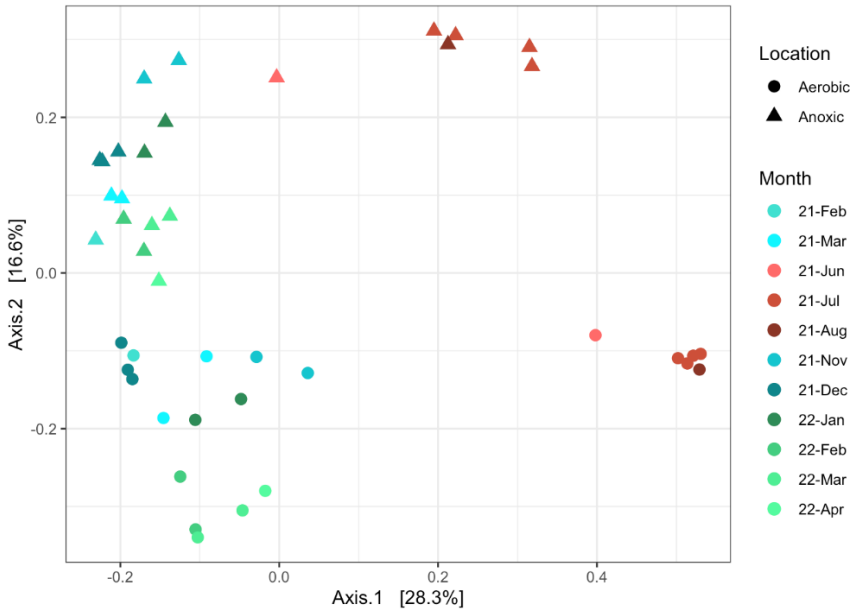

Figure 3-3 PCoA plots for the anoxic and aerobic suspended growth.

Overall, the two bioreactors used the same inoculum and received the same feed wastewater, but their microbial communities developed distinct structures. This may not be surprising, considering the apparent differences in aerobic and anaerobic metabolisms, but a detailed analysis regarding their microbial compositions (discussed in later sections) provides insight into what functional organisms appear under different conditions leading to performance optimization. Even though random processes of birth/death, speciation/extinction, and immigration can also influence community structure and lead to measurable differences (Dottorini et al., 2021, Ofiţeru et al., 2010, Zhou et al., 2013), random factors alone cannot explain the ordination pattern observed in this study. Differences between the aerobic and anoxic microbial communities were consistent over time, and their responses in different seasons were consistently distinct.

3.3.4 Microbial composition and taxonomic diversity

A total of 3,320 and 3,582 taxa in the Bacteria were found in the aerobic and anoxic communities. Subsampling at a library size of 7,537 sequences captured the majority of the richness for samples, with coverage estimation of 95.9 ± 0.5%. The two communities showed a

similar level of Alpha diversity (Shannon p = 0.45, Simpson p = 0.36) (Table 3-2). This similarity indicates that other selective forces besides electron acceptors, such as anaerobic and aerobic/anoxic cycling, plug flow-like conditions in the bioreactor, and SRTs, impacted species diversity.

Table 3-2 Diversity indices of microbial compositions in bioreactors.

	Shannon	Simpson
Aerobic	5.03 ± 0.33	0.98 ± 0.02
Anoxic	5.02 ± 0.18	0.98 ± 0.01

Both aerobic and anoxic communities were dominated by OTUs affiliated with Proteobacteria (36.80 ± 4.81% for the aerobic community; 36.09 ± 4.58% for the anoxic community), followed by Bacteroidota (28.77 ± 6.44%; 29.55 ± 3.68%) and Campylobacterota (8.84 ± 6.47%; 13.14 ± 7.39%). Proteobacteria and Bacteroidota are common predominant phyla present in municipal wastewater treatment plants (WWTPs) (Dueholm et al., 2022, Wu et al., 2019). They play a key role in nitrogen cycling and organics degradation (Nascimento et al., 2018). Other common phyla reported elsewhere, such as Actinobacteriota and Chloroflexi, showed low relative abundances in this study. Campylobacterota, which is less reported in AS studies, were abundant in both communities, especially during the cold season from November 2021 to March 2022 (11.93 ± 4.89%; 16.71 ± 5.14%)). Most of them belong to the family *Arcobacteraceae*, which can be seen as a waterborne pathogen and can cause human illness (Venâncio et al., 2022). Reasons behind their high relative abundance during the cold seasons are not clear, but previous studies suggested their presence correlates with high levels of fecal contamination (Collado et al., 2008, Lee et al., 2012).

The top abundant OTUs (mean relative abundance across the time-series samples >1%) were shown in Figure B 4. Comparison indicates that some species were with strong preference for either aerobic or anoxic conditions. The high abundance of OTU0013 (Genus: *Zoogloea*) (1.59 ±

1.66%) in the aerobic community agreed with the larger size of flocs developed in the aerobic reactor. *Zoogloea* can use both oxygen and nitrate as electron acceptors but grows faster in aerobic environments, so their proliferation in the aerobic bioreactor was logical. OTU0025, identified as the genera *Lentimicrobium*, was only abundant in the anoxic community. *Lentimicrobium* is an anaerobic bacterium, so they selectively proliferated in the oxygen-free conditions. Besides obligate organisms that were exclusive in one community over another, the anoxic and aerobic communities also shared common abundant species, i.e., OTU0001 (Genus: *Arcobacter*), OTU0002 (Genus: *Pseudarcobacter*), OTU0004 (Family: *Comamonadaceae*), OTU0003 (Genus: *Pseudarcobacter*), OTU0008 (Family: *Hydrogenophilaceae*). Those species, if growing, are likely to be process-critical species that have facultative heterotrophic denitrification capability. It is also possible that some shared abundant species were simply due to mass immigration with the influent source community (Dottorini et al., 2021). Continuous transport into the bioreactors from upstream influents, i.e., plant primary effluent, may have kept them abundant despite inactivity during the actual treatment stage. *Arcobacter*, for example, was reported among the incoming highly abundant genera in WWTPs but non-growing in the process tank (Kristensen et al., 2020).

3.3.5 Microbial community temporal dynamics

The bacterial TTR of the two communities was examined using the power law equation ($S = cT^w$) to characterize how the species changed with time. Cumulative observed OTUs were fitted to the equation to determine the steepness of the TTR slope (w), which measures the relative species turnover rate. In this study, the power law model displayed a strong fit ($R^2 > 0.97$) to the molecular characterization of community dynamics (Figure 3-4). The calculated exponent values were 0.561 for the anoxic and 0.556 for the aerobic community. Both values fell within the typical ranges reported previously (Guo et al., 2019, Hai et al., 2014, Van Der Gast et al., 2008).

TTR models have been used as informative indicators of the ability of a microbial community to support and maintain a balanced assemblage of organisms, including decreasing temporal

scaling exponents responding to increasing selective pressure (Rivett et al., 2021). Species turnover rates can be influenced by community diversity and the spatial scale of observation. Theory predicts that the decline in species turnover occurs in more diverse communities that have greater temporal stability, as was validated in previous microbial studies (Hai et al., 2014, Rivett et al., 2021). Overall, the exponent values for the aerobic and anoxic communities were remarkably close ($p > 0.05$), suggesting a similar species turnover along the time span over which the communities were observed.

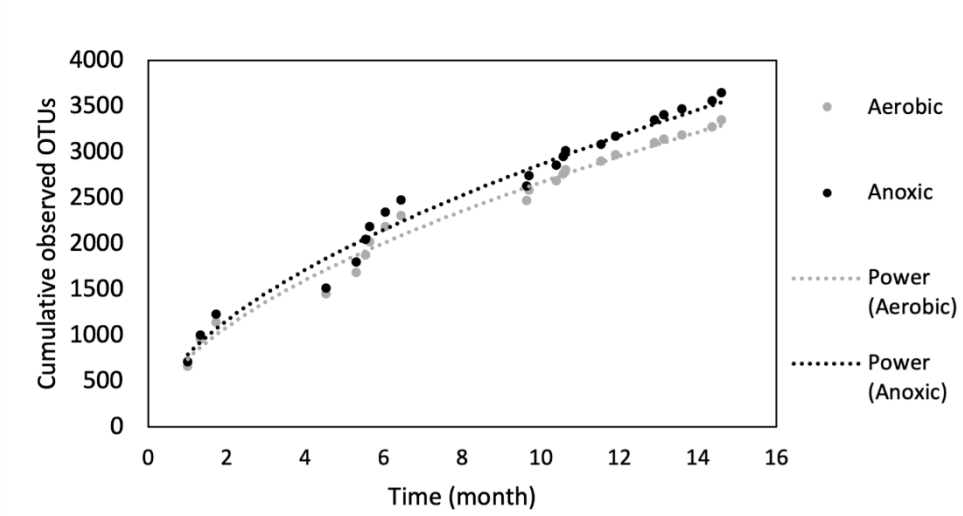

Figure 3-4 Taxa-time relationship and least-squares nonlinear regression power law fit between time and cumulative observed OTUs in the aerobic and anoxic bioreactors.

The core microbiome also reflects microbial temporal dynamics as it describes a community that is constantly associated with a given environment (Neu et al., 2021, Xia et al., 2018). In this study, we identified core members in both the anoxic and aerobic suspended growth communities (Figure B 5). The anoxic suspended growth community contained 218 loose core taxa (79.71 ± 5.61%), 98 general core taxa (60.34 ± 15.47%), and 41 strict core taxa (41.50 ± 12.17%). In the aerobic community, there were 247 loose core genera (78.81 ± 8.00%), 103 general core genera (56.59 ± 16.81%), and 28 strict core genera (28.20 ± 6.62%). Results showed that a large persistent population adapted to the anoxic condition imposed. The presence of core microbiome is important in modeling to predict and diagnose process functions for anoxic suspended growth, as persistent

populations (especially persistently abundant organisms) may make essential contributions to treatment performance and temporal stability (Saunders et al., 2016).

3.3.6 Diversity within functional guilds

Insight into which bacteria are responsible for nutrient removal is critical to improve BNR processes, particularly anoxic BNR processes as there is such little information about them in full systems. Therefore, the taxonomy diversity of well-described nitrifiers, denitrifiers, PAOs, and GAOs was examined in this study. As the bioreactors were not designed to nitrify, the relative abundances of nitrifiers were less than 0.04% in most of the samples (Figure 3-5 a & b). An enrichment of nitrifiers occurred in the aerobic community during the summer months (2.12 ± 0.63%) with both abundant AOBs (*Nitrosomonas* and *Nitrospira*) and NOBs (*Nitrospira* and *Nitrotoga*). This can be attributed to the fact that the growth rate of nitrifiers peaked during the summertime, and the SRT of the aerobic bioreactor (8-10 days) during that period was much longer than typical washout conditions. It is well-known that nitrification is an "all or nothing" proposition (Grady et al., 2011), and nitrate production may have interfered with the preceding anaerobic phase in the aerobic bioreactor at that time (data not shown). However, the nitrifiers were washed out after the SRT was reduced. The presence of low abundant nitrifiers in the anoxic bioreactor was likely due to immigration via the influent wastewater. Nitrate concentrations were consistently low enough (<1 mg-N/L) during the anaerobic phase in the anoxic bioreactor and were not considered to have interfered with anaerobic functions.

Among the known genera, denitrifiers (non-PAO and non-GAO) made up of 3.25 ± 2.31% and 3.48 ± 1.68% for the aerobic and anoxic communities (Figure 3-5 c & d). *Zoogloea* (1.59 ± 1.66%) and *Rhodoferax* (0.96 ± 0.62%) were the top abundant genera in the aerobic bioreactor, while *Thauera* (1.90 ± 1.07%) and *Rhodoferax* (1.30 ± 0.67%) were most abundant in the anoxic bioreactor. Besides being important to the denitrification process, both *Zoogloea* and *Thauera* are also known as floc-formers (Thomsen et al., 2007). Compared to *Zoogloea*, *Thauera* are more

versatile in use of available substrates such as sulfur species and are, thereby, more capable of living in an oxygen-free environment. A previous study reported that *Thauera* can utilize sulfide as the electron donor for denitrification and store intracellular elemental sulfur (Liang et al., 2020). Sulfur granules were also observed in the anoxic biomass samples by microscopic examination. Deeper knowledge about the ecophysiology of *Thauera* may ensure the presence of denitrification and help control for settleable floc properties in anoxic suspended growth.

Biological phosphorus removal is accomplished by PAOs, with four genera identified in this study (Figure 3-5 e & f). *Ca.* Accumulibacter and *Tetrasphaera*, two well-described PAO genera that have received intensive investigations (S. He et al., 2007, Marques et al., 2017, Nguyen et al., 2011, Stokholm-Bjerregaard et al., 2017), were less represented in the anoxic bioreactor. The relative abundance of *Ca.* Accumulibacter in the anoxic bioreactor was 0.52 ± 0.53% while the number in the aerobic bioreactor was almost double (1.02 ± 1.09%). *Tetrasphaera* accounted for only 0.03 ± 0.04% of the total population in the anoxic bioreactor but five times more (0.15 ± 0.09%) in the aerobic bioreactor. The denitrification capability of different *Ca.* Accumulibacter clades have been well-documented (Carvalho et al., 2007, Díez-Montero et al., 2016, Filipe and Daigger, 1999, Flowers et al., 2009, H. Gao et al., 2019). While most previous studies used synthetic wastewater, Díez-Montero et al., 2016 recorded the evolution of denitrifying PAOs in an anaerobic-anoxic sludge blanket treating municipal wastewater. Our study revealed the feasibility to enrich denitrifying PAOs in the suspended growth for municipal wastewater treatment. Process optimization and finer-resolution-diversity of the denitrifying PAOs will need future investigations.

The recognized putative PAO genera *Dechloromonas* were abundant with high occurrence frequencies in both bioreactors. While members of *Dechloromonas* have been shown to behave according to the PAO phenotype, a potential GAO phenotype in situ was also reported previously (McIlroy et al., 2016, Nielsen et al., 2019). Metabolic information retrieved from metagenome-assembled genomes revealed glycogen accumulation genes encoded in *Dechloromonas* members, suggesting the possibility that *Dechloromonas can* exhibit different metabolisms (polyphosphate-

and glycogen-based phenotypes) depending on environmental conditions (Petriglieri et al., 2021). A high relative abundance of *Dechloromonas* was identified in the anoxic bioreactor (2.06 ± 1.79%)., and future analysis needs to investigate their metabolism under the anoxic condition.

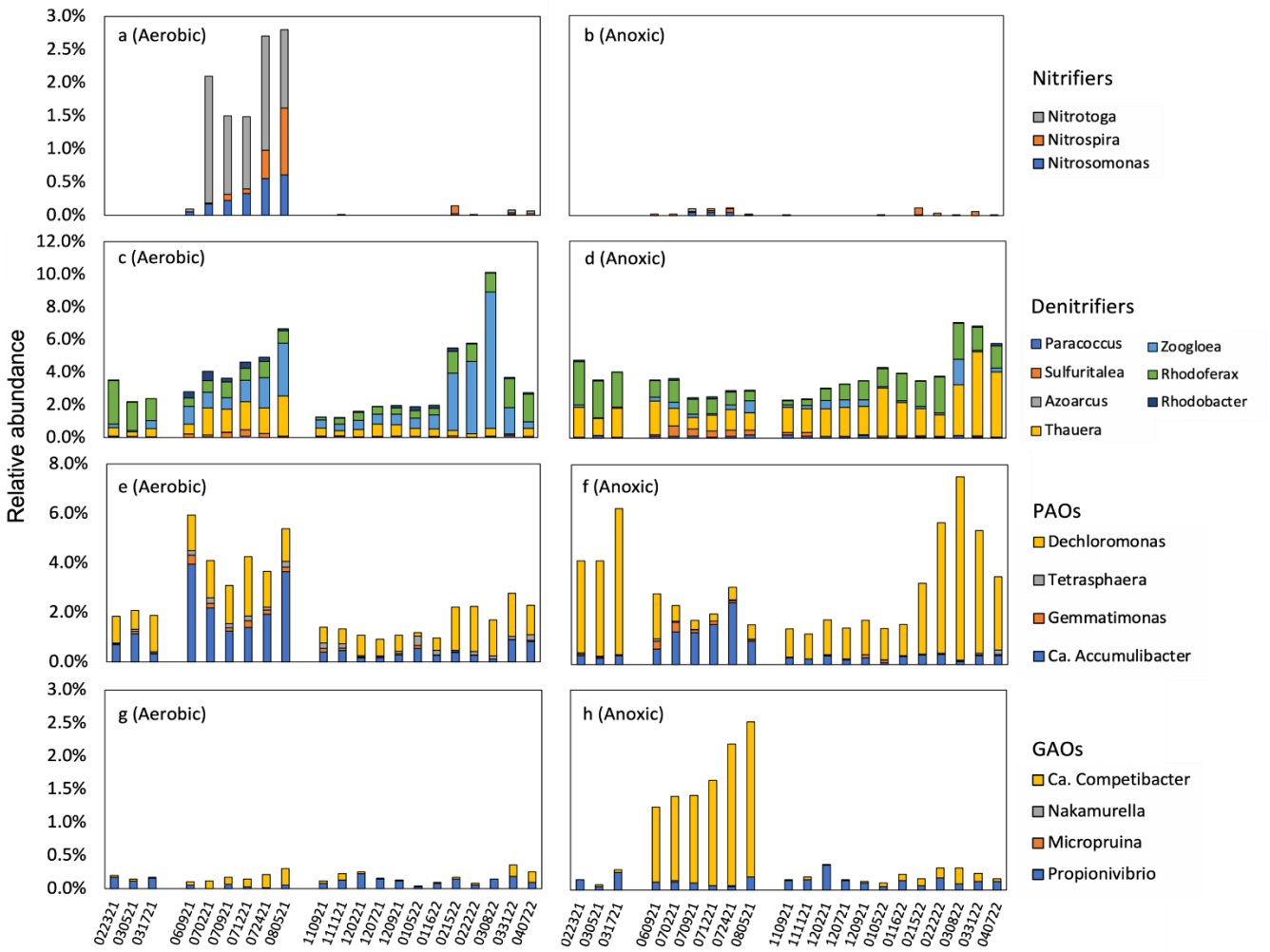

Figure 3-5 Diversity of genera belonging to major functional groups. The x-axis indicated the sampling dates (e.g., 022321 = February 23, 2021).

Low relative abundance of recognized GAOs was found in both bioreactors (Figure 3-5 g & h), suggesting that GAOs were not as competitive as PAOs. Although the relative abundance of *Ca*. Competibacter in the anoxic bioreactor surged during June to August 2021, a moderate phosphorus percentage removal of 58.0 % was still achieved in the anoxic bioreactor during that period.

3.3.7 Stochastic and deterministic processes controlling microbial temporal dynamics

Microbial temporal dynamics is shaped by both stochastic (e.g., random birth/death, immigration) and deterministic (e.g., niche-related selection) processes (Van Der Gast et al., 2008, Zhang et al., 2022, Zhou and Ning, 2017). Understanding the mechanisms (stochastic vs. deterministic) governing community diversity and dynamics is important to manage and control the microbial community. In the context of environmental engineering of practical biological treatment systems, determining which mechanisms are driving factors is desired to help better optimize system performance. To disentangle the stochastic and deterministic assembly in this study, two types of null model analysis were employed. In the first null model analysis, NST and SES values were calculated (Table 3-3). The value of NST for the anoxic community (64.1%) was higher than that for the aerobic community (53.8%), suggesting higher stochasticity in assembly of the anoxic community. A similar result was revealed by the modified RC metrics based NMDS plots (Figure 3-6). Samples from the anoxic bioreactor were clustered farther apart, indicating that they were less deviant to the null expectation and more shaped by stochastic factors (Zhou et al., 2014).

Table 3-3 Normalized Stochasticity (NST) and Standard effect size (SES) values for the aerobic and anoxic suspended growth.

Group	Normalized Stochasticity (NST)	Standard effect size (SES)
Aerobic	0.538	3.59
Anoxic	0.641	2.79

One might expect that microbial temporal assembly in anoxic suspended growth would be more niche-related and less random than in the aerobic community, as the presence of nitrate as the electron acceptor may create a higher selective pressure, filtering out microorganisms incapable of anaerobic metabolisms. However, the null model analysis indicated that the anoxic

community assembly was more stochastic than aerobic community assembly. This could be attributed to the occasionally longer SRTs in the anoxic bioreactor. It has been reported that stochastic processes generally become more pronounced at long SRTs, possibly due to the increased microbial immigration rates from the feed wastewater (Zhang et al., 2022). Long SRTs could intensify nutrient competition between functional groups and weaken their ability to resist external disturbances (Sun et al., 2020). Thus, the anoxic community occasionally operated at longer SRTs could be more disturbed by the continuous immigration from the influent wastewater. In addition, lower net specific growth rates in the anoxic bioreactor may have intensified drift or fluctuations in population size due to random birth or death events (Evans et al., 2017).

On the other hand, both communities exhibited SES values of over 2 and, therefore, deterministic factors also played significant roles in regulating microbial community structures (Ning et al., 2019). The significance of deterministic assembly was also reflected by the large number of species in the core microbiome observed in both communities. However, the role of stochastic processes in anoxic microbial assembly cannot be overlooked. Compared to conventional aerobic suspended growth, random processes, such as immigration via the influent source community, were more significant in driving community assembly in the anoxic suspended growth. Therefore, the anoxic suspended growth may be less controllable than the conventional aerobic suspended growth, but it may be less subject to changes in environmental variables (pH, temperature, etc.) at the same time.

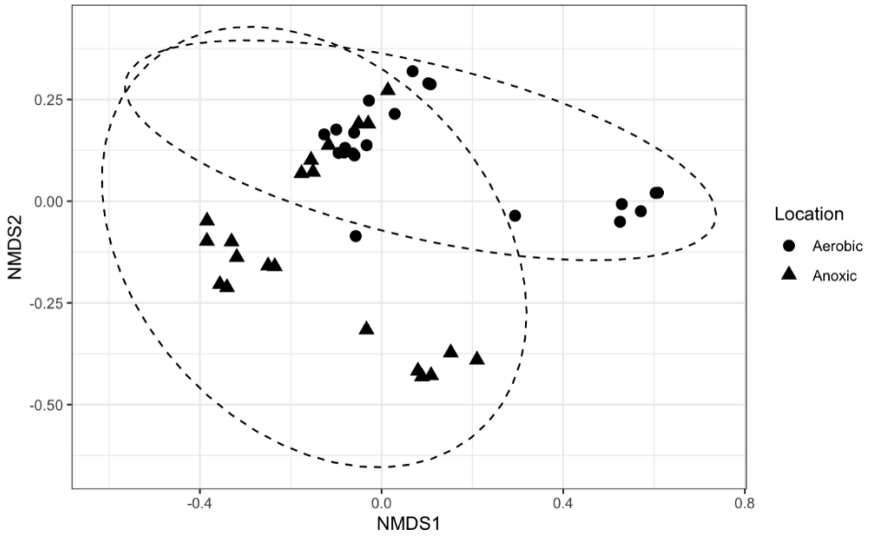

Figure 3-6 NMDS plots based on the modified RC metrics. Stress: 0.16.

3.4 Conclusions and future research needs

A fully anoxic suspended growth is appealing in BNR processes due to considerable aeration reduction and improved carbon processing efficiency. With the development of hybrid MABR technology, implementation of a fully anoxic suspended growth community in the resulting hybrid process became practical. Our study comparatively investigated the anoxic microbial community compared to a conventional aerobic community via microscopic and molecular methods. Results from this study provide a basis for understanding how an anoxic alternative differs from conventional aerobic communities and may facilitate a wider adoption of the anoxic suspended growth for improving the carbon and energy efficiency of BNR processes.

Microscopic examination showed that flocs formed under the anoxic condition had less filamentous backbones and were more diffuse with internal voids, implying reduced bio-flocculation capacity and easily sheared flocs. This study quantified the colloidal carbon concentrations in the effluents, but did not distinguish the fraction from the influent passing through the treatment versus the fraction released from flocs due to hydraulic shear force. The efficiency of the process operation varies based on the type of carbon present: enhanced production

of microbial extracellular polymer substances (EPS) or addition of flocculants can significantly improve the aggregation of influent colloidal particles, while encouraging the growth of low-DO filaments makes stronger floc structures and thus reduce the colloidal carbon dispersed from flocs. Future research is needed to identify the source to allow adjustment of the treatment process accordingly to minimize the potential for carbon breakthrough in the effluent. Future studies also need to quantify the flocculation rates andEPS contents in the biomass to determine the proper amount of oxygen for micro-aeration that improves floc strength, flocculation capacity, and effluent quality without sacrificing the carbon processing benefits of a fully anoxic suspended growth.

Thauera, *Thiothrix*, and *Trichococcus* were identified as important floc-formers and filaments in anoxic suspended growth, so deeper knowledge about their ecophysiology can help these systems achieve good floc properties. As phylogenetic diversity exists within each filament morphotype, the identification of filamentous bacteria was with uncertainties. Fluorescence in situ hybridization (FISH) with species-targeted probes can better identify and visualize filaments, which can be pursued in future research.

Community level analysis based on 16S rRNA gene sequencing provided insights into the microbial composition and diversity of the anoxic suspended growth. Though a distinctly different microbial community adapted to the anoxic condition, it showed a similar degree of diversity and temporal dynamics compared to the conventional aerobic community. This is important because diversity and dynamics of communities are often related to functional redundancy and process stability (Briones and Raskin, 2003). Recognizing the similarities between the anoxic and aerobic communities can lead to a better integration of existing knowledge and strategies to design and control the anoxic suspended growth process.

A variety of well-described filaments, denitrifiers, and PAOs sustainably adapted to the anoxic condition. Since bacterial identification at the species level is a challenge for 16S rRNA gene V4 region-based analysis, some members within the functional guilds were either unclassified or

poorly described (i.e., those with only a MiDAS placeholder species name). More specific and quantitative functional traits-based methods, such as GeoChip (Shi et al., 2019) and metagenomic sequencing (Singleton et al., 2021), are needed in the future research to identify the process-critical and novel members on the species level.

Null model analysis in this study indicated that the anoxic community had a more stochastic assembly pattern than the aerobic community. This was likely due to the longer SRTs and lower net growth rates in the anoxic bioreactor. On the other hand, deterministic assembly was still significant in the anoxic community, and the general core microbiome encompassed 98 genera, representing a great portion of the total population. Different microbial groups may differ greatly in the assembly mechanisms, however, as some populations are under strong selection pressure while others have highly random birth/death events. This type of difference was not discerned by the whole community level analysis in this study. Future research is needed to apply individual taxa/lineages based analysis, such as phylogenetic bin-based mull model (iCAMP) (Ning et al., 2020), to quantify the ecological drivers that govern the temporal assembly of various microbial groups.

Reference

APHA. (2005) *Standard Methods for the Examination of Water and Wastewater*, 21st ed.; Washington, DC, USA: American Public Health Association, American Water Works Association, and Water Environment Federation.

APHA. (2012) *Standard Methods for the Examination of Water and Wastewater*, 22nd ed.; Washington, DC, USA: American Public Health Association, American Water Works Association, and Water Environment Federation.

Bajaj, M.; Gallert, C.; Winter, J. (2010) Effect of phenol addition on COD and nitrate removal in an anoxic suspension reactor. *Bioresource Technology*, **101** (14), 5159–5167.

Briones, A.; Raskin, L. (2003) Diversity and dynamics of microbial communities in engineered environments and their implications for process stability. *Current Opinion in Biotechnology*, **14** (3), 270–276.

Carlson, A. L.; He, H.; Yang, C.; Daigger, G. T. (2021) Comparison of hybrid membrane aerated biofilm reactor (MABR)/suspended growth and conventional biological nutrient removal processes. *Water Science and Technology*, wst2021062.

Carvalho, G.; Lemos, P. C.; Oehmen, A.; Reis, M. A. M. (2007) Denitrifying phosphorus removal: Linking the process performance with the microbial community structure. *Water Research*, **41** (19), 4383–4396.

Chase, J. M.; Kraft, N. J. B.; Smith, K. G.; Vellend, M.; Inouye, B. D. (2011) Using null models to disentangle variation in community dissimilarity from variation in α-diversity. *Ecosphere*, **2** (2), art24.

Chudoba, J. (1985) Control of Activated Sludge Filamentous Bulking-VI. Formulation of basic principles, **19** (8), 1017–1022.

Collado, L.; Inza, I.; Guarro, J.; Figueras, M. J. (2008) Presence of Arcobacter spp. in environmental waters correlates with high levels of fecal pollution: Correlation of Arcobacter with fecal pollution. *Environmental Microbiology*, **10** (6), 1635–1640.

Daigger, G.; Carlson, A.; Chen, X.; Johnson, B. R. (2019) Coupled Anoxic Suspended Growth and Membrane Aerated Biofilm Reactor Process Options. *Proceedings of the 92nd Annual Water Environment Federation Technical Conference and Exhibition*; Presented at the WEFTEC, Chicago, IL.

Díez-Montero, R.; De Florio, L.; González-Viar, M.; Herrero, M.; Tejero, I. (2016) Performance evaluation of a novel anaerobic–anoxic sludge blanket reactor for biological nutrient removal treating municipal wastewater. *Bioresource Technology*, **209**, 195–204.

Dottorini, G.; Michaelsen, T. Y.; Kucheryavskiy, S.; Andersen, K. S.; Kristensen, J. M.; Peces, M.; Wagner, D. S.; et al. (2021) Mass-immigration determines the assembly of activated sludge microbial communities. *Proc. Natl. Acad. Sci. U.S.A.*, **118** (27), e2021589118.

Dueholm, M. K. D.; Nierychlo, M.; Andersen, K. S.; Rudkjøbing, V.; Knutsson, S.; MiDAS Global Consortium; Arriaga, S.; et al. (2022) MiDAS 4: A global catalogue of full-length 16S rRNA gene sequences and taxonomy for studies of bacterial communities in wastewater treatment plants. *Nat Commun*, **13** (1), 1908.

Eikelboom, D. (2000) *Process Control of Activated Sludge Plants by Microscopic investigationn*; UK: IWA Publising.

Evans, S.; Martiny, J. B. H.; Allison, S. D. (2017) Effects of dispersal and selection on stochastic assembly in microbial communities. *ISME J*, **11** (1), 176–185.

Filipe, C. D. M.; Daigger, G. T. (1999) Evaluation of the Capacity of Phosphorus-Accumulating Organisms To Use Nitrate and Oxygen as Final Electron Acceptors: A Theoretical Study on Population Dynamics. *water environ res*, **71** (6), 1140–1150.

Flowers, J. J.; Cadkin, T. A.; McMahon, K. D. (2013) Seasonal bacterial community dynamics in a full-scale enhanced biological phosphorus removal plant. *Water Research*, **47** (19), 7019–7031.

Flowers, J. J.; He, S.; Yilmaz, S.; Noguera, D. R.; McMahon, K. D. (2009) Denitrification capabilities of two biological phosphorus removal sludges dominated by different 'Candidatus Accumulibacter' clades. *Environmental Microbiology Reports*, **1** (6), 583–588.

Gabb, D. M. D.; Still, D. A.; Ekama, G. A.; Jenkins, D.; Marais v., G. R. (1991) The selector effect on filamentous bulking in long sludge age activated sludge systems. *Water Science and Technology*, **23** (4–6), 867–877.

Gao, H.; Liu, M.; Griffin, J. S.; Xu, L.; Xiang, D.; Scherson, Y. D.; Liu, W.-T.; et al. (2017) Complete Nutrient Removal Coupled to Nitrous Oxide Production as a Bioenergy Source by Denitrifying Polyphosphate-Accumulating Organisms. *Environ. Sci. Technol.*, **51** (8), 4531–4540.

Gao, H.; Mao, Y.; Zhao, X.; Liu, W.-T.; Zhang, T.; Wells, G. (2019) Genome-centric metagenomics resolves microbial diversity and prevalent truncated denitrification pathways in a denitrifying PAO-enriched bioprocess. *Water Research*, **155**, 275–287.

Gao, Y.; Guo, L.; Shao, M.; Hu, F.; Wang, G.; Zhao, Y.; Gao, M.; et al. (2020) Heterotrophic denitrification strategy for marine recirculating aquaculture wastewater treatment using mariculture solid wastes fermentation liquid as carbon source: Optimization of COD/NO3−-N ratio and hydraulic retention time. *Bioresource Technology*, **304**, 122982.

Gonzalez-Martinez, A.; Rodriguez-Sanchez, A.; Loosdrecht, M. C. M. van; Gonzalez-Lopez, J.; Vahala, R. (2016) Detection of comammox bacteria in full-scale wastewater treatment bioreactors using tag-454-pyrosequencing. *Environ Sci Pollut Res*, **23** (24), 25501–25511.

Grady, L.; Daigger, G.; Love, N.; Filipe, C. (2011) *Biological Wastewater Treatment*, 3rd ed.; CRC Press LLC.

Guo, X.; Zhou, X.; Hale, L.; Yuan, M.; Ning, D.; Feng, J.; Shi, Z.; et al. (2019) Climate warming accelerates temporal scaling of grassland soil microbial biodiversity. *Nat Ecol Evol*, **3** (4), 612–619.

Haegeman, B.; Hamelin, J.; Moriarty, J.; Neal, P.; Dushoff, J.; Weitz, J. S. (2013) Robust estimation of microbial diversity in theory and in practice. *ISME J*, **7** (6), 1092–1101.

Hai, R.; Wang, Y.; Wang, X.; Li, Y.; Du, Z. (2014) Bacterial Community Dynamics and Taxa-Time Relationships within Two Activated Sludge Bioreactors. (J. Vera, Ed.)*PLoS ONE*, **9** (3), e90175.

He, H.; Wagner, B. M.; Carlson, A. L.; Yang, C.; Daigger, G. T. (2021) Recent progress using membrane aerated biofilm reactors for wastewater treatment. *Water Science and Technology*, **84** (9), 2131–2157.

He, S.; Gall, D. L.; McMahon, K. D. (2007) " Candidatus Accumulibacter" Population Structure in Enhanced Biological Phosphorus Removal Sludges as Revealed by Polyphosphate Kinase Genes. *Appl Environ Microbiol*, **73** (18), 5865–5874.

Henze, M.; Gujer, W.; Mino, T.; Loosedrecht, M. van. (2000) *Activated Sludge Models ASM1, ASM2, ASM2d and ASM3*, Vol. 5; London: IWA Publising. Retrieved from https://iwaponline.com/ebooks/book/96/

Jarvis, P.; Jefferson, B.; Parsons, S. A. (2005) Measuring Floc Structural Characteristics. *Rev Environ Sci Biotechnol*, **4** (1–2), 1–18.

Jenkins, D.; Richard, M.; Daigger, G. (2003) *Manual on the Causes and Control of Activated Sludge Bulking, Foaming, and Other Solids Separation Problems*, 3rd ed.; CRC Press.

Jimenez, J. A.; La Motta, E. J.; Parker, D. S. (2005) Kinetics of Removal of Particulate Chemical Oxygen Demand in the Activated-Sludge Process. *Water Environment Research*, **77** (5), 437–446.

Kozich, J. J.; Westcott, S. L.; Baxter, N. T.; Highlander, S. K.; Schloss, P. D. (2013) Development of a Dual-Index Sequencing Strategy and Curation Pipeline for Analyzing

Amplicon Sequence Data on the MiSeq Illumina Sequencing Platform. *Appl. Environ. Microbiol.*, **79** (17), 5112–5120.

Kristensen, J. M.; Nierychlo, M.; Albertsen, M.; Nielsen, P. H. (2020) Bacteria from the Genus *Arcobacter* Are Abundant in Effluent from Wastewater Treatment Plants. (N.-Y. Zhou, Ed.)*Appl Environ Microbiol*, **86** (9), e03044-19.

Lee, C.; Agidi, S.; Marion, J. W.; Lee, J. (2012) Arcobacter in Lake Erie Beach Waters: an Emerging Gastrointestinal Pathogen Linked with Human-Associated Fecal Contamination. *Appl Environ Microbiol*, **78** (16), 5511–5519.

Letelier-Gordo, C. O.; Martin Herreros, M. (2019) Denitrifying granules in a marine Upflow Anoxic Sludge Bed (UASB) reactor. *Aquacultural Engineering*, **84**, 42–49.

Liang, Z.; Sun, J.; Zhan, C.; Wu, S.; Zhang, L.; Jiang, F. (2020) Effects of sulfide on mixotrophic denitrification by *Thauera* -dominated denitrifying sludge. *Environ. Sci.: Water Res. Technol.*, **6** (4), 1186–1195.

Marques, R.; Santos, J.; Nguyen, H.; Carvalho, G.; Noronha, J. P.; Nielsen, P. H.; Reis, M. A. M.; et al. (2017) Metabolism and ecological niche of Tetrasphaera and Ca. Accumulibacter in enhanced biological phosphorus removal. *Water Research*, **122**, 159–171.

McIlroy, S. J.; Starnawska, A.; Starnawski, P.; Saunders, A. M.; Nierychlo, M.; Nielsen, P. H.; Nielsen, J. L. (2016) Identification of active denitrifiers in full-scale nutrient removal wastewater treatment systems: Identifying active denitrifiers in activated sludge. *Environ Microbiol*, **18** (1), 50–64.

Meerburg, F. A.; Vlaeminck, S. E.; Roume, H.; Seuntjens, D.; Pieper, D. H.; Jauregui, R.; Vilchez-Vargas, R.; et al. (2016) High-rate activated sludge communities have a distinctly different structure compared to low-rate sludge communities, and are less sensitive towards environmental and operational variables. *Water Research*, **100**, 137–145.

Moussavi, G.; Ghodrati, S.; Mohseni-Bandpei, A. (2014) The biodegradation and COD removal of 2-chlorophenol in a granular anoxic baffled reactor. *Journal of Biotechnology*, **184**, 111–117.

Nascimento, A. L.; Souza, A. J.; Andrade, P. A. M.; Andreote, F. D.; Coscione, A. R.; Oliveira, F. C.; Regitano, J. B. (2018) Sewage Sludge Microbial Structures and Relations to Their Sources, Treatments, and Chemical Attributes. *Front. Microbiol.*, **9**, 1462.

Neu, A. T.; Allen, E. E.; Roy, K. (2021) Defining and quantifying the core microbiome: Challenges and prospects. *Proc. Natl. Acad. Sci. U.S.A.*, **118** (51), e2104429118.

Nguyen, H. T. T.; Le, V. Q.; Hansen, A. A.; Nielsen, J. L.; Nielsen, P. H. (2011) High diversity and abundance of putative polyphosphate-accumulating Tetrasphaera-related bacteria in

activated sludge systems: Tetrasphaera-related bacteria in activated sludge systems. *FEMS Microbiology Ecology*, **76** (2), 256–267.

Nielsen, P. H.; Kragelund, C.; Seviour, R. J.; Nielsen, J. L. (2009) Identity and ecophysiology of filamentous bacteria in activated sludge. *FEMS Microbiol Rev*, **33** (6), 969–998.

Nielsen, P. H.; McIlroy, S. J.; Albertsen, M.; Nierychlo, M. (2019) Re-evaluating the microbiology of the enhanced biological phosphorus removal process. *Current Opinion in Biotechnology*, **57**, 111–118.

Ning, D.; Deng, Y.; Tiedje, J. M.; Zhou, J. (2019) A general framework for quantitatively assessing ecological stochasticity. *Proc. Natl. Acad. Sci. U.S.A.*, **116** (34), 16892–16898.

Ning, D.; Yuan, M.; Wu, L.; Zhang, Y.; Guo, X.; Zhou, X.; Yang, Y.; et al. (2020) A quantitative framework reveals ecological drivers of grassland microbial community assembly in response to warming. *Nat Commun*, **11** (1), 4717.

Nittami, T.; Batinovic, S. (2022) Recent advances in understanding the ecology of the filamentous bacteria responsible for activated sludge bulking. *Letters Applied Microbiology*, lam.13634.

Ofiţeru, I. D.; Lunn, M.; Curtis, T. P.; Wells, G. F.; Criddle, C. S.; Francis, C. A.; Sloan, W. T. (2010) Combined niche and neutral effects in a microbial wastewater treatment community. *Proc. Natl. Acad. Sci. U.S.A.*, **107** (35), 15345–15350.

Peces, M.; Dottorini, G.; Nierychlo, M.; Andersen, K. S.; Dueholm, M. K. D.; Nielsen, P. H. (2022) Microbial communities across activated sludge plants show recurring species-level seasonal patterns. *ISME COMMUN.*, **2** (1), 18.

Petriglieri, F.; Singleton, C.; Peces, M.; Petersen, J. F.; Nierychlo, M.; Nielsen, P. H. (2021) "Candidatus Dechloromonas phosphoritropha" and "Ca. D. phosphorivorans", novel polyphosphate accumulating organisms abundant in wastewater treatment systems. *ISME J*, **15** (12), 3605–3614.

Pinto, A. J.; Xi, C.; Raskin, L. (2012) Bacterial Community Structure in the Drinking Water Microbiome Is Governed by Filtration Processes. *Environ. Sci. Technol.*, **46** (16), 8851–8859.

Ravin, N. V.; Rudenko, T. S.; Smolyakov, D. D.; Beletsky, A. V.; Rakitin, A. L.; Markov, N. D.; Fomenkov, A.; et al. (2021) Comparative Genome Analysis of the Genus Thiothrix Involving Three Novel Species, Thiothrix subterranea sp. nov. Ku-5, Thiothrix litoralis sp. nov. AS and "Candidatus Thiothrix anitrata" sp. nov. A52, Revealed the Conservation of the Pathways of Dissimilatory Sulfur Metabolism and Variations in the Genetic Inventory for Nitrogen Metabolism and Autotrophic Carbon Fixation. *Front. Microbiol.*, **12**, 760289.

Rivett, D. W.; Mombrikotb, S. B.; Gweon, H. S.; Bell, T.; Gast, C. van der. (2021) Bacterial communities in larger islands have reduced temporal turnover. *ISME J*, **15** (10), 2947–2955.

Rognes, T.; Flouri, T.; Nichols, B.; Quince, C.; Mahé, F. (2016) VSEARCH: a versatile open source tool for metagenomics. *PeerJ*, **4**, e2584.

Roy, D.; McEvoy, J.; Blonigen, M.; Amundson, M.; Khan, E. (2017) Seasonal variation and ex-situ nitrification activity of ammonia oxidizing archaea in biofilm based wastewater treatment processes. *Bioresource Technology*, **244**, 850–859.

Saunders, A. M.; Albertsen, M.; Vollertsen, J.; Nielsen, P. H. (2016) The activated sludge ecosystem contains a core community of abundant organisms. *ISME J*, **10** (1), 11–20.

Schloss, P. D. (2008) Evaluating different approaches that test whether microbial communities have the same structure. *ISME J*, **2** (3), 265–275.

Schloss, P. D.; Westcott, S. L.; Ryabin, T.; Hall, J. R.; Hartmann, M.; Hollister, E. B.; Lesniewski, R. A.; et al. (2009) Introducing mothur: Open-Source, Platform-Independent, Community-Supported Software for Describing and Comparing Microbial Communities. *Appl Environ Microbiol*, **75** (23), 7537–7541.

Shi, Z.; Yin, H.; Van Nostrand, J. D.; Voordeckers, J. W.; Tu, Q.; Deng, Y.; Yuan, M.; et al. (2019) Functional Gene Array-Based Ultrasensitive and Quantitative Detection of Microbial Populations in Complex Communities. (S. M. Gibbons, Ed.)*mSystems*, **4** (4), e00296-19.

Singleton, C. M.; Petriglieri, F.; Kristensen, J. M.; Kirkegaard, R. H.; Michaelsen, T. Y.; Andersen, M. H.; Kondrotaite, Z.; et al. (2021) Connecting structure to function with the recovery of over 1000 high-quality metagenome-assembled genomes from activated sludge using long-read sequencing. *Nat Commun*, **12** (1), 2009.

Stokholm-Bjerregaard, M.; McIlroy, S. J.; Nierychlo, M.; Karst, S. M.; Albertsen, M.; Nielsen, P. H. (2017) A Critical Assessment of the Microorganisms Proposed to be Important to Enhanced Biological Phosphorus Removal in Full-Scale Wastewater Treatment Systems. *Front. Microbiol.*, **8**, 718.

Sun, C.; Zhang, B.; Chen, Z.; Qin, W.; Wen, X. (2020) Sludge retention time affects the microbial community structure: A large-scale sampling of aeration tanks throughout China. *Environmental Pollution*, **261**, 114140.

Thomsen, T. R.; Kong, Y.; Nielsen, P. H. (2007) Ecophysiology of abundant denitrifying bacteria in activated sludge: Ecophysiology of denitrifying bacteria in activated sludge. *FEMS Microbiology Ecology*, **60** (3), 370–382.

Van Der Gast, C. J.; Ager, D.; Lilley, A. K. (2008) Temporal scaling of bacterial taxa is influenced by both stochastic and deterministic ecological factors: Temporal scaling of bacterial taxa. *Environmental Microbiology*, **10** (6), 1411–1418.

Veen, W. L. van; Kooij, D. van der; Geuze, E. C. W. A.; Vlies, A. W. van der. (1973) Investigations on the sheathed bacteriumHaliscomenobacter hydrossis gen.n., sp.n., isolated from activated sludge. *Antonie van Leeuwenhoek*, **39** (1), 207–216.

Venâncio, I.; Luís, Â.; Domingues, F.; Oleastro, M.; Pereira, L.; Ferreira, S. (2022) The Prevalence of Arcobacteraceae in Aquatic Environments: A Systematic Review and Meta-Analysis. *Pathogens*, **11** (2), 244.

Wágner, D. S.; Peces, M.; Nierychlo, M.; Mielczarek, A. T.; Thornberg, D.; Nielsen, P. H. (2022) Seasonal microbial community dynamics complicates the evaluation of filamentous bulking mitigation strategies in full-scale WRRFs. *Water Research*, **216**, 118340.

Walters, W.; Hyde, E. R.; Berg-Lyons, D.; Ackermann, G.; Humphrey, G.; Parada, A.; Gilbert, J. A.; et al. (2016) Improved Bacterial 16S rRNA Gene (V4 and V4-5) and Fungal Internal Transcribed Spacer Marker Gene Primers for Microbial Community Surveys. (H. Bik, Ed.)*mSystems*, **1** (1), e00009-15.

Wang, B.; Peng, D.; Zhang, X.; Wang, X. (2016) Structure and formation of anoxic granular sludge—A string-bag hypothesis. *Front. Environ. Sci. Eng.*, **10** (2), 311–318.

Wang, Q.; Garrity, G. M.; Tiedje, J. M.; Cole, J. R. (2007) Naïve Bayesian Classifier for Rapid Assignment of rRNA Sequences into the New Bacterial Taxonomy. *Appl Environ Microbiol*, **73** (16), 5261–5267.

Wells, G. F.; Park, H.-D.; Eggleston, B.; Francis, C. A.; Criddle, C. S. (2011) Fine-scale bacterial community dynamics and the taxa–time relationship within a full-scale activated sludge bioreactor. *Water Research*, **45** (17), 5476–5488.

Wu, L.; Ning, D.; Zhang, B.; Li, Y.; Zhang, P.; Shan, X.; Zhang, Q.; et al. (2019) Global diversity and biogeography of bacterial communities in wastewater treatment plants. *Nat Microbiol*, **4** (7), 1183–1195.

Xia, Y.; Wen, X.; Zhang, B.; Yang, Y. (2018) Diversity and assembly patterns of activated sludge microbial communities: A review. *Biotechnology Advances*, **36** (4), 1038–1047.

Zhang, L.; Guo, K.; Wang, L.; Xu, R.; Lu, D.; Zhou, Y. (2022) Effect of sludge retention time on microbial succession and assembly in thermal hydrolysis pretreated sludge digesters: Deterministic versus stochastic processes. *Water Research*, **209**, 117900.

Zhou, J.; Deng, Y.; Zhang, P.; Xue, K.; Liang, Y.; Van Nostrand, J. D.; Yang, Y.; et al. (2014) Stochasticity, succession, and environmental perturbations in a fluidic ecosystem. *Proc. Natl. Acad. Sci. U.S.A.*, **111** (9). Retrieved from https://pnas.org/doi/full/10.1073/pnas.1324044111

Zhou, J.; Liu, W.; Deng, Y.; Jiang, Y.-H.; Xue, K.; He, Z.; Van Nostrand, J. D.; et al. (2013) Stochastic Assembly Leads to Alternative Communities with Distinct Functions in a Bioreactor Microbial Community. (J. Handelsman, Ed.)*mBio*, **4** (2), e00584-12.

Zhou, J.; Ning, D. (2017) Stochastic Community Assembly: Does It Matter in Microbial Ecology? *Microbiol Mol Biol Rev*, **81** (4), e00002-17.

CHAPTER IV

Hybrid MABR Process Achieves Intensified Nitrogen Removal While N_2O Emissions Remain Low

Published as:

He, H. and Daigger, G. T. (2023). The hybrid MABR process achieves intensified nitrogen removal while N_2O emissions remain low. *Water Research.* Accepted.

4.1 Introduction

Membrane-aerated biofilm reactors (MABRs) rely on gas-permeable membranes to support the growth of biofilms and supply oxygen into the biofilm via bubble-less aeration (He et al., 2021). Bubble-less aeration in MABRs offers high oxygen transfer efficiency and at a low energy input (Côté et al., 2015; Peeters et al., 2017). In MABRs, oxygen and soluble substrates (organic carbon or ammonia) diffuse into the biofilm from opposite directions, consequently creating a counter-diffusional biofilm with distinct concentration profiles (He et al., 2021). The MABR biofilm accommodates both oxygen-rich, oxygen-limited, and oxygen-depleted biofilm layers, housing diverse ecological niches for a range of functional microbiota. Most recently,

researchers and practitioners have coupled MABR units with activated sludge suspended growth as a hybrid process. The hybrid MABR process represents a full-scale solution to upgrade the biological nitrogen removal capacity of existing facilities and to create new facilities with increased sustainability features compared to traditional technologies. Commercial applications world-wide have demonstrated many benefits of the hybrid MABR process, including robust treatment performance (Chang et al., 2022; Mei et al., 2019; Silveira et al., 2022; Sun et al., 2020), bioaugmentation (Corsino and Torregrossa, 2022; Houweling et al., 2018; Shechter et al., 2020), and energy savings (Guglielmi et al., 2020; Houweling et al., 2018; Peeters et al., 2017; Shechter et al., 2020).

To date, most of the hybrid MABR processes submerge the MABR units into the unaerated suspended growth zones for simultaneous nitrification and denitrification, but aerated suspended growth zones are still maintained as the largest portion of the bioreactor volumes for further nitrification (Corsino and Torregrossa, 2022; Houweling et al., 2018; Peeters et al., 2017; Shechter et al., 2020; Silveira et al., 2022; Uri-Carreno et al., 2021). Maintaining a large aerobic zone is not desirable, however, as it requires significant aeration energy to deliver oxygen into the wastewater and also increases the extent to which influent carbon is oxidized rather than used for nitrogen removal (He et al., 2022). Given the unique feature of the hybrid MABR process, that an aerobic biofilm presents in the anoxic tank to produce nitrate for denitrification, economic benefits can be potentially maximized if most, or all, of the required nitrification is accomplished by the biofilm rather than by the suspended growth. The aerobic zone and corresponding aeration energy can be significantly reduced. The process can also be operated at shorter solid retention times (SRTs), which translate into smaller bioreactor volumes, smaller land usage, lower capital costs, and increased carbon capture.

In the previous modeling work published by our group (Carlson et al., 2021), we demonstrated that the hybrid MABR can produce high quality effluents with only 2% of the total suspended growth volume being aerated. However, the previous work used steady-state simulations without considering the system dynamic responses to influent variations. In reality, the strength and volume of wastewater entering the treatment plant are changing as a result of human activity patterns, and peak flow events can often present difficulties at a treatment process. In this regard, further investigations are needed to examine the dynamic behavior of the hybrid MABR process under changing conditions and its ability to mitigate peak flow events.

Oxidation-reduction potential (ORP) is an important water quality variable employed to monitor the redox conditions in bioreactors (Khanal and Huang, 2003; Luccarini et al., 2017). Field observations demonstrated that ORP in the bulk mixed liquor suspended growth surrounding the MABR biofilm requires control (Silveira et al., 2022; Uri-Carreno et al., 2021). Specifically, low ORP (anaerobic) conditions must be avoided in the bulk to minimize sulfate reduction activities that may cause nitrification upset in the biofilm (Flores-Alsina et al., 2023; Uri-Carreño et al., 2023). During peak loading events, the bulk mixed liquor may periodically become anaerobic (low ORP signals) because of the rapid consumption of nitrate via denitrification. Anaerobic conditions are unwanted because the promoted sulfate reduction results in more formation of 1) H_2S, which can diffuse into the biofilm and compete with nitrifiers for oxygen, and 2) FeS precipitates when Fe is added in the process such as for the purpose of chemical phosphorus removal. FeS can coat the biofilm and hinder mass transfer. Therefore, in this study we use ORP based aeration control in the MABR bulk mixed liquor to mitigate the effects of sulfur species and ensure robust nitrification in the biofilm.

Another key question is related to greenhouse gas (GHG) emissions from the hybrid MABR process, with increased attention to nitrous oxide (N_2O) emissions from nitrification and denitrification processes. Many studies demonstrated the potential of MABRs to greatly reduce N_2O emissions (Houweling, 2021; Kinh et al., 2017b, 2017a; Li et al., 2023). The mitigation effects are due to the unique microbial stratification in the biofilm, so that N_2O produced in the inner biofilm zone can be consumed in the outer zone. However, most of the studies focused on N_2O emissions from the MABR as a stand-alone unit, and an evaluation within the context of the whole hybrid process is still lacking. In addition, methane (CH_4) is also a potent GHG with a 100-year global warming potential 25 times higher than that of CO_2 (Wang et al., 2021). Previous studies reported that the direct CH_4 emissions from wastewater sector account for up to 79% of the Scope 1 emissions (direct GHG emissions from a facility) (Song, Zhu, et al., 2023). However, despite recognition of CH_4 emissions of WWTPs, CH_4 from the hybrid MABR process has received far less attention than N_2O emissions. To our knowledge, CH_4 emissions from the hybrid MABR process have not been reported before. Therefore, the total GHG emissions including both N_2O and CH_4 emissions need attention to get a holistic picture of the hybrid MABR process carbon footprint.

A wastewater treatment process should be considered as an integrated process, where process units (i.e., clarifiers, bioreactors, etc.) are linked together with complex interactions. In this regard, plant-wide modelling is an important tool to develop potential operation and control strategies. Previous work by our group using a plant-wide modelling approach demonstrated efficient performance and significant economic advantages for the hybrid MABR process in comparison to conventional activated sludge (Carlson et al., 2021). This paper extends the previous work with dynamic simulations to capture process behavior in response to diurnal loadings. The main objective of this study is to: 1) investigate viability of ORP based aeration controls to maximize the achievable nitrification in the MABR biofilm, 2) evaluate the nitrogen removal performance of the hybrid MABR under different temperature scenarios, and 3) evaluate the direct GHG emissions from the hybrid MABR including both N_2O and CH_4 emissions to get a holistic picture of the hybrid MABR process' carbon footprint.

4.2 Method

4.2.1 Model development

SUMO v.21 (Dynamita, France) was adopted as the simulation platform. The MABR model was constructed based on the commercial ZeelungTM 2.0 MABR module by Suez (Yang et al., 2022a, 2022b), and thereby the aeration and configuration parameters embedded in the model (e.g., air supply pressure, membrane thickness, packing density, etc.) reflect the consensus design and operation of full-scale hybrid MABRs at the present time. Details of the MABR model were described by (Yang et al., 2022b). Briefly, it is a fixed-thickness and one-dimensional biofilm model. It calculates the oxygen concentrations in the biofilm based on aeration settings, gas diffusion rates, and mass balances, which allows it to simulate biofilm activities under conditions of varying oxygen availability. The biofilm is divided into three layers: from the gas to liquid phase the biofilm has an inner layer adjacent to the membrane aeration, a middle layer, and an outer layer adjacent to the bulk mixed liquor (Supporting Information: Figure C 1). Biofilm specifications replicate previously published setups (Carlson, He, et al., 2021) and are shown in Table C 1.

The plant-wide biokinetic model was established based on Sumo2S (Dynamita, France). Sumo2S is a commercially available model which upgraded the typical biological and physio-chemical reactions occurring in wastewater treatment systems for COD, nitrogen, and phosphorus

with iron/sulfur/phosphorus (Fe/S/P) cycles (Hauduc et al., 2019). The model implemented both abiotic chemical reactions and biological transformations. To account for N2O emissions, we extended the nitritation model embedded in Sumo2S with two N2O pathways (Pocquet et al., 2016), namely autotrophic denitrification of nitrite (NN pathway) and incomplete hydroxylamine oxidation (ND pathway) (Figure C 2). 4-step denitrification via NO3, NO2, NO, and N2O was added into the model in parallel to 4-step nitrification. Relevant kinetic stoichiometry and rate expressions were obtained from Sumo4N (Dynamita, France). Lastly, we added aerobic growth and decay processes for methanotrophs, taken from (Delgado Vela, Gordon, et al., 2022), to investigate the fate of CH_4. The resulting integrated model, SumoMSN, was applied for all simulations. Detailed stoichiometry and kinetics are presented in the supporting information (SI).

Sulfide inhibition of nitrification was not taken into account in the model. The sulfide concentrations under the operating conditions of interest were significantly less than the values needed for inhibition to occur. The response of nitrifying communities to sulfide varied from study to study, and consensus inhibition constants are lacking for modeling efforts. The reported inhibition constants from activated sludge studies ranged widely from 7.8 to 150 gS/m^3 for AOBs and 2.4 to 10 gS/m^3 for nitrite-oxidizing bacteria (NOB) (Delgado Vela et al., 2018; Flores-Alsina et al., 2023; Kouba et al., 2017; Zhou et al., 2014). Whatever the constants, those reported values are at least one order of magnitude higher than the simulated sulfide concentrations under the operating conditions of interest (data present in later sections). For these reasons, sulfide inhibition of nitrification was not included in the model.

4.2.2 Process simulated

The configuration of the hybrid MABR process is shown in Figure 4-1 System configuration for the hybrid MABR process. The primary clarifier was set to be a non-reactive point separator to simulate suspended solid removal. For the secondary clarifier, the three-compartment clarifier model was used to simulate reactive biological reactions. The MABR bioreactor had a volume of 2000 m^3 with a total media surface area of 250,000 m^3. The downstream swing zone also had a volume of 2000 m^3.

An hourly diurnal influent flow was generated using the Sumo Influent Tool based on a medium plant size (average flowrate = 24,000 m3/d) (Figure C 3). Model default values of the

state variable based influent, which reflect a typical municipal wastewater, were used to set up the influent concentrations. Table 4-1 summarizes the influent wastewater flows and key state variable concentrations. In this study, the influent flowrate had hourly variations while influent concentrations remained constant for all the simulations. The ammonia loading rates (1.5~2.5 gN/m2/d) (average loading = 2.4 gN/m2/d), resulting from the varying influent flowrates, were within the typical range used to design commercial hybrid MABR system (He et al., 2021; Houweling and Daigger, 2019).

Table 4-1 Influent wastewater characteristics.

Parameters	Value	Units
Influent flow	24,000 ± 2,986 (mean ± std, dynamic)	m^3/d
Chemical oxygen demand (COD)	420.5	$gCOD/m^3$
Biological oxygen demand, 5 days (BOD_5)	183.5	$gCOD/m^3$
Dissolved methane (CH_4)	Non-detectable	$gCOD/m^3$
Total nitrogen (TN)	32.26	gN/m^3
Ammonia (NHx)	24.00	gN/m^3
Total phosphorus	4.15	gP/m^3
Total suspended solid (TSS)	183.8	$gTSS/m^3$
Hydrogen sulfide (H_2S)	1.00	gS/m^3

A modified Ludzack-Ettinger (MLE) process was simulated as an activated sludge benchmark for comparison. We select the MLE process because it is a long-standing, widely accepted, and effective process for biological nitrogen removal with well-documented system behaviors. The MLE process consists of designated anoxic and aerobic zones with a mixed liquor recirculation of 400% (Figure 4-2). Multiple tanks (2 ANX and 3 AER) were used to simulate hydrodynamic dispersion in the full-size activated sludge process. The total volume of the bioreactors was varied to maintain a comparable mixed liquor suspended solid (MLSS) concentration to the hybrid MABR process. The aerobic bioreactors accounted for 70% of the total bioreactor volume for all simulations. The same influent characteristics as described in Table 1 were used for the MLE process.

The SRT for both the hybrid MABR and MLE processes was controlled by adjusting the wastage flow rate. The SRT was varied based on effluent quality indicators -- effluent ammonia and effluent total inorganic nitrogen (TIN) concentrations. This study considered effluent TIN as the metric of effluent total nitrogen (TN) performance because TIN captures the performance of nitrification and denitrification, whereas the organic nitrogen components of TN are wastewater specific.

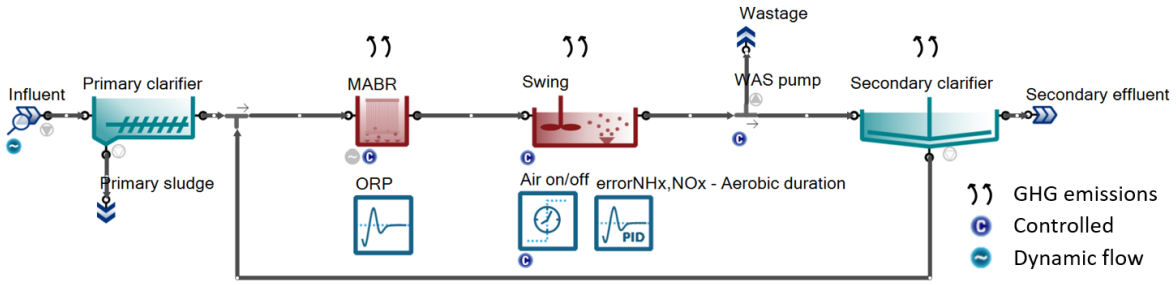

Figure 4-1 System configuration for the hybrid MABR process.

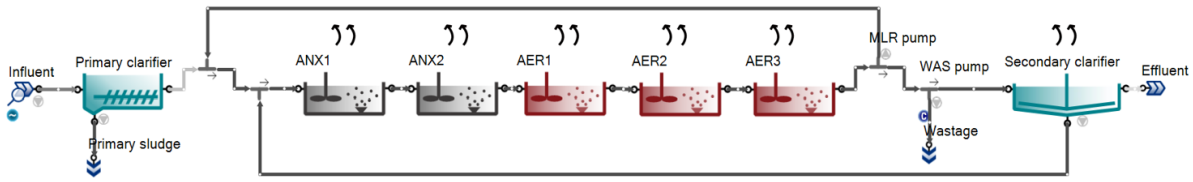

Figure 4-2 System configuration for the MLE process.

Two water temperature scenarios were simulated to test the resilience of the hybrid MABR process for biological nitrogen removal. Simulations were conducted at 20oC and 10oC to analyze the scenario of optimal nitrifier growth (20oC) and the scenario where the nitrification activities in the suspended growth portion are stressed (10oC). The temperature dependency in the model was formalized in accordance with the Arrhenius equation. The Arrhenius coefficients are listed in SI.

4.2.3 Aeration control strategies in the hybrid MABR process

Aeration controls were used in the hybrid MABR process to manage influent variations and ensure consistent nitrogen removal performance. An ORP-based feedback control was used in

the MABR zone (Figure 4-1). The controller adjusts the aeration rate in the bulk mixed liquor surrounding the biofilm to maintain a desired ORP setpoint. Model equations for ORP signals are added into SI (Table C 2-Table C 3). In the Swing zone, a cascade control strategy was used to optimize total nitrogen removal. The cascade control strategy includes a PID controller "errorNHx-NOx", with the target of maintaining equal NHx and NOx concentrations in the tank effluent, and a time-based ON/OFF controller "Air on/off", which regulates intermittent aeration. The controller settings, presented in SI (Table C 4, Table C 5, Table C 6), were selected based on various gain sets.

Aeration controllers were not used in the MLE process simulations. The MLE process is a mature technology with well-established operational conditions. Therefore, to simplify computational effort, DO concentrations in the MLE process were set to be fixed values (Anoxic tank DO = 0 mg/L, Aerobic tank DO = 2.0 mg/L). Those values were selected based on typical operating conditions in practice (Grady et al., 2011).

4.2.4 Greenhouse gas (GHG) evaluation

The scope of the GHG accounting in this study included direct GHG emissions (CH_4 and N_2O) from the bioreactors and secondary clarifiers. GHG accounting practice considers CO_2 emissions from wastewater treatment processes to be biogenic and part of the natural carbon cycles (Ross et al., 2020), and therefore this study did not include direct CO_2 emissions in the GHG inventory. This study focuses on the Scope 1 emissions (direct GHG emissions from wastewater treatment process) guided by Intergovernmental Panel on Climate Change. Therefore, indirect emissions from electricity were not considered, although they would be significantly less for the hybrid MABR process due to reduced energy requirements. CH_4 and N_2O emissions were normalized to CO_2 equivalents (CO_2-eq) based on their global warming potential (GWP) (Abulimiti et al., 2022):

$$GHG_{CO2\text{-}eq} = GHG_{CH4}*25 + GHG_{N2O}*298$$

Parameters for the MOB growth and decay processes were taken from a recent lab-scale model (Delgado Vela, Gordon, et al., 2022), and have not yet been tested in full-scale WWTPs. Therefore, a sensitivity analysis was conducted to assess the influence of the parameter values on CH_4 emissions. The sensitivity analysis followed the method described by (Daelman et al., 2014). Five MOB parameters were included: yield (Y_{MOB}), maximum specific growth rate (μ_{MOB}), decay rate

(b_{MOB}), half-saturation of O_2 ($K_{O2, MOB}$), and half-saturation of CH_4 ($K_{CH4, MOB}$). Each parameter was varied between 75% and 125% of the default value, using the methane emission rate as the output variable.

4.3 Results and discussion

4.3.1 Impacts of MABR bulk ORPs on sulfur and ammonia uptake in the biofilm

Numerous steady-state simulations were conducted to examine the effects of sulfur species on biofilm nitrification under a range of MABR bulk ORPs. In this step, we used steady state simulations (at the constant influent flowrate of 24000 m3/d), instead of dynamic simulations with diurnal flows, to capture the impacts of ORPs and to exclude influences of the varying ammonia loadings on biofilm nitrification.

The model demonstrated the behavior observed in full-scale systems, where low ORP conditions have shown a strong negative correlation with the MABR biofilm nitrification rate and overall nitrogen removal performance (Silveira, Cadee, et al., 2022; Uri-Carreno, Nielsen, et al., 2021). According to the results, when the MABR ORP increased from -80 to -50 mV, ammonia uptake rates in the biofilm almost doubled, and the resulting ammonia concentrations in the bulk mixed liquor dropped significantly (Figure 4-3a). The fraction of nitrification oxygen consumption of the total oxygen consumption also increased from 15% to 80 %, indicating the majority of oxygen consumption in the biofilm was used to oxidize ammonia instead of carbon oxidation or sulfide oxidation (Figure C 4). With higher ammonia removed in the biofilm, the bulk ammonia concentration decreased from 17 gN/m3 to an average of 3 gN/m3, and this represented over a 5-fold reduction in the effective ammonia loads that must be removed by the mixed liquor to reach the effluent discharge limit. Nitrate production in the biofilm also significantly increased as a result of nitrification (Figure C 5).

ORP is a water quality variable employed to characterize the redox capacity of the system (Wang et al., 2022). ORP signals are widely used in wastewater treatment plants (WWTPs) in monitoring and control of process tanks to ensure effluent quality standards under variable influent loadings (Luccarini et al., 2017; Wang et al., 2022). The negative impacts of low ORPs on biofilm nitrification have been observed in both cold climate (Uri-Carreno et al., 2021) and warm climate

regions (Silveira et al., 2022). Uri-Carreño, Nielsen, et al., 2023 suggested that the promoted formation of sulfide species under anaerobic conditions was a potential cause. Active sulfate reducing activities occur in the bulk mixed liquor at low ORP conditions. Due to the lack of air stripping in the MABR bulk, the formed H_2S would diffuse into the biofilm and compete with nitrifiers for oxygen. FeS precipitation also occurred under low ORP conditions, and it can coat the biofilm and hinder the mass transfer. This needs attention especially when external Fe is fed into the process, such as for the chemical phosphorus removal.

The biofilm layer adjacent to the bulk mixed liquor but furthest from the inner membrane aeration appeared to be the most sensitive zone to MABR bulk ORP variations. With the MABR bulk ORP increasing from -80 mV to -50 mV, while sulfide concentrations in the other biofilm layers did not change significantly due to their access to oxygen supplied through the membrane lumen, one magnitude reduction was observed in the outer biofilm layer as the H2S concentration dropped from 1.1 to 0.13 gS/m3, and the FeS concentration dropped from 2.9 to 0.49 gS/m3, respectively. For the outer biofilm layer alone, the ammonia uptake rate increased significantly from 16 mg N/L/h to 111 mg N/L/h with the MABR bulk ORP increase from -80 mV to -50 mV.

Carbon oxidation was another cause to explain the low nitrification rate in the biofilm under low ORP conditions. The BOD_5 and biomass profiles are presented Figure C 6-Figure C 7. Increased bulk ORPs contributed to the oxidation of BOD_5 in the bulk liquid, preventing its diffusion into the biofilm and providing a competitive advantage to nitrifiers in the biofilm. The modeling results indicated a sweet spot range, from – 50 mV to -20mV, for the MABR bulk ORP control. The overall sulfide reduction rates (SRR) and sulfide oxidation rates (SOR) in the biofilm decreased sharply over this range (Figure 4-3b), suggesting the oxygen competition exerted by sulfide oxidation was effectively mitigated. The highest H2S concentration within the system was 0.32 gS/m3, well below the reported value of 1.0 gS/m3 that the activated sludge can tolerate without inhibition effects (Bejarano-Ortiz et al., 2015). Oxygen uptake for carbon oxidation in the biofilm was also approaching to the minimum. The MABR bulk ammonia was maintained at a low value of 2.4 gN/m3, so the fraction of influent ammonia removed in the biofilm was maximized and the effect of ammonia load on the mixed liquor was minimized. The biofilm was able to remove an average of 87.5% of the influent ammonia in this ORP range. With most of the ammonia removed in the biofilm, the process provides added safety factor and resilience if nitrification in the mixed liquor decreases (e.g., due to cold temperatures). The modeling results indicated

minimal improvements when the ORP was increased beyond -20 mV, and further increase led to decreased nitrification oxygen uptake rates in the biofilm because of accelerated ammonia uptakes in the suspended growth (Figure C 8). Also, high ORPs are also not ideal because they might negatively impact the development of denitrifying populations (Silveira et al., 2022; Uri-Carreño et al., 2023).

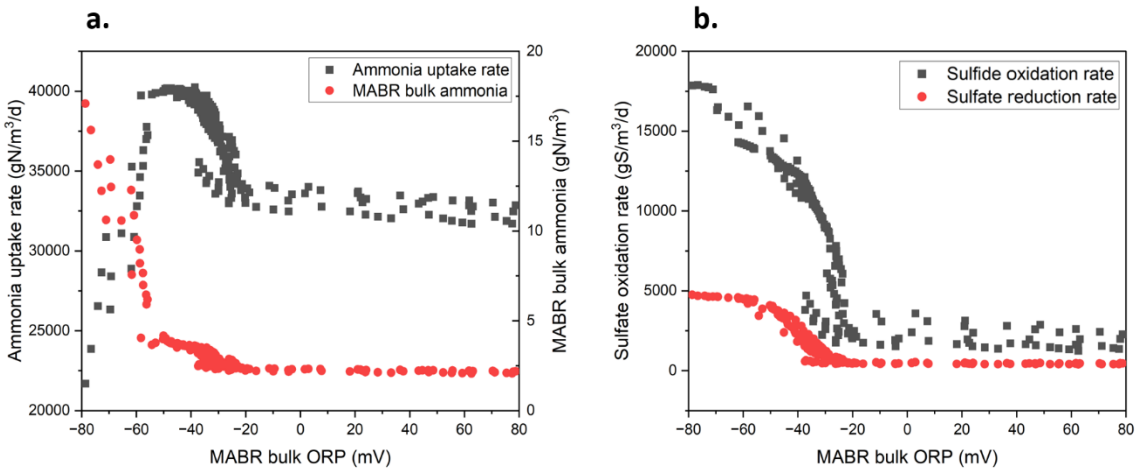

Figure 4-3 Ammonia uptake rate, MABR bulk ammonia concentration, sulfide oxidation rate, and sulfate reduction rate in the biofilm under a range of ORPs.

4.3.2 Biological nitrogen removal performance of the hybrid MABR

Dynamic simulations were conducted to evaluate the biological nitrogen removal performance of the hybrid MABR process under diurnal loadings. The model reflected the changes in air flows, DO concentrations, and nitrogen species concentrations in response to the varying loadings. The DO profiles and aeration supplies under aeration controls are illustrated in Figure C 9-Figure C 10. Overall, the hybrid MABR adjusted to the varying conditions and showed robust nitrogen removal performance. The ammonia loading and removal rate are shown in Figure C 11.

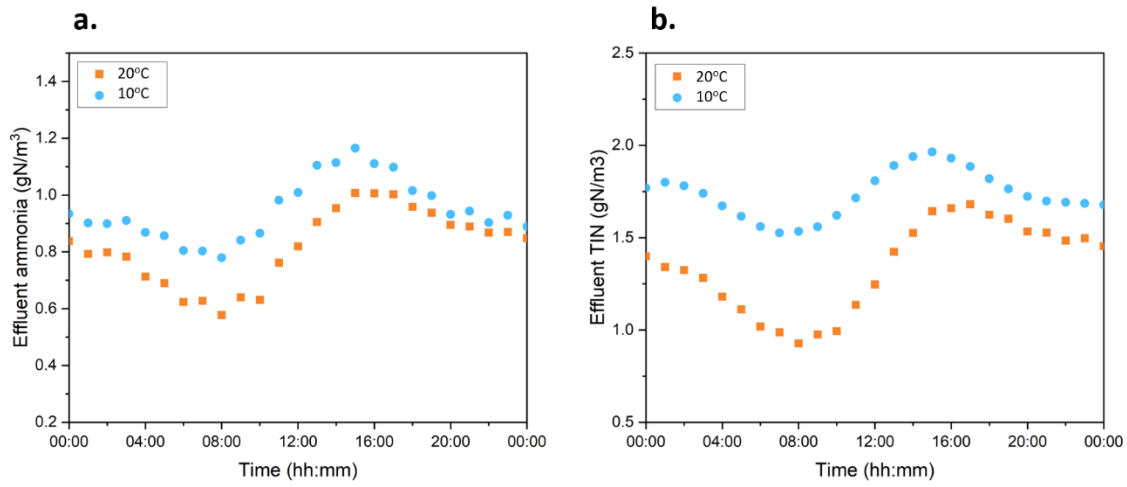

Figure 4-4 Diurnal variations of the ammonia and total inorganic nitrogen (TIN) concentrations in the hybrid MABR effluents under 20oC and 10oC.

At a SRT of 4 days, the hybrid MABR produced high quality effluents regardless of the temperature (Figure 4-4). Under diurnal loadings, the peak concentrations of the effluent ammonia and TIN were 1.0 and 1.6 gN/m^3 at 20ºC. At a colder temperature of 10ºC, the hybrid MABR system could also achieve intensive nitrogen removal without the need to operate at a longer SRT. The peak concentrations of the effluent ammonia and TIN were 1.2 and 1.9 gN/m^3 at 10ºC. This result is significant as for conventional activated sludge, a design SRT longer than 10 days is common for the temperature of 10ºC (Houweling and Daigger, 2019). In the hybrid MABR, the low suspended growth SRT of 4 days can be maintained at 10ºC because nitrification was mostly accomplished in the biofilm. The aeration controls dynamically corresponded to the temperature change, and increased aeration supply and higher DO concentrations at the low temperature compensated the reduced growth rates. At 20ºC, the average AOB and NOB in the biofilm were 10,689 and 7,260 gCOD/m^3, while at 10ºC, their concentrations increased to 12,002 and 8,233 gCOD/m^3, respectively. The activities in the biofilm layers also dynamically changed in response to the temperature change. When the temperature dropped from 20ºC to 10ºC, the biofilm layer closer to the bulk mixed liquor became more active, with the ammonia uptake rates increased from 882 to 927 mgN/L/h. Meanwhile, the ammonia uptake rate in the biofilm layer far most to the bulk mixed liquor decreased from 468 to 361 mgN/L/h. In addition, more nitrifiers shifted to the attached growth in the biofilm when the temperature dropped. At 20ºc, the average AOB and NOB in the biofilm were 10,689 and 7,260 gCOD/m^3, while at 10ºC, their concentrations increased to

12,002 and 8,233 gCOD/m^3, respectively. The results agreed with other studies that the impacts of temperature were masked by the dynamic changes of active layers in the biofilm (Long et al., 2020; Martin et al., 2017).

Table 4-2 Performance comparison for biological nitrogen removal.

Temperature (°C)	20 °C		10 °C	
	Hybrid MABR	MLE	Hybrid MABR	MLE
Operation				
Bioreactor Volume (m3)	4000	4700	4000	12000
MABR Area (m2)	250000	N/A	250000	N/A
MABR Applied Ammonia Flux (g-N/m2-day)	2.4	N/A	2.4	N/A
Suspended Growth SRT (Days)	4	5	4	14
Suspended Growth MLSS (mg/L)	2693	2671	2716	2503
Actual oxygen requirement AOR (kg/day)	3670	3759	3655	4260
Energy				
Aeration energy (kW)*	58. 7	104.4	54.8	118.3
Anoxic mixing/MLR (kW)**	N/A	13.4	N/A	24.4
Effluent quality				
Effluent TIN (mg-N/L)	1.3	3.9	1.7	4.8
Effluent NHx-N (mg-N/L)	0.89	0.84	0.9	0.83
**The calculation assumed: MABR membrane aeration efficiency = 5 kg O2/kW-hr; Suspended growth aeration efficiency = 1.5 kg O2/kW-hr*				
***Anoxic zone mixing energy = 5 W/m3 Mixed Liquor Recirculation rate = 400%. Head = 0.5m. Pump efficiency = 85%.*				

The results above indicated significant performance and economic advantages for the hybrid MABR system. Table 4-2 summarizes a series of comparisons between the hybrid MABR and conventional MLE processes to illustrate these differences. In general, the hybrid MABR process required a lower SRT and smaller bioreactor volumes, while achieving complete

nitrification and more than 50% lower effluent TIN concentration. An average effluent TIN for the MLE process of around 4 gN/m^3 was indicated, which would meet some discharge standards, but not in places like Chesapeake Bay region or Florida (Chesapeake Bay Program, 2023; The Florida Senate, 2022). The hybrid MABR process, however, could further lower the effluent TIN concentrations to be < 2 gN/m^3 even under the cold temperature. The result illustrated the great opportunity for process intensification in existing facilities.

The hybrid MABR provided the most benefit at 10°C. Low water temperature during colder months are often challenges for conventional treatments to successfully achieve desired nitrogen removal. Modeling results also reflect these challenges: for the MLE process at 10°C, the maximum nitrification oxygen uptake rate dramatically decreased to 1.9 $gO_2/m^3/d$, in comparison with the rate of 10.5 $gO_2/m^3/d$ at 20°C. Due to the significantly stressed nitrification activity under the cold temperature, the MLE process required a much longer SRT (14 days) to achieve complete nitrification at 10°C, which translated into a bioreactor volume 3 times larger than the hybrid MABR. In the hybrid MABR system, however, the nitrification activities in the biofilm were relatively insensitive to the temperature drop. The model predicted a nitrification rate in the biofilm of 1.92 $gN/m_2/d$ at 20°C and a slightly higher value of 1.96 $gN/m^2/d$ at 10°C. Under both temperatures, roughly 89% of the influent ammonia was removed in the biofilm. The modeling results are in line with field observations that nitrification in the biofilm was insensitive to the temperature, and the nitrifying activity shifted from the mixed liquor to the biofilm as temperatures decreased (Houweling and Daigger, 2019). With the biofilm adding a safety factor to compensate the nitrification loss, the hybrid MABR process can provide greater benefit when mixed liquor nitrification is stressed, in this case due to the colder temperature. As cold conditions usually govern the bioreactor and SRT design, hybrid MABR provides an opportunity to achieve high quality effluents with a fraction of the bioreactor volume and SRT needed compared to conventional technologies.

Examination of the process energy in Table 4-2 shows that the hybrid MABR produced high effluent quality with an energy consumption half that of the MLE process. The biggest difference comes in the aeration energy consumption. Actual oxygen requirement (AOR) was reduced in the hybrid MABR, and the bubble-less aeration in the MABR lumen greatly improved the aeration efficiency in terms of kgO_2/kwh (Longo et al., 2016). Ancillary energy reductions were in pumping and mixing. In the MLE process, mixed liquor recirculation (MLR), which

recycles the sludge mixture from the aerobic bioreactor to the upstream anoxic bioreactor by pumping (Figure 4-2), is essential for highly efficient nitrogen removal (Grady et al., 2011). As the amount of dentification is controlled by the MLR rate, high MLR rates (400% of the influent flowrate in this study) are typical to ensure high quality effluent. In the hybrid MABR, the nitrifying biofilm upstream can produce nitrate for subsequent denitrification, so MLR is eliminated which cuts the pumping energy further. Mechanical mixing in the anoxic zones is not needed for the hybrid MABR process, so mixing energy can also be saved.

4.3.3 Direct GHG emissions

4.3.3.1 Hybrid MABR significantly reduced N_2O emissions

The model predicted that significant GHG emission reduction can be achieved in the hybrid MABR process along with intensified nitrogen removal performance compared to the conventional alternative. The total GHG emission from the hybrid MABR was 316 kgCO2eq/d, and the value for the MLE process was 3 times higher at 971 kgCO2eq/d (Figure 4-5a). The most significant reduction was in N_2O emissions: 126 kgCO2eq/d from the hybrid MABR vs. 902 kgCO2eq/d from the MLE process.

As depicted in Figure 4-5b, over 70% of the total N_2O emissions for the hybrid MABR process were from the swing zone. Even though the N_2O production rate in the swing zone was low (0.037 mg N/L/h), aeration events intensified gas stripping to the atmosphere and, therefore, led to higher emission rates. MABR off-gas also contributed a considerable fraction of total N_2O emissions (16.3%) as a result of active nitrification activities, while the MABR bulk mixed liquor emitted the least amount of N_2O.

Modeling results are in line with field observations of full-scale MABRs that the counter-diffusional biofilm geometry presented a N_2O sink (Houweling, 2021; Kinh et al., 2017b, 2017a). In the model, N_2O was mainly produced in the middle biofilm layer via the ND pathway (mean production rate = 16 mg N/L/h), while the produced N_2O was most actively consumed in the same biofilm layer via denitrification (15 mg N/L/h). Heterotrophic denitrification also contributed to N_2O production and mostly occurred in the outer biofilm layer (4.1 mg N/L/h). Given that the ND pathway in the biofilm dominated N_2O production, for the hybrid MABR process investigated in

this work, reduced aeration supply in the MABR bulk liquid helped reduce N_2O production in the biofilm as a result of lower nitrification activities.

Greenhouse gases are not created equal. Due to their abilities to absorb heat and long residence time in the atmosphere, N_2O emissions exert the highest greenhouse effect (GWP_{N2O} = 298 GWP_{CO2}), thereby becoming a significant concern relative to global climate change. During biological nitrogen removal, N_2O emissions largely depend on process operation (Soares, 2020). Fluctuating and low DO conditions are well-known factors conductive to produce N_2O emissions, and DO concentrations in the hybrid MABR indeed fluctuated due to diurnal influent loadings and aeration controls. However, N_2O emissions from the hybrid MABR compared favorably with the MLE process. The average N_2O emissions from the hybrid MABR were 0.05 ± 0.02 % of the total nitrogen load, while the value was on average one order of magnitude lower than those from the MLE process (0.4 ± 0.03 %). The results reflect the great potential for the hybrid MABR to achieve intensive nitrogen removal while N_2O emissions remain low. It also brings economic advantages if exhaust gas post-treatment would be implemented to minimize carbon footprint, as the airflow required for exhaust gas post-treatment can be significantly reduced.

N_2O gas emissions from MABRs have been quantified in previous studies, so experimental data are available to be relied upon supporting modeling results. Comparative studies consistently reported lower N_2O emissions from MABRs than from conventional biofilm reactors and activated sludge processes (Houweling, 2021; Kinh et al., 2017b). Several trends of the modeling results in the present study have also been reported in full-scale hybrid MABRs: 1) The MABR off-gas from the membrane lumen emits more N_2O than the MABR bulk mixed liquor. The lack of stripping leads to lower emissions from the MABR bulk, but the N_2O generated by AOBs in the biofilm can escape into the air with the off-gas; 2) N_2O emissions are closely related to aeration events and diurnal variations, with more emissions coinciding with (higher) aeration supply and peak loading events. Future work should undertake to better understand the partitioning of N_2O between the MABR exhaust gas and bulk liquid phases.

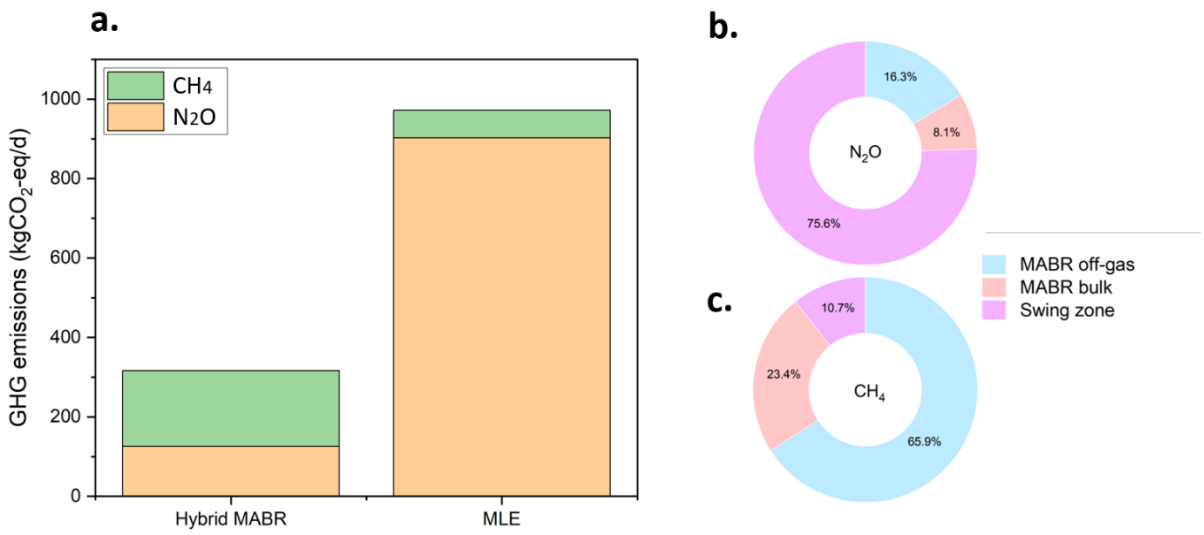

Figure 4-5 a: CH_4, N_2O emissions (normalized to CO2-eq) from the hybrid MABR and MLE process. Partitioning of N_2O (b) and CH_4 (c) between the MABR off-gas, MABR bulk liquid, and swing zone in the hybrid MABR process. The emissions from the secondary clarifier were minimal and not included in the graph.

4.3.3.2 Hybrid MABR emitted more CH_4 because of methanogen growth in the biofilm

Interestingly, CH_4 appeared to be the dominant GHG from the hybrid MABR, accounting for 60% of the total CO_2-eq (Figure 4-5a). In comparison to the CH_4 emission rate of 69.8 $kgCO_2eq/d$ from the MLE process, the CH_4 emission rate from the hybrid MABR was 2.7 times higher (189.9 $kgCO_2eq/d$), although the resulting contribution to total GHG emissions was modest. The majority of the CH_4 emissions in the hybrid MABR were contributed by the membrane off-gas (Figure 4-5c).

Because aerobic conditions prevail in the hybrid MABR and MLE processes, the process most relevant to methane emission is aerobic methane oxidation. A sensitivity analysis evaluated the uncertainty of the parameters used to characterize aerobic methane oxidation. The change of methane emissions from the hybrid MABR for a given change in the parameter values is shown in Figure 4-6a. The most influential parameters were μMOB and bMOB; when varying the μMOB and bMOB between 75% and 125% of their default values, CH4 emissions from the hybrid MABR ranged from 87% to 123% compared to the reference. However, the selection of aerobic methane

oxidation parameters did not change the overall comparison: under all scenarios simulated, the hybrid MABR consistently had at least 1.5 times higher CH4 emissions than the MLE (Figure 4-6b). Detailed data are present in Table C 7. We emphasize the need for experimental data to validate the modeling outcomes.

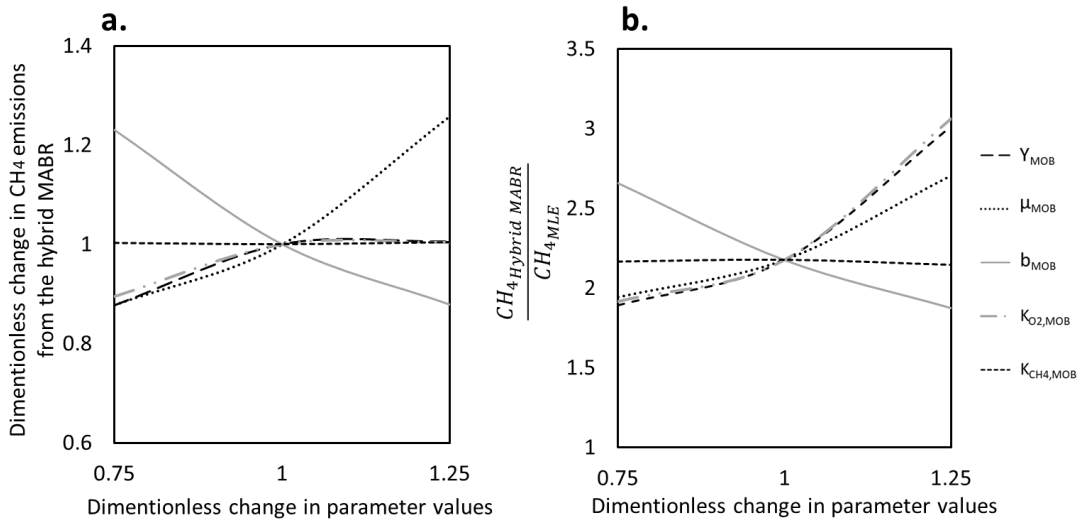

Figure 4-6 Dimensionless change in CH4 emissions from the hybrid MABR (a) and the ratio of total CH4 emissions from the hybrid MABR over the emissions from the MLE (b) versus relative change of methane-oxidizing bacteria yield (YMOB), maximum specific growth rate

In WWTPs, CH_4 emissions take place on the water line under two conditions: 1) anoxic conditions due to anaerobic respiration of methanogens, and 2) aerobic condition because a high aeration rate strips dissolved CH_4 into the atmosphere (Daelman et al., 2014, 2013, 2012; Wang et al., 2021). In our model, it was the first condition that led to the increased CH_4 emissions from the MABR off-gas. Due to the low DO, methanogen biomass was significantly more concentrated in the outer biofilm layer (average biomass concentration = 16.8 gCOD/m^3), while in suspended growth or inner biofilm layers the methanogens biomass was below 0.80 gCOD/m^3 (Figure 4-7). The more concentrated methanogen population in the outer biofilm layer may contribute to active production of CH_4 and increased CH_4 escaping from the membrane lumen. These results suggest that measurements of CH_4 emissions should be made in future studies to provide a holistic picture of direct GHG emissions from the hybrid MABR process.

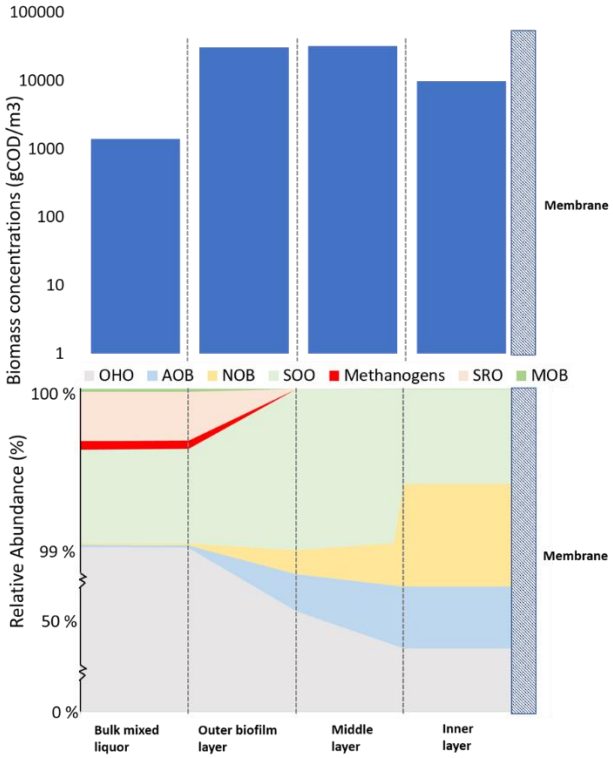

Figure 4-7 Upper: biomass concentrations in the MABR bulk and biofilm layers. Lower: biomass fractions of ammonia oxidizing bacteria (AOB), nitrite oxidizing bacteria (NOB), methanogens (acidoclastic and hydrogenotrophic methanogens), sulfide oxidizing organism (SOO), ordinary heterotrophic organisms (OHO), methane oxidizing bacteria (MOB), and sulfate reducing organisms (SRO).

4.4 Challenges and limitations of the proposed model

The model results presented in this paper demonstrate that the hybrid MABR can achieve resilient nitrogen removal performance with significant energy and GHG reductions. The model will be a useful tool to enable the development, testing and comprehensive evaluation of the hybrid MABR process. In the following section, we discuss the applicability and limitations of the proposed model.

4.4.1 General applicability of the present model

The present model is appropriate to evaluate a hybrid MABR process for biological nitrogen removal. The model of the MABR unit is based on the ZeelungTM MABR and reflects typical design and operational conditions in practice. The MABR unit was sized based on a mid-

size plant design, but it can be scaled to different situations. The mechanistic model consists of consensus kinetic and stoichiometry values that are proven to be robust to describe real-world municipal wastewater treatment plants (Jenkins and Wanner, 2014; Wanner et al., 2006).

The present model did not consider sulfide inhibitions as one of the operational goal was to minimize the the sulfide formation within the. For future extrapolations, incorporating the sulfide inhibition into the mechanistic model may be important if it is of specific interest. Relevant kinetic parameters need experimental efforts as the microbial response to sulfide could be case-specific.

The framework for biofilm reactor modeling practice is fully applicable to the proposed model (Rittmann et al., 2018). Extrapolations of the modeling outcomes to real hybrid MABR plants would require calibration and validation with measured data. Sampling campaign and experiments for data collection should be carefully designed so as to correspond to the operating conditions that are encountered in the practical operation of a hybrid MABR process.

4.4.2 GHG emissions needs experimental validation

The mechanistic models of N_2O and CH_4 production have reached a maturity that facilitates site-specific predictions and development of mitigation strategies, and they are appropriate for this comparative analysis. In this study, the N_2O model incorporated multiple pathways (NN, ND, heterotrophic denitrification), and it is suitable to be used under varying oxygenation conditions (Peng et al., 2015). For systems with constant DO concentrations, other N_2O models may be preferred (Spérandio et al., 2022)

Measured data of N_2O and CH_4 emissions are needed to verify the modeling outcomes. While N_2O emissions have been reported for stand-alone MABR units, the data for the whole hybrid MABR process is still lacking. CH_4 emissions from the hybrid MABR are not available at the present time. The sensitivity analysis indicated that the hybrid MABR had increased CH_4 emissions than the conventional MLE process, regardless of the kinetic values. The modeling results are significant as there are reasons to suggest that there might be increased emissions from the hybrid MABR process over the conventional activated sludge: the oxygen-depleted biofilm layer may provide the ecological niche for methanogen growth. Future research should measure CH_4 emissions from the hybrid MABR to validate the model predictions.

4.4.3 The use of ORP signals for process control

ORP-based oxygenation for setpoint control is not new, and the setpoint values varied for case-specific purposes (Almenglo et al., 2016; Chen et al., 2002; Khanal and Huang, 2003). The value selected in the current model was based on the ORP vs. ammonia uptake rate to maximize the nitrification in the biofilm (Figure 2). As ORP is an indirect signal of the balance between electron donors vs. acceptors within the process, direct adoption of the setpoint value from one study to a different study may not be appropriate. For any extrapolation of this model, characterization of ORP-rate or ORP-concentration correlation is necessary to provide substantial physiological information and determine proper ORP setpoints.

4.5 Conclusions

The main findings from this study are summarized in the following:

1) The model reflected the field observations that low ORPs in the MABR bulk mixed liquor negatively affect nitrification performance in the biofilm. The ORP-based aeration control in the MABR bulk mixed liquor was an effective strategy to mitigate oxygen competition exerted by sulfide oxidation.

2) The hybrid MABR process was resilient against diurnal flow and loading variations and water temperatures. With dynamic loadings, the hybrid process produced high quality effluents (average NHx<1 gN/m^3, TIN<2 gN/m^3) under both 20°C and 10°C scenarios.

3) The hybrid MABR process provided the highest value at the cold temperature (10°C) in comparison with conventional activated sludge (MLE). The hybrid MABR process offers the potential to shrink the bioreactor volume by 3 fold and cut the process energy by half, while also achieving superior nitrogen removal.

4) The total GHG emissions from hybrid MABR process were significantly lower than those from the MLE process. The model suggested increased CH_4 emissions from the MABR off-gas, and future measurements should be made to validate the results.

5) The relative contributions of N_2O and CH_4 emissions were closely related to MABR bulk aeration. With the tradeoff between CH_4 and N_2O emissions, the total direct GHG emissions can potentially be minimized by manipulating the aeration settings.

Reference

Abulimiti, A., Wang, X., Kang, J., Li, L., Wu, D., Li, Z., Piao, Y., Ren, N., 2022. The trade-off between N2O emission and energy saving through aeration control based on dynamic simulation of full-scale WWTP. Water Res. 223, 118961. https://doi.org/10.1016/j.watres.2022.118961

Almenglo, F., Ramírez, M., Gómez, J.M., Cantero, D., 2016. Operational conditions for start-up and nitrate-feeding in an anoxic biotrickling filtration process at pilot scale. Chem. Eng. J. 285, 83–91. https://doi.org/10.1016/j.cej.2015.09.094

Bejarano-Ortiz, D.I., Huerta-Ochoa, S., Thalasso, F., Cuervo-López, F. de M., Texier, A.-C., 2015. Kinetic Constants for Biological Ammonium and Nitrite Oxidation Processes Under Sulfide Inhibition. Appl. Biochem. Biotechnol. 177, 1665–1675. https://doi.org/10.1007/s12010-015-1844-3

Carlson, A.L., He, H., Yang, C., Daigger, G.T., 2021. Comparison of hybrid membrane aerated biofilm reactor (MABR)/suspended growth and conventional biological nutrient removal processes. Water Sci. Technol. wst2021062. https://doi.org/10.2166/wst.2021.062

Chang, M., Liang, B., Zhang, K., Wang, Y., Jin, D., Zhang, Q., Hao, L., Zhu, T., 2022. Simultaneous shortcut nitrification and denitrification in a hybrid membrane aerated biofilms reactor (H-MBfR) for nitrogen removal from low COD/N wastewater. Water Res. 211, 118027. https://doi.org/10.1016/j.watres.2021.118027

Chen, K.-C., Chen, C.-Y., Peng, J.-W., Houng, J.-Y., 2002. Real-time control of an immobilized-cell reactor for wastewater treatment using ORP. Water Res. 36, 230–238. https://doi.org/10.1016/S0043-1354(01)00201-9

Chesapeake Bay Program, 2023. Wastewater [WWW Document]. URL https://www.chesapeakebay.net/issues/threats-to-the-bay/wastewater

Corsino, S.F., Torregrossa, M., 2022. Achieving complete nitrification below the washout SRT with hybrid membrane aerated biofilm reactor (MABR) treating municipal wastewater. J. Environ. Chem. Eng. 10, 106983. https://doi.org/10.1016/j.jece.2021.106983

Côté, P., Peeters, J., Adams, N., Hong, Y., Long, Z., Ireland, J., 2015. A New Membrane-Aerated Biofilm Reactor for Low Energy Wastewater Treatment: Pilot Results. Proc. Water Environ. Fed. 2015, 4226–4239. https://doi.org/10.2175/193864715819540883

Daelman, M.R.J., Van Eynde, T., van Loosdrecht, M.C.M., Volcke, E.I.P., 2014. Effect of process design and operating parameters on aerobic methane oxidation in municipal WWTPs. Water Res. 66, 308–319. https://doi.org/10.1016/j.watres.2014.07.034

Daelman, M.R.J., van Voorthuizen, E.M., van Dongen, L.G.J.M., Volcke, E.I.P., van Loosdrecht, M.C.M., 2013. Methane and nitrous oxide emissions from municipal wastewater treatment – results from a long-term study. Water Sci. Technol. 67, 2350–2355. https://doi.org/10.2166/wst.2013.109

Daelman, M.R.J., van Voorthuizen, E.M., van Dongen, U.G.J.M., Volcke, E.I.P., van Loosdrecht, M.C.M., 2012. Methane emission during municipal wastewater treatment. Water Res. 46, 3657–3670. https://doi.org/10.1016/j.watres.2012.04.024

Delgado Vela, J., Dick, G.J., Love, N.G., 2018. Sulfide inhibition of nitrite oxidation in activated sludge depends on microbial community composition. Water Res. 138, 241–249. https://doi.org/10.1016/j.watres.2018.03.047

Flores-Alsina, X., Uri-Carreno, N., Nielsen, P.H., Gernaey, K.V., 2023. Modelling the impacts of operational conditions on the performance of a full-scale membrane aerated biofilm reactor. Sci. Total Environ. 856, 158980. https://doi.org/10.1016/j.scitotenv.2022.158980

Grady, L., Daigger, G., Love, N., Filipe, C., 2011. Biological Wastewater Treatment, 3rd ed. CRC Press LLC.

Guglielmi, G., Coutts, D., Houweling, D., Peeters, J., 2020. Full-scale application of MABR technology for upgrading and retrofitting an existing WWTP: performances and process modeling. Environ. Eng. Manag. J. 19, 1781–1789. https://doi.org/10.30638/eemj.2020.169

Hauduc, H., Wadhawan, T., Johnson, B., Bott, C., Ward, M., Takács, I., 2019. Incorporating sulfur reactions and interactions with iron and phosphorus into a general plant-wide model. Water Sci. Technol. 79, 26–34. https://doi.org/10.2166/wst.2018.482

He, H., Carlson, A.L., Nielsen, P.H., Zhou, J., Daigger, G.T., 2022. Comparative analysis of floc characteristics and microbial communities in anoxic and aerobic suspended growth processes. Water Environ. Res. 94. https://doi.org/10.1002/wer.10822

He, H., Wagner, B.M., Carlson, A.L., Yang, C., Daigger, G.T., 2021. Recent progress using membrane aerated biofilm reactors for wastewater treatment. Water Sci. Technol. 84, 2131–2157. https://doi.org/10.2166/wst.2021.443

Hiatt, W.C., Grady, C.P.L., 2008. An Updated Process Model for Carbon Oxidation, Nitrification, and Denitrification. Water Environ. Res. 80, 2145–2156. https://doi.org/10.2175/106143008X304776

Houweling, D., 2021. Eliminating N2O Emissions to Zero: ZeeLung^{TM} MABR Shows the Way.

Houweling, D., Daigger, G.T., 2019. Intensifying Activated Sludge Using Media-Supported Biofilms, 1st ed. CRC Press. https://doi.org/10.1201/9780429260278

Houweling, D., Long, Z., Peeters, J., Adams, N., Côté, P., Daigger, G., Snowling, S., 2018. Nitrifying below the "Washout" SRT: Experimental and Modelling Results for a Hybrid MABR / Activated Sludge Process. Proc. Water Environ. Fed. 2018, 1250–1263. https://doi.org/10.2175/193864718825137944

Jenkins, D., Wanner, J., 2014. Activated Sludge - 100 Years and Counting. IWA Publishing.

Khanal, S.K., Huang, J.-C., 2003. ORP-based oxygenation for sulfide control in anaerobic treatment of high-sulfate wastewater. Water Res. 37, 2053–2062. https://doi.org/10.1016/S0043-1354(02)00618-8

Kinh, C.T., Riya, S., Hosomi, M., Terada, A., 2017a. Identification of hotspots for NO and N2O production and consumption in counter- and co-diffusion biofilms for simultaneous nitrification and denitrification. Bioresour. Technol. 245, 318–324. https://doi.org/10.1016/j.biortech.2017.08.051

Kinh, C.T., Suenaga, T., Hori, T., Riya, S., Hosomi, M., Smets, B.F., Terada, A., 2017b. Counter-diffusion biofilms have lower N2O emissions than co-diffusion biofilms during simultaneous nitrification and denitrification: Insights from depth-profile analysis. Water Res. 124, 363–371. https://doi.org/10.1016/j.watres.2017.07.058

Kouba, V., Proksova, H., Wiesinger, H., Vejmelkova, D., Bartacek, J., 2017. Good servant, bad master: sulfide influence on partial nitritation of sewage. Water Sci Technol 76. https://doi.org/10.2166/wst.2017.490

Li, J., Feng, M., Zheng, S., Zhao, W., Xu, X., Yu, X., 2023. The membrane aerated biofilm reactor for nitrogen removal of wastewater treatment: Principles, performances, and nitrous oxide emissions. Chem. Eng. J. 460, 141693. https://doi.org/10.1016/j.cej.2023.141693

Long, Z., Oskouie, A.K., Kunetz, T.E., Peeters, J., Adams, N., Houweling, D., 2020. Simulation of Long-Term Performance of an Innovative Membrane-Aerated Biofilm Reactor. J. Environ. Eng. 146, 04020041. https://doi.org/10.1061/(ASCE)EE.1943-7870.0001705

Longo, S., d'Antoni, B.M., Bongards, M., Chaparro, A., Cronrath, A., Fatone, F., Lema, J.M., Mauricio-Iglesias, M., Soares, A., Hospido, A., 2016. Monitoring and diagnosis of energy consumption in wastewater treatment plants. A state of the art and proposals for improvement. Appl. Energy 179, 1251–1268. https://doi.org/10.1016/j.apenergy.2016.07.043

Luccarini, L., Pulcini, D., Sottara, D., Di Cosmo, R., Canziani, R., 2017. Monitoring denitrification by means of pH and ORP in continuous-flow conventional activated sludge processes. DESALINATION WATER Treat. 61, 319–325. https://doi.org/10.5004/dwt.2017.11119

Martin, K., Sathyamoorthy, S., Houweling, D., Long, Z., Peeters, J., Snowling, S., 2017. A Sensitivity Analysis of Model Parameters Influencing the Biofilm Nitrification Rate: Comparison between the Aerated Biofilm Reactor (MABR) and Integrated Fixed Film Activated Sludge (IFAS) Process. Proc. Water Environ. Fed. 2017, 257–265. https://doi.org/10.2175/193864717822155759

Mei, X., Liu, J., Guo, Z., Li, P., Bi, S., Wang, Yong, Yang, Y., Shen, W., Wang, Yihan, Xiao, Y., Yang, X., Zhou, B., Liu, H., Wu, S., 2019. Simultaneous p-nitrophenol and nitrogen removal in PNP wastewater treatment: Comparison of two integrated membrane-aerated bioreactor systems. J. Hazard. Mater. 363, 99–108. https://doi.org/10.1016/j.jhazmat.2018.09.072

Peeters, J., Adams, N., Long, Z., Côté, P., Kunetz, T., 2017. Demonstration of innovative MABR low-energy nutrient removal technology at Chicago MWRD. Water Pract. Technol. 12, 927–936. https://doi.org/10.2166/wpt.2017.096

Peng, L., Ni, B.-J., Ye, L., Yuan, Z., 2015. Selection of mathematical models for N2O production by ammonia oxidizing bacteria under varying dissolved oxygen and nitrite concentrations. Chem. Eng. J. 281, 661–668. https://doi.org/10.1016/j.cej.2015.07.015

Pocquet, M., Wu, Z., Queinnec, I., Spérandio, M., 2016. A two pathway model for N 2 O emissions by ammonium oxidizing bacteria supported by the NO/N 2 O variation. Water Res. 88, 948–959. https://doi.org/10.1016/j.watres.2015.11.029

Rittmann, B.E., Boltz, J.P., Brockmann, D., Daigger, G.T., Morgenroth, E., Sørensen, K.H., Takács, I., van Loosdrecht, M., Vanrolleghem, P.A., 2018. A framework for good biofilm reactor modeling practice (GBRMP). Water Sci. Technol. 77, 1149–1164. https://doi.org/10.2166/wst.2018.021

Ross, B.N., Lancellotti, B.V., Brannon, E.Q., Loomis, G.W., Amador, J.A., 2020. Greenhouse gas emissions from advanced nitrogen-removal onsite wastewater treatment systems. Sci. Total Environ. 737, 140399. https://doi.org/10.1016/j.scitotenv.2020.140399

Shechter, R., Downing, L., Gordon, K., Nathan, N., 2020. First Full-Scale Activated Sludge Retrofit Using a Spirally-Wound MABR: Results and Model Evaluation. Presented at the Proceedings of the Water Environment Federation. https://doi.org/10.2175/193864718825157591

Silveira, I.T., Cadee, K., Bagg, W., 2022. Startup and initial operation of an MLE-MABR treating municipal wastewater. Water Sci. Technol. 85, 1155–1166. https://doi.org/10.2166/wst.2022.045

Soares, A., 2020. Wastewater treatment in 2050: Challenges ahead and future vision in a European context. Environ. Sci. Ecotechnology 2, 100030. https://doi.org/10.1016/j.ese.2020.100030

Spérandio, M., Lang, L., Sabba, F., Nerenberg, R., Vanrolleghem, P., Domingo-Félez, C., Smets, B.F., Duan, H., Ni, B.-J., Yuan, Z., 2022. Modelling N2O production and emissions, in:

Ye, L., Porro, J., Nopens, I. (Eds.), Quantification and Modelling of Fugitive Greenhouse Gas Emissions from Urban Water Systems. IWA Publishing, pp. 167–196. https://doi.org/10.2166/9781789060461_0167

Sun, Z., Li, M., Wang, G., Yan, X., Li, Y., Lan, M., Liu, R., Li, B., 2020. Enhanced carbon and nitrogen removal in an integrated anaerobic/anoxic/aerobic-membrane aerated biofilm reactor system. RSC Adv. 10, 28838–28847. https://doi.org/10.1039/D0RA04120C

The Florida Senate, 2022. Sweage disposal facilities; advanced and secondary waste treatment [WWW Document]. URL https://m.flsenate.gov/Statutes/403.086

Uri-Carreno, N., Nielsen, P.H., Gernaey, K., Flores-Alsina, X., 2021. Long-term operation assessment of a full-scale membrane-aerated biofilm reactor under Nordic conditions 779. https://doi.org/10.1016/j.scitotenv.2021.146366

Uri-Carreño, N., Nielsen, P.H., Gernaey, K.V., Wang, Q., Nielsen, U.G., Nierychlo, M., Hansen, S.H., Thomsen, L., Flores-Alsina, X., 2023. The effects of low oxidation-reduction potential on the performance of full-scale hybrid membrane-aerated biofilm reactors. Chem. Eng. J. 451, 138917. https://doi.org/10.1016/j.cej.2022.138917

Wang, S., Liu, Q., Li, J., Wang, Z., 2021. Methane in wastewater treatment plants: status, characteristics, and bioconversion feasibility by methane oxidizing bacteria for high value-added chemicals production and wastewater treatment. Water Res. 198, 117122. https://doi.org/10.1016/j.watres.2021.117122

Wang, X., Wu, Y., Chen, N., Piao, H., Sun, D., Ratnaweera, H., Maletskyi, Z., Bi, X., 2022. Characterization of Oxidation-Reduction Potential Variations in Biological Wastewater Treatment Processes: A Study from Mechanism to Application. Processes 10, 2607. https://doi.org/10.3390/pr10122607

Wanner, O., Eberl, H., Morgenroth, E., Noguera, D., Picioreanu, C., Rittmann, B.E., Loosdrecht, M., 2006. Mathematical Modeling of Biofilms. IWA Publishing.

Yang, C., Belia, E., Daigger, G.T., 2022a. Automating process design by coupling genetic algorithms with commercial simulators: a case study for hybrid MABR processes. Water Sci. Technol. 86, 672–689. https://doi.org/10.2166/wst.2022.234

Yang, C., Houweling, D., He, H., Daigger, G.T., 2022b. Available online sensors can be used to create fingerprints for MABRs that characterize biofilm limiting conditions and serve as soft sensors. Water Sci. Technol. 86, 2270–2287. https://doi.org/10.2166/wst.2022.323

Zhou, Z., Xing, C., An, Y., Hu, D., Qiao, W., Wang, L., 2014. Inhibitory effects of sulfide on nitrifying biomass in the anaerobic-anoxic-aerobic wastewater treatment process: Inhibitory effects of sulfide on nitrifying biomass in WWTP. J. Chem. Technol. Biotechnol. 89, 214–219. https://doi.org/10.1002/jctb.4104

CHAPTER V
Conclusions, Significance, and Future Research Needs

5.1 Conclusions and significance

The research objective of this dissertation is to add knowledge to our understanding of the hybrid MABR process for the sustainable biological nutrient removal (BNR) practice. This dissertation specifically focused on a new hybrid MABR concept where the nitrification process primarily occurs in the biofilm component and decouples from the suspended growth. This work began with a literature review that synthesized and updated the present knowledge base about hybrid MABRs, especially with a focus on recent commercial experiences from pilot-, demonstration-, and full-scale systems (Chapter 2). This work then investigated the tradeoffs of eliminating traditional aeration from the suspended growth by providing community-level insights into fully anoxic suspended growth operation (Chapter 3). And finally, taking all the lessoned learned, this dissertation presents a functional dynamic model as a refined example of how the hybrid MABR can be operated to achieve optimal results (Chapter 4). The main conclusions and engineering significance are summarized as follows.

5.1.1 The hybrid MABR intensifies biological nitrogen removal with sustainable features

The hybrid MABR has unique capacities to develop solutions for process intensification, energy savings, and carbon footprint reductions. We find that the benefits offered by the hybrid MABR cannot be denied. The literature review incorporated valuable outcomes from the MABR workshop at the International Water Association (IWA) Biofilms 2020 conference, where we received significant inputs from researchers, practitioners, and MABR vendors. Existing

commercial applications have shown robust simultaneous nitrification and denitrification (SND) and improved nitrification rates in hybrid MABRs. With MABR units dropped in activated sludge tanks, operators are able to increase the biomass inventory and treatment capacity in order to meet stringent discharge standards without additional footprints. The seeding effect of the MABR biofilm also allows complete nitrification under typical suspended growth washout SRTs. The dynamic model indicates that the MABR biofilm adds safety factor and resilience: the activities in the biofilm are relatively insensitive to loading and temperature variations compared with the suspended growth, and the dynamic change of active biofilm layers can mask the effects of varying conditions.

Significantly lower total inorganic nitrogen (TIN) concentration at short SRTs is also achievable in the hybrid MABR. As the MABR is located in the upstream zone of the suspended growth bioreactor, internal mixed liquor recirculation is not required to direct nitrate to the anoxic zone. Essentially all the nitrate generated in the biofilm passes directly into the anoxic zone for denitrification. The dynamic model suggests that a TIN concentration of less than 2 g N/m^3 is achieved in the hybrid MABR at a suspended growth SRT of 4 days. The process also offers the benefits of shrinking the bioreactor volume by 3-fold and cutting the energy consumption by half compared to conventional activated sludge.

Finally, the hybrid MABR can steer companies closer to low carbon and net zero emission goals. The comparative results from dynamic models suggest that the hybrid MABR generates only 1/3 of the total GHG emissions than the conventional activated sludge. This feature of the hybrid MABR will enable climate change mitigation and carbon footprint reduction in biological nitrogen removal processes.

5.1.2 Aeration is important in the suspended growth

Aeration into the suspended growth provides the important function of managing the floc structure. The 16s rRNA gene sequencing and floc morphology examination indicate that flocs developed under the fully anoxic condition lack sufficient filamentous backbones. This translates into easily sheared flocs, reduced flocculation capacity, and reduced non-soluble particles removal. The occurrence of insufficient filaments is well-studied in activated sludge processes. In practice, a standard strategy applied in BNR systems when insufficient filamentous backbones are present

is to provide a modest amount of oxygen into the upstream zone with readily biodegradable organic matter present to encourage the growth of low-DO filaments.

Aeration is also important to control the oxidation-reduction potential (ORP) conditions in the MABR bulk mixed liquor to balance the electron acceptor supply and demand. Recent commercial demonstrations using full-scale MABR modules indicate that low ORP conditions in the bulk mixed liquor surrounding the MABR biofilm negatively correlates to reduced nitrification rate in the biofilm and overall nitrogen removal. The dynamic model suggests that the nitrifiers are outcompeted by ordinary heterotrophs and sulfide oxidizers under low ORP conditions. This unwanted situation can be avoided by providing a modest amount of air into the MABR bulk mixed liquor to balance electron acceptor supply and demand, as indicated by ORP measurements. With the increase in bulk ORPs, carbon oxidation and sulfide oxidation in the biofilm can be minimized so that the nitrification rate in the biofilm is maximized.

Aeration closely relates to process GHG emissions from the hybrid MABR. Intensified aeration events increase the portion of nitrogen being transformed into N_2O as a result of higher nitrifier activities, leading to more N_2O emissions. In contrast, CH_4 emissions decrease with the increase in air supply due to the aerobic methane oxidation process. With the tradeoff between CH_4 and N_2O emissions, the total direct GHG emissions can potentially be minimized by aeration controls.

5.1.3 Extensive knowledge of the activated sludge can be transmitted to the anoxic suspended growth operation

The microbial ecology analysis investigates the inherent microbiological aspects of the suspended growth community adapted to fully anoxic operation. The comparative community-level analysis suggests that the anoxic community and aerobic counterpart developed distinct compositional structures, but their diversity, temporal dynamics, and assemblage patterns are similar. A variety of well-described functional microbial growth in the conventional activated sludge process can sustainably adopt to the anoxic suspended growth. Our findings also highlight the influence of niche-related factors on shaping anoxic community composition. Understanding these conditions and their impacts on the community structure provide insights into process development and maintenance. The fact that their microbial diversity and temporal dynamics are similar suggests that both systems are functioning in a comparable manner. Therefore, our

extensive knowledge of operation and control for aerobic activated sludge processes can generally be applied to anoxic systems.

As discussed in 5.1.2, the "weaker structure" of the anoxic flocs and insufficient filaments are fixable. This occurrence may represent another advantage of the anoxic suspended growth operation, as bulking and foaming issues resulted from excessive filaments will be much less likely to occur. In practice, managing the insufficient filaments situation is more straightforward (by increasing the aeration) than controlling excessive filaments in which multiple operational factors (e.g., SRT, F/M ratio, etc.) may come into play (Daigger, 2023).

5.2 Future research needs

With almost a decade of in-the-field trials and testing, the hybrid MABR technology has matured over recent years. However, it is still a young technology with many research questions and practical considerations to be addressed. Despite the progress made in this dissertation, future research in the following engaging topics remains to be expanded in order to facilitate a wider adoption of hybrid MABR technology.

5.2.1 Modeling practice needs experimental validation

Ultimately, the modelling outcomes need to be tested and validated via prototype processes. The bench-scale hybrid MABR at the Ann Arbor Wastewater Treatment Plant, Michigan, US and pilot-scale process in Nanjing, China will provide opportunities to evaluate the aeration control and operational conditions of interest, and add knowledge to nitrogen removal performance in hybrid MABRs with different municipal wastewater characteristics (Chinese vs. US wastewaters). In both cases, a comprehensive wet chemistry analysis is necessary to measure the concentration profiles within the system, including but not limited to suspended solids, chemical oxygen demand (COD), nitrate, ammonia, and dissolved oxygen (DO). Sampling campaigns and experiments for data collection should be carefully designed to correspond to the operating conditions that are encountered in the practical operation of a hybrid MABR process. Batch tests are needed to quantify the nitrification rate in the biofilm and denitrification rate in the suspended growth in response to different aeration settings. Measured data of N_2O and CH_4 emissions are also important to verify the modeling outcomes.

5.2.2 Microbial ecology in the biofilm needs future investigation

In the hybrid MABR configuration of interest, the MABR biofilm nitrifies the majority of influent ammonia load, and thereby the suspended growth is largely unaerated. Chapter 3 investigated the process microbial ecology in the unaerated suspended growth component for such a hybrid MABR configuration, and more research is needed to characterize the biofilm component. Amplicon gene sequencing coupled with statistical models is needed to provide community level insights as well as tackle the nitrifying populations, i.e., ammonia-oxidizing bacteria (AOBs) and nitrite-oxidizing bacteria (NOBs).

Though the MABR would often be considered as an aerobic biofilm technology given the oxygenation provided through the membrane lumen, a deeper anaerobic biofilm stratum is likely to exist due to the complex internal structure and considerable heterogeneity in the biofilm. The dynamic model indicated a concentrated biomass of methanogens grew in the outer layer of the biofilm and led to increased CH_4 emissions. Future research needs to add biomolecular techniques, such as qPCR and quantitate fluorescent in situ hybridization (FISH), to confirm and quantify the anaerobic populations and their activities in the MABR biofilm.

5.2.3 Aeration controls need optimization

Oxygen deliver into the hybrid MABR process is critical to achieve successful nitrogen removal while achieving significant economic advantages in comparison to the conventional alternatives. The floc characterization in Chapter 3 and modeling practice in Chapter 4 indicate that properly controlled aeration in the hybrid MABR process can bring maximum benefits by optimizing use of the individual system components (biofilm and suspended growth). ORP-based PI control and TIN-based PID control were applied in Chapter 4 with objectives of maximizing the biofilm nitrification rate and overall nitrogen removal efficiency. Many other control strategies, e.g., ammonia-based aeration control (ABAC), have been developed and used in activated sludge, but only limited practice incorporates the control algorithms for the operation in commercial-scale hybrid MABRs. The selection of control strategies is essentially a multi-criteria problem, with several types of objectives (effluent quality, greenhouse gas emissions, and energy consumption) that must be taken into consideration simultaneously. Future research is needed to comparatively

explore the feasibility and techno-economic outcomes of various control algorithms in hybrid MABRs.

5.2.4 Combined biological nitrogen and phosphorus need future investigation

Biological phosphorus removal can occur with addition of an upstream anaerobic zone for hydrolysis of particulate and colloidal organic carbon to generate volatile fatty acids (VFAs) that power phosphorus-accumulating organisms (PAOs). In Chapter 3, we identified that a variety of well-described PAOs and denitrifying PAOs can sustainability adapt to the anoxic suspended growth, but their relative abundances were consistently lower than the populations growing in the aerobic counterpart. Research in parallel (Carlson, 2023) also demonstrated sustained biological phosphorus removal activities in the fully anoxic suspended growth, but less efficient use of VFAs limited the overall performance. Ultimately, the anoxic suspended growth needs to be coupled with the MABR biofilm to form the hybrid MABR process. The underlying questions include what species are functioning and where they are growing (biofilm layers or suspended growth).

A key question is how the sizing of the anaerobic zone would impact biological phosphorus removal as well as nitrogen removal. A sufficiently sized anaerobic zone is required to generate VFAs for successful biological phosphorus removal, while the downstream MABR zone performs nitrogen removal from anaerobically treated wastewater. However, sulfide concentrations in the anaerobic effluent may reach the values needed for inhibition to occur. Future research is needed to properly size the anaerobic zone for VFAs production while minimizing its impact on the MABR biofilm. Combined control strategies, such as flow control along with the ORP-based aeration control, will need further investigation and optimization to avoid the detrimental effects of anaerobic conditions on nitrification.

Reference

Carlson, A. L. (2023) Advanced Analytical Methods for Assessing Biological Nutrient Removal in Membrane Wastewater Treatment Systems. [Doctoral dissertation, University of Michigan]. Deep Blue DOI: https://dx.doi.org/10.7302/7510.

Daigger, G. T. (2023) Personal Communication.

APPENDICES

Appendix A: Supplementary Information for Chapter 2 - IWA MABR Workshop Breakout Session Notes

Date: Dec 6, 2020
Location: Online

A-1 Imagining the Future – Exploring New Applications for MABR; Jeff Peeters, Suez Water Technologies & Solutions

1. Main commercial application today is process intensification – increasing capacity and/or improving nutrient removal in existing tanks
2. Benefits of MABR compared to MBBR/IFAS include:
    a. Much more energy-efficient
    b. Ability to direct oxygen directly to location in process
3. MABR mimics biology – transfer of O_2 and nutrients from the inside rather than outside
4. New/future application ideas:
    a. Improving current application
        i. MABR in aerobic (or swing) reactors
        ii. Integration with EBPR (in biofilm or in suspension)
        iii. Shifting share of biofilm in hybrid process from 25-50% of treatment to 80%+… is there a limit with biofilm thickness control?
        iv. Peak trimming
    b. New applications in wastewater treatment
        i. MABR enabled AMX – mainstream & sidestream
        ii. N2O mitigation and/or recovery

iii.

iv. MABR in a water reuse system, e.g.; in combination with MBR

v. Effluent ammonia polishing, e.g.; overcome high energy costs for MBBR (mixing limited)

c. New applications outside wastewater treatment

i. Transfer of H_2, e.g.; biogas

ii. Transfer of CO_2, e.g.; algae, alkalinity

A-2 MABR Process Engineering: What We Know for Sure, what we are Still Contemplating; Ronen Shechter, Fluence

Discussion subjects

1. Process staging and IFAS mode: what happens downstream at low loading rate / low concentration? How does MABR influence nitrifiers fraction in the ML? How does MABR operate at low ammonia – is it just low rate by Monod or lower?
2. Mixing frequency – not just scouring, also influences mass transfer. We know that (see last slide on my flash presentation Tue). How is it or how should it be considered in process design –and how can it be modeled?
3. Challenges or Suggestions of the design of MABR reactor: (1) Seasonal community change - how to balance it? and (2) Advection based supply of electron donor or acceptor through the membrane.
4. Phosphate removal with MABR? - With a single stage of MABR might be challenging, but hybridization with other techniques would work
5. How operate MABR? especially advection and diffusion. Flux by advection is vulnerable to detachment. So, Advection based MABR is very challenging
6. Hybridization process with MABR in Anoxic tank - Employ Air as a circulating and mixing forc
7. What is the tips for the starting-up MABR? Answer) (1) Having heterotroph base layer is not ideal if you plan to enrich nitrifying biofilm.
8. Treat higher rates in anoxic tanks where ammonia concentrations are highest
9. How much air is needed for internal mixing and for helping advection?

Notes from Jam board

< Session 1 >

1. Treat higher rates in anoxic tanks where ammonia concentrations are highest
2. Super selection of different communities using different approaches and nitrifiers are best for MABR
3. How operate MABR? especially advection and diffusion. Flux by advection is vulnerable to detachment. So, Advection based MABR is very challenging
4. Regarding process staging, the MABR + polishing for biofilm is logical.
5. Challenges or suggestions of the design of MABR reactor: (1) Seasonal community change - how to balance it? and (2) Advection based supply of electron donor and acceptor through the membrane
6. How to design for TN remove - internal circulation into the MABR or a downstream anoxic volume

< Session 2 >

1. Hybridization process with MABR in Anoxic tank - Employ Air as a circulating and mixing force.
2. What are the tips for the starting-up MABR? Answer) (1) Having heterotroph base layer is not ideal if you plan to enrich nitrifying biofilm.....
3. Phosphate removal with MABR? - With a single stage of MABR might be challenging, but hybridization with other techniques would work. How much air is needed for internal mixing and for helping advection?

A-3 MABR Biofilm Thickness Control; Barry Heffernan, Oxymem

Round 1:

1. Difference between pure biofilm and IFAS biofilm with AS in terms of biofilm control and importance:
    a. Carbon process differently: in pure biofilms all carbon is processed in the biofilm, in IFAS with AS carbon is processed by both biofilms and suspended growth
        i.
2. Carbon concentrations or loads, which is more important in terms of impact on biofilm growth
    a. Load gets into the biofilm
    b. High concentration of COD is not a problem for system of treating COD
    c. Low concentration of COD may cause a problem of biofilm thickness for systems doing nitrification because of the potential massive carbon loading for biofilm growth
3. Lessons learned from trickling filters:
    a. Hydraulic application rate to prevent excess biofilm
    b. For MABR biofilms: when is necessary to exert biofilm control and when is not?
4. What problems are caused by excessive biofilms?
    a. Substrate diffusion limitations
    b. Clogging and channeling
    c. the challenge is to let massive flows enter membrane
    d. Mass transfer resistance
    e. Too thick biofilm results in structural problems and biomass loss, need time for its rebuild
    f. Temperature related issues: not seen
5. Can system be less susceptible to the temperature variation due to hot air seeding biofilm & can hot air keep the biofilm temperature:
    a. Hot air cannot change much temperature of system because of the massive thermo mass of water
    b. Heat generated by biodegradation of COD keeps the temperature of liquid
6. Will too thick biofilm cause massive structural loss?

a. A gas scouring system is used to prevent and unclog too thick biofilm
b. Exhausted gas is collected to scour air bubbles onto the biofilm continuously (Suez) or intermittently (OxyMem), also for mixing
c. Oxymem biofilm control: 2-3 mins/day scouring for energy saving, use inert gas to measure biofilm thickness

Round 2:

1. Oxymem biofilm thickness control:
    a. One blower for process air for aeration, and another for large bubbles scouring for thickness control
    b. biofilm thickness indicator, scouring decision processor
    c. Use inert gas (Argon) and pressure decay test to measure relative biofilm thickness, which is used to control the scouring blower
2. Oxymem findings:
    a. For municipal system with pure biofilm: control scouring can increase nitrification rates (more than doubled)
    b. The amount of oxygen transferring the membrane is not changing: too low COD-over aeration-no denitrification
3. Suez biofilm thickness control:
    a. Bubble generators underneath the membrane
    b. Process air collected to generate bubbles for biofilm thickness control and mixing
4. Do you control thickness in hybrid biofilms?
    a. Yes, use the same control system
    b. Self-control: winter-higher SRT-thicker biofilm, summer-lower SRT-thinner biofilm
5. Hybrid MBBR vs. MABR:
    a. MBBR: cannot be placed at the beginning of the plant for nitrification due to outcompete of nitrifiers, no active biofilm thickness control but rely on the shear
    b. MABR: cannot stop nitrification
6. Pure biofilm system:
    a. Nitrifiers are close to membrane
    b. Heterotrophs near bulk liquid
    c. SND
    d. Loading rate controls the thickness is more important than active controls
    e. Biofilm density more important
    f. Enough COD loadings result in no DO in the bulk liquid and SND with no flocs
7. Hybrid biofilm system:
    a. Prefer nitrifiers in the biofilm but heterotrophs in the bulk liquid (never happen)
    b. Competition is always there
    c. MABR cannot be put in an anaerobic tank because O2 and nitrate will consume VFA and inhibit bio-P

8. EPS production in pure and hybrid biofilms:
    a. Differences are expected but more research is needed

A-4 Modeling MABR's; Kelly Gordon, Black & Veatch

Session 1:

1. Question: What MABR question are you trying to answer through modeling, and what type of MABR model do you use to answer it? Why do you choose this model?
    a. What model complexity is required?
        i. Speed is important in terms of number of layers
        ii. 15-20 layers could be an optimum but could be impractical
        iii. What is a reasonable oxygen concentration within the membrane? This can create super-saturation and potential voids in the biofilm.
    b. What is the number of layers, and how does it relate to solving ODEs?
        i. How important is hydrolysis? Rate of attachment and solids transfer of particulates is important, since it makes the top layer appear similar to the bulk liquid sludge
    c. How complex do the models have to be?
2. Sticky notes: (stickies are grouped by theme)
    a. How to model MABRs with regard to complexity:
        i. "How do we include variable density in the layered biofilm models and still maintain the mass transfer between layers?"
        ii. "I am most interested in spatial/continuum models. My background is in fluid/structural interactions. Is it more realistic to have layered biofilms? The layers must be dynamic?
        iii. "My background is to use biofilm models to model granules. My question is that does anyone observe the phenomena that except for oxygen, other substrates (like ammonia, nitrite, nitrate, and phosphorus have a small change in concentration?" - could be caused by number of layers, fully penetrated biofilm, or insufficient biomass (density/thickness)
        iv. "Few years from now how complex are we looking to make our models? Will a "simplified model" be able to still answer our questions?" practicality tradeoff between time and accuracy (think of goal of model and question being asked). Can machine learning be incorporated to make faster, more efficient models?
    b. Metabolisms:
        i. "Anammox + MABR"

3. Overall summary of breakout room themes:
    a. Model complexity in terms of runtime and accuracy

i. Layers vs. continuum
ii. Biomass density
iii. Solids attachment and detachment
iv. Simplified model and machine learning

Session 2:

1. Will void space disturb modeling?
2. How is aeration modeled and what is the impact of scouring? How does this result with modeling biofilm thickness – it makes everything complicated!
3. Do you have continuous vs. discontinuous scouring?
4. How do you measure attachment and detachment?
    a. Biofilm thickness is the key user input and will control the attachment and detachment rate
    b. Need to think about "nitrifier SRT"
    c. Concept of interlayer mixing is important
    d. Not just the outer layer is detached
    e. Impact of seeding?
        i. How is this validated with experimental models?
    f. Are most of the practitioner models using detachment as proportional to thickness?
    g. For anammox MABRs, how important is detachment?
5. For initial conditions for MABR modeling, how important is the starting community? (depend on the question/goal and type of model)
    a. How long is process performance increased for a membrane that is pre-seeded?
    b. Growth rates are important here!
    c. How were the initial conditions in literature chosen?
6. Overall summary of breakout room themes:
    a. Importance of attachment/detachment
        i. interlayer mixing
        ii. Seeding
        iii. Biofilm thickness
        iv. scouring
    b. Seeding and initial conditions

Appendix B: Supplementary Information for Chapter 3

B-1 Code

Please refer to github.com/huanqihe/Anoxicsuspendedgrowth.

B-2 Tables and figures

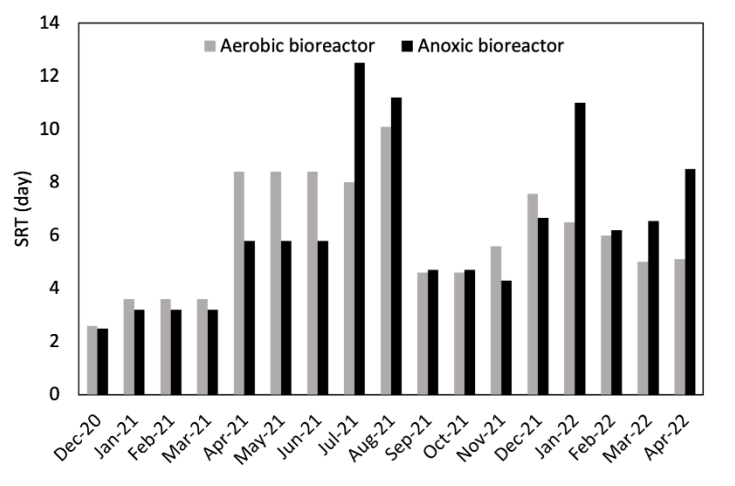

Figure B 1 Monthly average SRTs of the aerobic and anoxic bioreactors from December 2020 to April 2022.

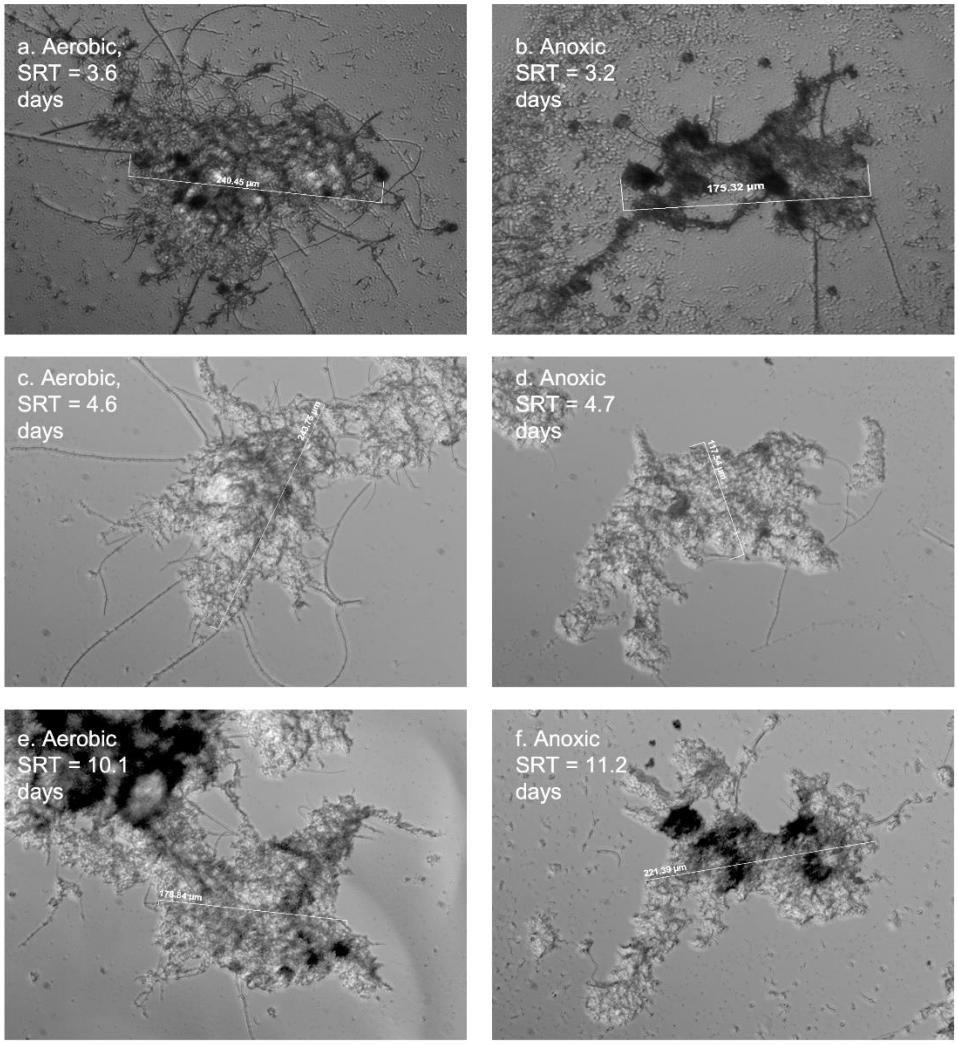

Figure B 2 Aerobic and anoxic flocs observation based on light microscopy examination (200x magnification direct illumination)

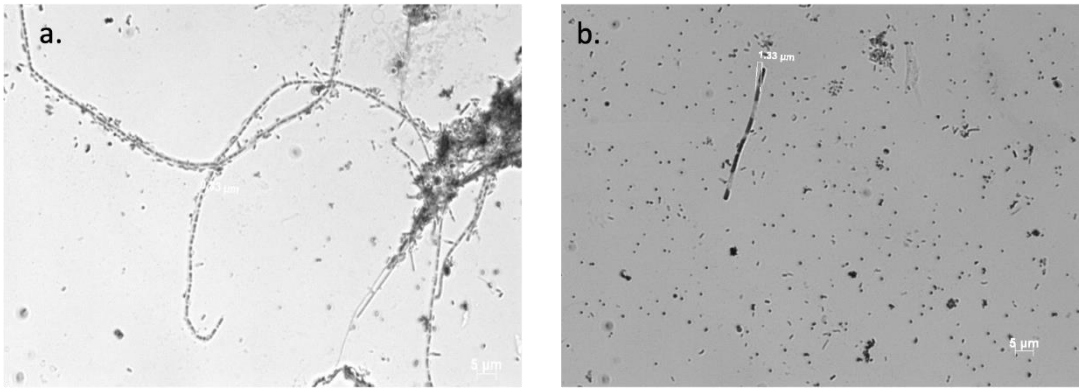

Figure B 3 Dispersed growth observed in the aerobic (a) and anoxic (b) suspended growth under 1000x magnification direct illumination. Suspended growth SRTs: aerobic = 10.1 days, anoxic = 11.2 days.

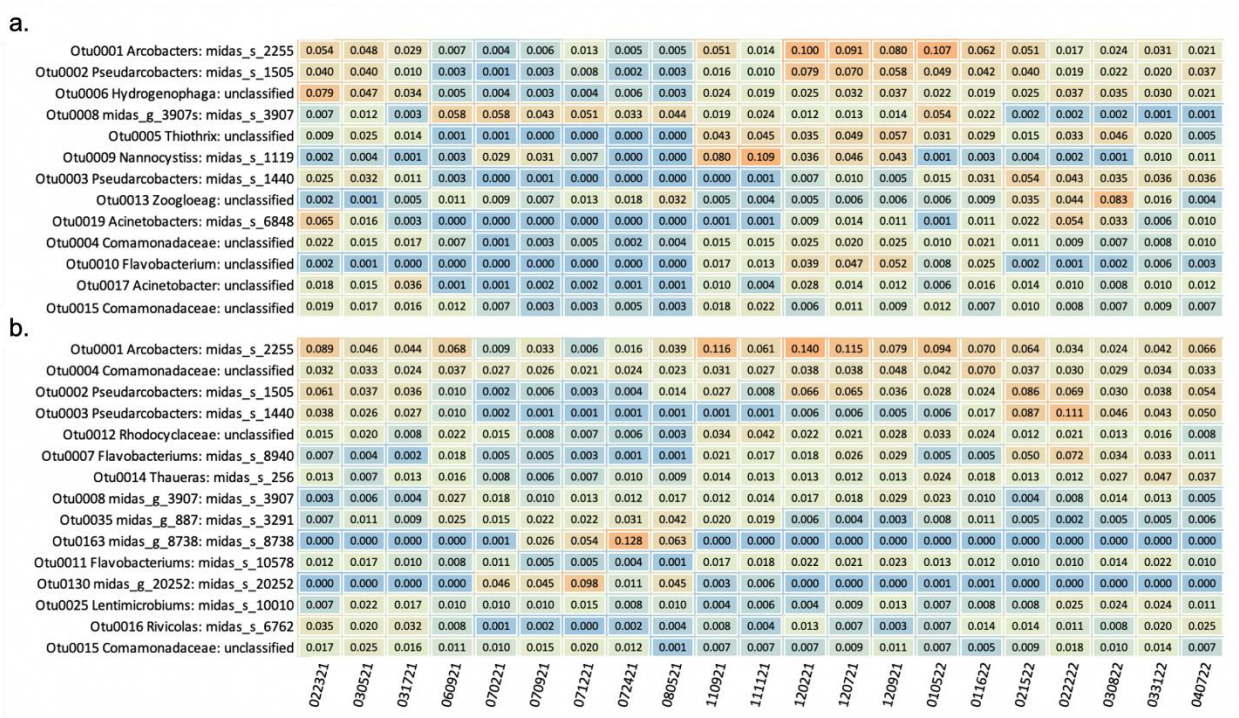

Figure B 4 The taxonomy and relative abundances of the top OTUs (mean relative abundance > 1%) in the aerobic community (a) and anoxic community (b). The x-axis indicated the sampling dates (e.g., 022321 = February 23, 2021).

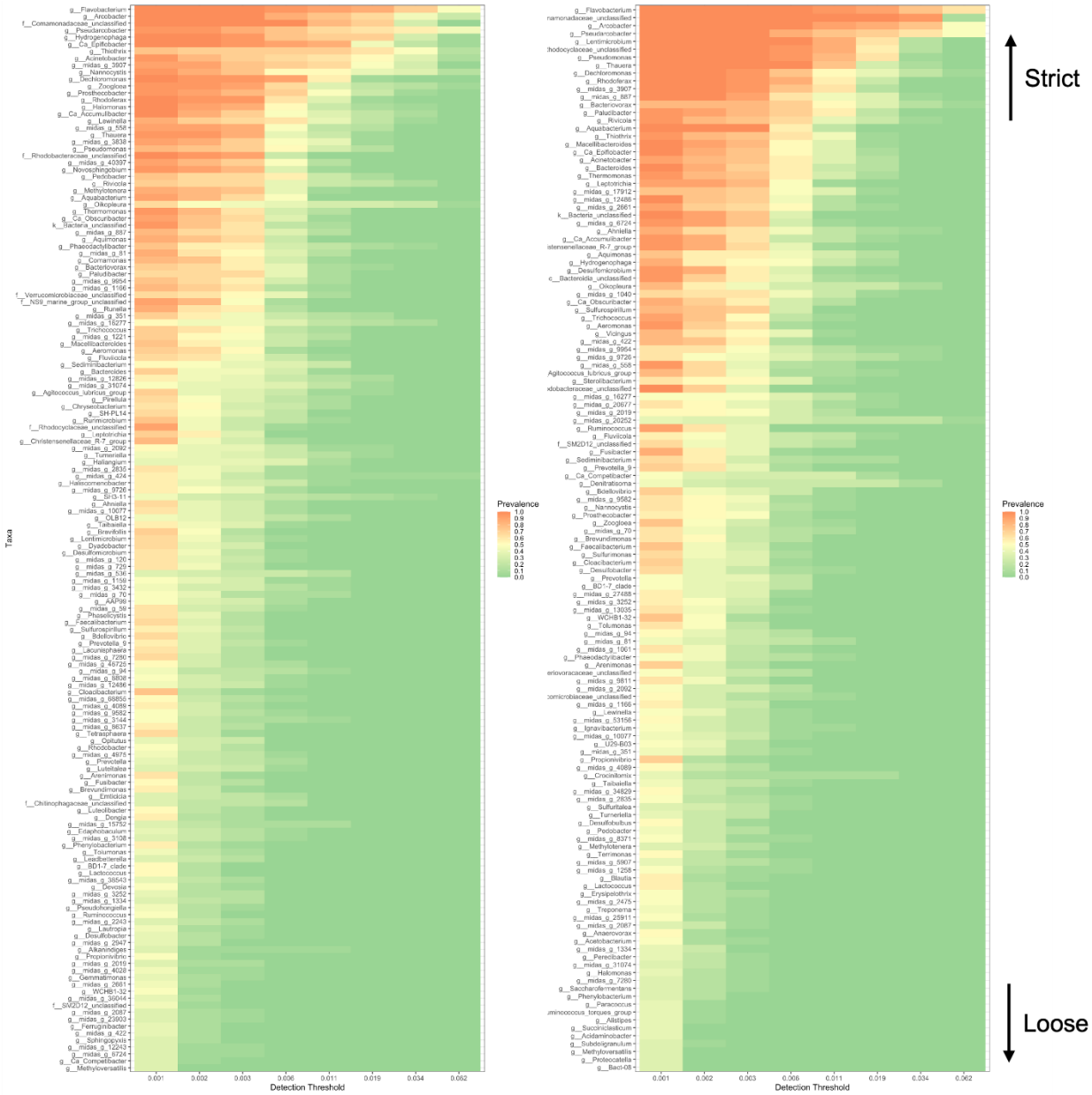

Figure B 5 Core microbiome in the aerobic community (left) and anoxic community (right).

Appendix C: Supplementary Information for Chapter 4

C-1 Code

For codes implemented in this study and the SumoMSN library, please refer to github.com/huanqihe/DynamichybridMABR.

C-2 Tables and figures

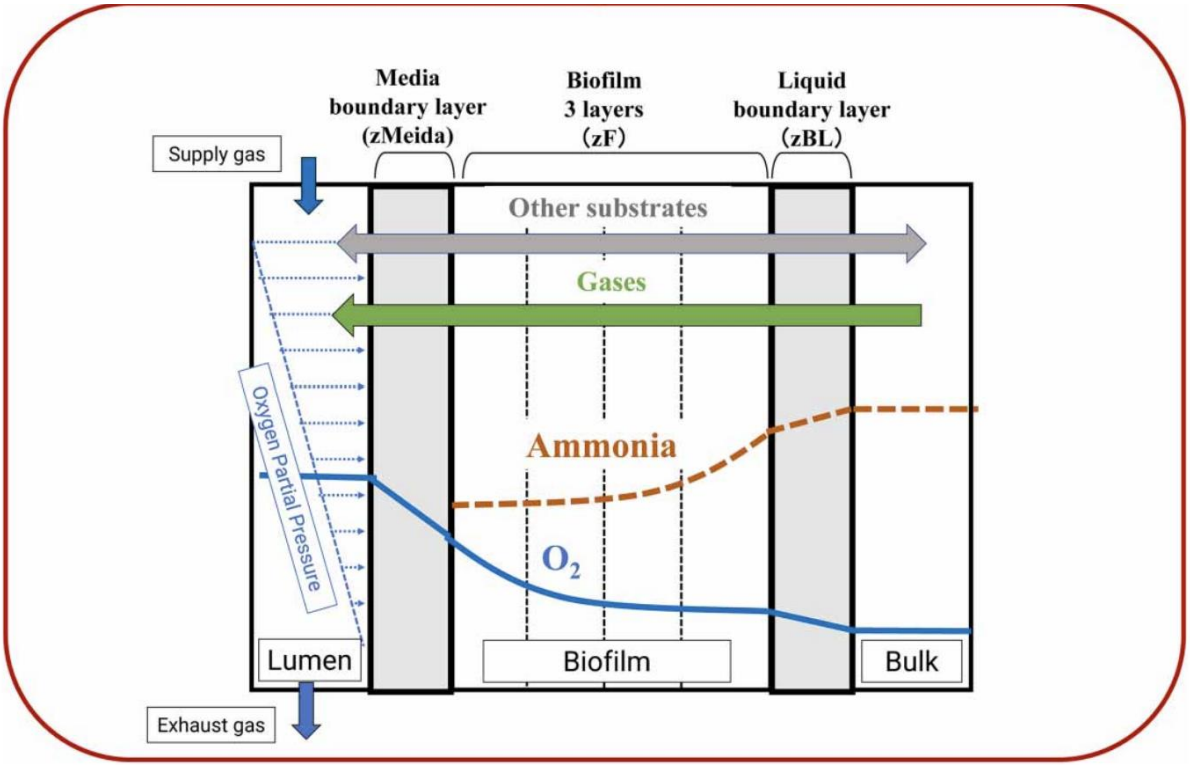

Figure C 1 Schematic presentation of the MABR model by (Yang, Houweling, et al., 2022).

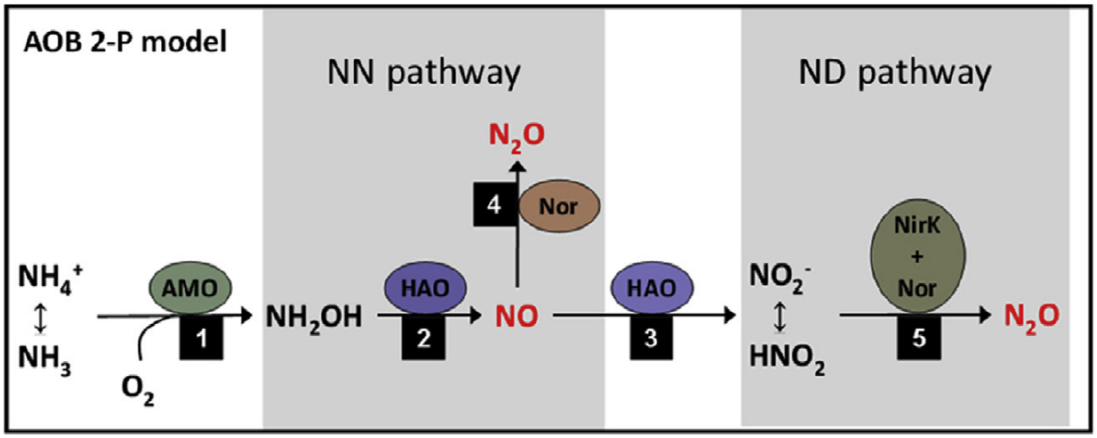

Figure C 2 Schematic presentation of the reactions involved in 4-step nitrification (adopted from (Pocquet, Wu, et al., 2016)).

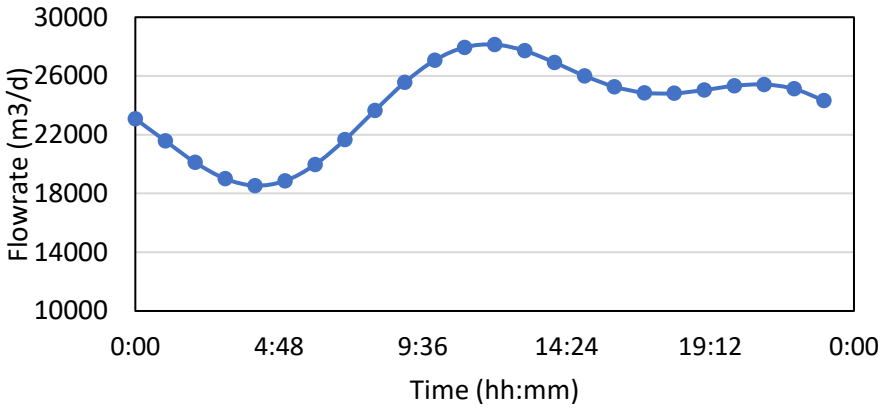

Figure C 3 Diurnal flow of the influent wastewater. Generated by Sumo Influent Tool based on a medium sized plant.

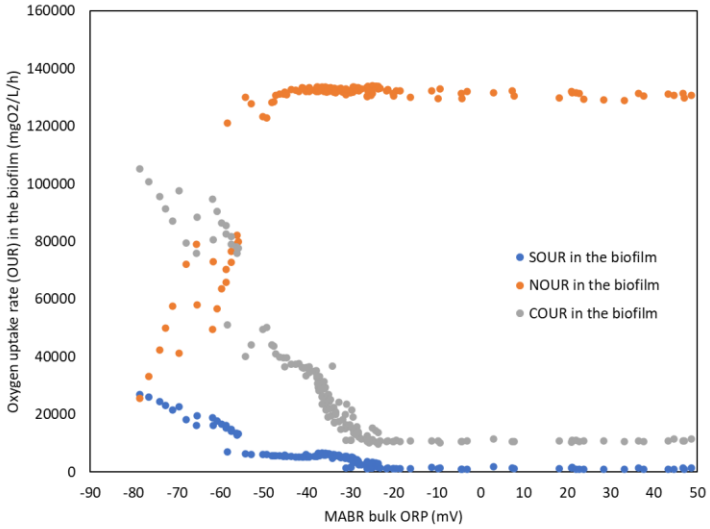

Figure C 4 Oxygen uptake rate for sulfide oxidation (SOUR), nitrification (NOUR) and carbon oxidation (COUR) in the MABR biofilm with different bulk ORPs.

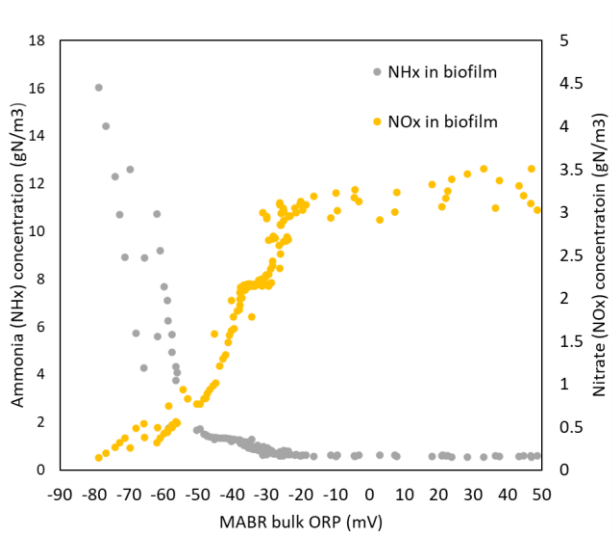

Figure C 5 NOx concentrations in the biofilm along with different ORPs.

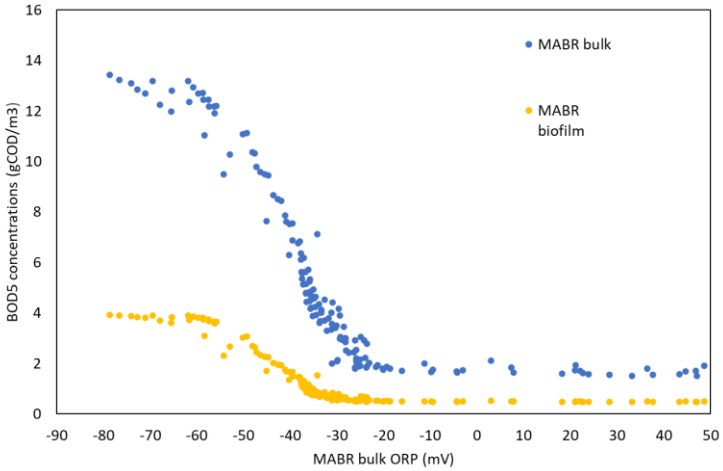

Figure C 6 BOD_5 concentrations in the MABR bulk and biofilm along with different ORPs.

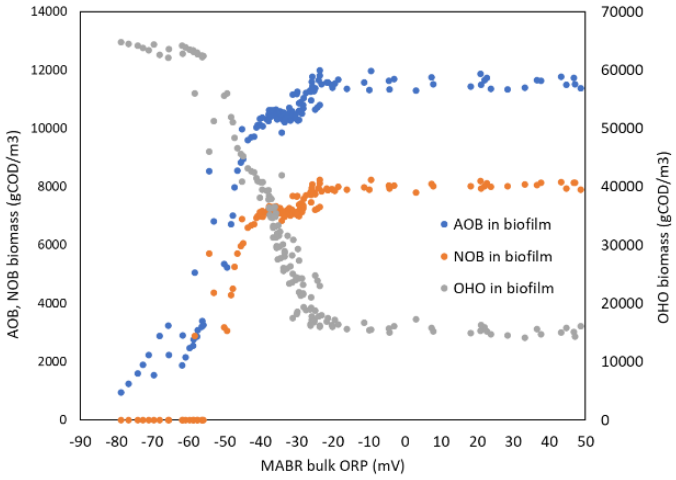

Figure C 7 AOB, NOB, and OHO biomass concentrations in the MABR biofilm along with different ORPs.

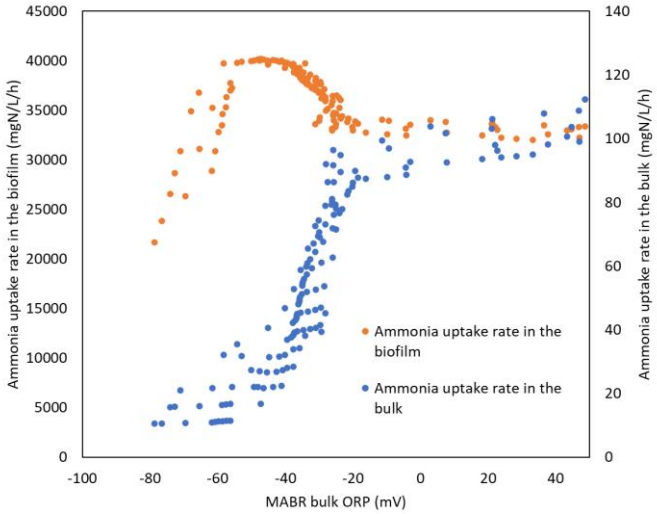

Figure C 8 Ammonia uptake rate in the biofilm and suspended growth bulk mixed liquor along with different bulk ORPs.

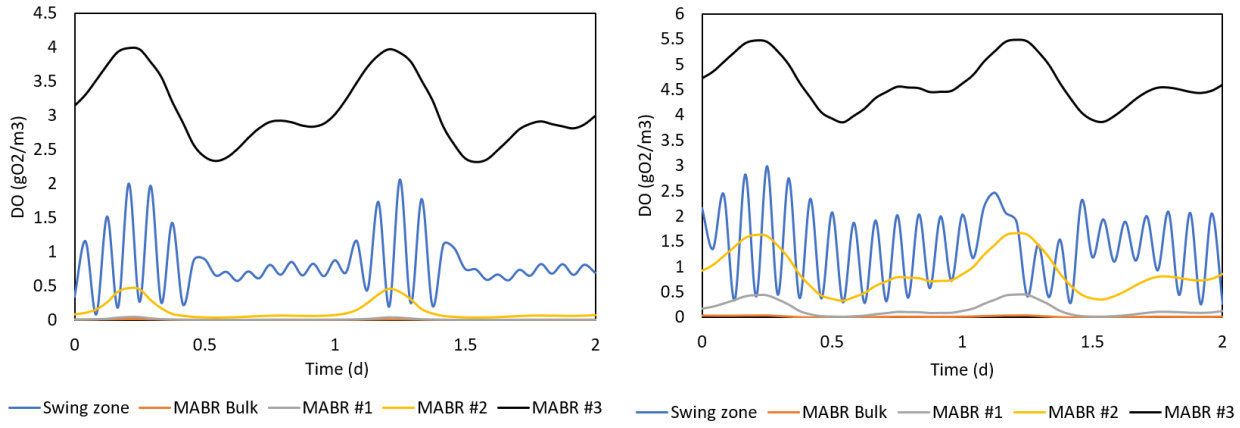

Figure C 9 Dissolved oxygen (DO) profiles in the hybrid MABR process at 20°C (left) and 10°C (right). MABR#1-#3 represents the 3 layers in the biofilm, #1: outer layer adjacent to the MABR bulk mixed liquor; #2: middle layer; #3: inner layer adjacent to the membrane.

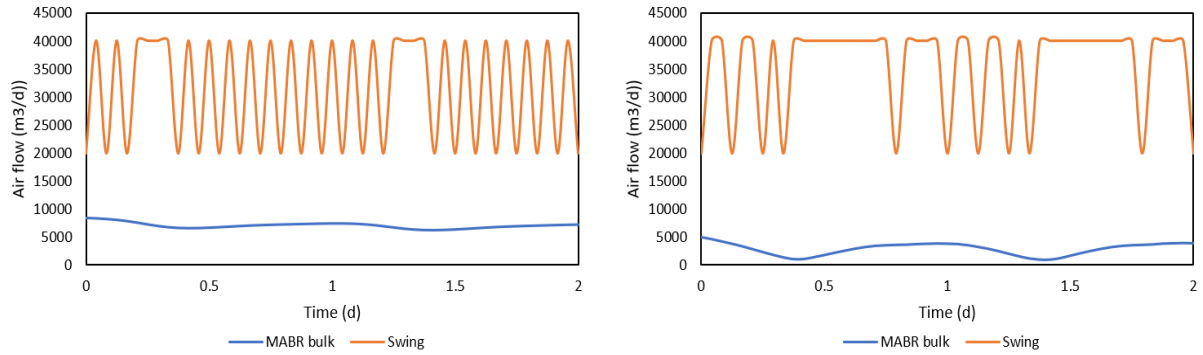

Figure C 10 Air flows into the MABR bulk mixed liquor and swing zone in the hybrid MABR process at 20°C (left) and 10°C (right). Air flows were quantified @ standard conditions (NTP: 20 °C, 1 atm).

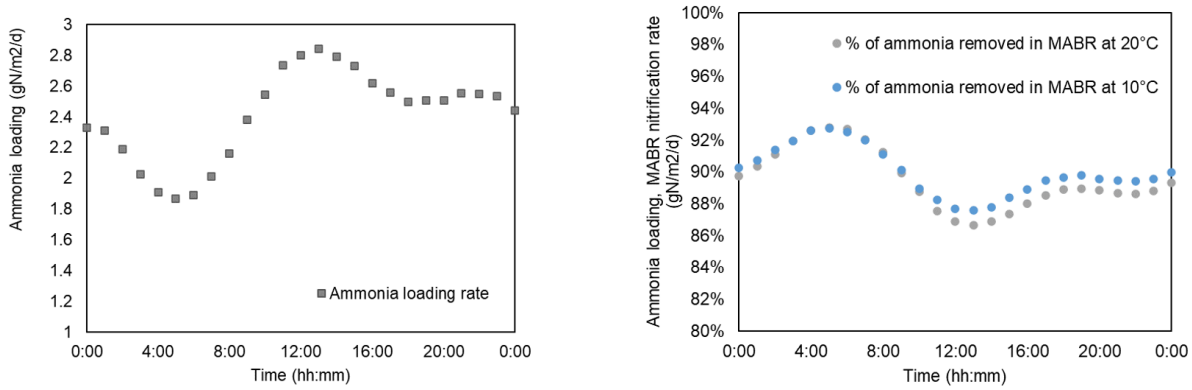

Figure C 11 Ammonia loading rate (left) and ammonia removal percentage in the MABR (right).

Table C 1 MABR biofilm specification setups.

Symbol	Name	Value	Unit
zF	Biofilm thickness	175	mm
zBL	Boundary layer thickness	40	mm
XTSS,spec	Biofilm specific mass	10	gTSS/m^2
n	Number of biofilm layers	3	

Table C 2 ORP kinetic expressions in SumoMSN.

Symbol	Name	Expression	Unit
ORP_{O2}	Oxidation-reduction potential due to dissolved oxygen	$ORP_{base}+(ORP_{max,SO2}-ORP_{base})*S_{O2}/(K_{ORP,SO2}+S_{O2})$	mV
ORP_{NOx}	Oxidation-reduction potential due to dissolved nitrate (anoxic)	$ORP_{base}+(ORP_{max,SNOx}-ORP_{base})*S_{NOx}/(K_{ORP,SNOx}+S_{NOx})$	mV

$S_{H2,CH4,H2S}$	Combined concentration of hydrogen, methane and hydrogen sulfide in COD	$S_{H2} + S_{CH4} + S_{H2S}$	g COD.m^{-3}
$ORP_{H2,CH4,H2S}$	Oxidation-reduction potential due to dissolved hydrogen, methane and hydrogen sulfide (anaerobic)	$ORP_{base} * (S_{H2,CH4,H2S})/(K_{ORP,H2,CH4,H2S} + S_{H2,CH4,H2S})$	mV
ORP	Oxidation-reduction potential	$Max(ORP_{O2;}ORP_{NOx;}ORP_{H2,CH4,H2S})$	mV

Table C 3 ORP constants in SumoMSN.

Symbol	Name	Default Value	Unit
ORP_{base}	Base ORP value	-300	mV
$ORP_{max,SO2}$	ORP max for dissolved oxygen	300	mV
$ORP_{max,SNOx}$	ORP max for dissolved nitrate	70	mV
$K_{ORP,SO2}$	Half-saturation of dissolved oxygen for ORP	0.05	g O2.m^{-3}
$K_{ORP,SNOx}$	Half-saturation of NO_x for ORP	0.1	g N.m^{-3}
$K_{ORP,H2,CH4,H2S}$	Half-saturation of dissolved hydrogen, methane and hydrogen sulfide for anaerobic ORP	5	g COD.m^{-3}

Table C 4 ORP controller settings. Type: Continuous P controller.

Symbol	Name	Value	Unit	Comment
CVsetp	Controlled variable setpoint	-40	mV	
MVmax	Maximum of the manipulated variable	10000	m3/d at NTP	
control	Controller on/off flag	1		
MVmin	Minimum of the manipulated variable	0	m3/d at NTP	
direction	Controller direction (1: direct; -1: inverse)	1	Unitless	E.g. DO-Qair is direct, MLSS-Qwas is inverse
	Controller initialization			
Symbol	Name	Value	Unit	Comment
MV,0	Initial value of manipulated variable	5000	m3/d at NTP	
	Gains			

Symbol	Name	Value	Unit	Comment
KP	Proportional gain	500	m3 gas.d-1 at NTP.mV-1	

Table C 5 Air on/off controller settings. Type: Time based on off controller.

Symbol	Name	Value	Unit
MVhigh	High value of the manipulated variable	40000	m3/d at NTP
MVlow	Low value of the manipulated variable	20000	m3/d at NTP
control	Controller on/off flag	1	
tcycle	Cycle length	2	h
ton	Duration while the manipulated variable (MV) is set to high	1	h
toffset	Start offset	0	h

Table C 6 errorNHx,NOx controller settings. Type: PID controller

Symbol	Name	Value	Unit	Comment
CVsetp	Controlled variable setpoint	0	g N/m3	
MVmin	Minimum of the manipulated variable	0.5	h	
MVmax	Maximum of the manipulated variable	1.5	h	
direction	Controller direction (1: direct; -1: inverse)	-1		E.g. DO-Qair is direct, MLSS-Qwas is inverse
control	Controller on/off flag	1		1 - controller is on, 0 - controller is off
MV,0	Initial value of the manipulated variable	1	h	
tcontrol,min	Controller time step in minutes	10	min	
	Gains			
Symbol	Name	Value	Unit	Comment
KP,PID	Proportional gain	0.1	MVUnit.CVUnit-1	
KI,PID	Integral gain	0.01	MVUnit.CVUnit-1.d-1	
KD,PID	Derivative gain	0.001	MVUnit.CVUnit-1.d	

	Discrete integration			
Symbol	Name	Value	Unit	Comment
n	Number of steps to store for 'I' control	10		

Table C 7 Total CH4 emissions from the hybrid MABR and MLE (kg/d) with changes in kinetic parameters of aerobic methane oxidation from 75%-125%.

Relative change in YMOB	Hybrid MABR	MLE
0.75	4.92	2.59
1	5.61	2.57
1.25	5.64	1.87

Relative change in bMOB	Hybrid MABR	MLE
0.75	6.91	2.59
1	5.61	2.57
1.25	4.93	2.62

Relative change in μMOB	Hybrid MABR	MLE
0.75	4.93	2.53
1	5.61	2.57
1.25	7.06	2.61

Relative change in KO2,MOB	Hybrid MABR	MLE
0.75	5.02	2.61
1	5.61	2.58
1.25	5.63	1.84

Relative change in KCH4,MOB	Hybrid MABR	MLE
0.75	5.62	2.59
1	5.61	2.57
1.25	5.63	2.62

C-3 Key kinetic matrix and rate expressions in the biokinetic model Sumo MSN

Ordinary heterotrophic organisms (OHO) kinetics matrix

j	S_{VFA}	S_B	S_{MEOL}	S_{NHx}	S_{NO3}	S_{NO2}	$S_{NO,OHO}$	S_{N2O}	S_{N2}	S_{O2}	S_{SO4}
1	$-1/Y_{OHO,VFA,ox}$			$-i_{N,BIO}$						$-(1-Y_{OHO,VFA,ox})/Y_{OHO,VFA,ox}$	$-i_{S,BIO}$
2	$-1/Y_{OHO,VFA,anox}$			$-i_{N,BIO}$	$-(1-Y_{OHO,VFA,anox})/(EEQ_{NO2,NO3}*Y_{OHO,VFA,anox})$	$(1-Y_{OHO,VFA,anox})/(EEQ_{NO2,NO3}*Y_{OHO,VFA,anox})$					$-i_{S,BIO}$
3	$-1/Y_{OHO,VFA,anox}$			$-i_{N,BIO}$		$-(1-Y_{OHO,VFA,anox})/(EEQ_{NO,NO2}*Y_{OHO,VFA,anox})$	$(1-Y_{OHO,VFA,anox})/(EEQ_{NO,NO2}*Y_{OHO,VFA,anox})$				$-i_{S,BIO}$
4	$-1/Y_{OHO,VFA,anox}$			$-i_{N,BIO}$			$-(1-Y_{OHO,VFA,anox})/(EEQ_{N2O,NO}*Y_{OHO,VFA,anox})$	$(1-Y_{OHO,VFA,anox})/(EEQ_{N2O,NO}*Y_{OHO,VFA,anox})$			$-i_{S,BIO}$
5	$-1/Y_{OHO,VFA,anox}$			$-i_{N,BIO}$				$-(1-Y_{OHO,VFA,anox})/(EEQ_{N2,N2O}*Y_{OHO,VFA,anox})$	$(1-Y_{OHO,VFA,anox})/(EEQ_{N2,N2O}*Y_{OHO,VFA,anox})$		$-i_{S,BIO}$
6		$-1/Y_{OHO,SB,ox}$		$-i_{N,BIO}$						$-(1-Y_{OHO,SB,ox})/Y_{OHO,SB,ox}$	$-i_{S,BIO}+1/Y_{OH}$

									$_{O,SB,ox}*i_{S,SB}$
7		$-1/Y_{OHO,SB,anox}$	$-i_{N,BIO}$	$-(1-Y_{OHO,SB,anox})/(EEQ_{NO2,NO3}*Y_{OHO,SB,anox})$	$(1-Y_{OHO,SB,anox})/(EEQ_{NO2,NO3}*Y_{OHO,SB,anox})$				$-i_{S,BIO}+1/Y_{OHO,SB,anox}*i_{S,SB}$
8		$-1/Y_{OHO,SB,anox}$	$-i_{N,BIO}$		$-(1-Y_{OHO,SB,anox})/(EEQ_{NO,NO2}*Y_{OHO,SB,anox})$	$(1-Y_{OHO,SB,anox})/(EEQ_{NO,NO2}*Y_{OHO,SB,anox})$			$-i_{S,BIO}+1/Y_{OHO,SB,anox}*i_{S,SB}$
9		$-1/Y_{OHO,SB,anox}$	$-i_{N,BIO}$			$-(1-Y_{OHO,SB,anox})/(EEQ_{N2O,NO}*Y_{OHO,SB,anox})$	$(1-Y_{OHO,SB,anox})/(EEQ_{N2O,NO}*Y_{OHO,SB,anox})$		$-i_{S,BIO}+1/Y_{OHO,SB,anox}*i_{S,SB}$
10		$-1/Y_{OHO,SB,anox}$	$-i_{N,BIO}$				$-(1-Y_{OHO,SB,anox})/(EEQ_{N2,N2O}*Y_{OHO,SB,anox})$	$(1-Y_{OHO,SB,anox})/(EEQ_{N2,N2O}*Y_{OHO,SB,anox})$	$-i_{S,BIO}+1/Y_{OHO,SB,anox}*i_{S,SB}$
11	$(1-Y_{OHO,SB,ana}-Y_{OHO,H2,ana,high})/Y_{OHO,SB,ana}$	$-1/Y_{OHO,SB,ana}$	$-i_{N,BIO}$						$-i_{S,BIO}+1/Y_{OHO,SB,ana}*i_{S,SB}$

12	(1-$Y_{OHO,SB,ana}$-$Y_{OHO,H2,ana,low}$)/$Y_{OHO,SB,ana}$	-1/$Y_{OHO,SB,ana}$		-$i_{N,BIO}$			-$i_{S,BIO}$ + 1/$Y_{OHO,SB,ana}$*$i_{S,SB}$
13			-1/$Y_{OHO,SMEOL,ox}$	-$i_{N,BIO}$		-(1-$Y_{OHO,SMEOL,ox}$)/$Y_{OHO,SMEOL,ox}$	-$i_{S,BIO}$
14				-f_E*($i_{N,XE}$-$i_{N,BIO}$)			(1-f_E)*$i_{S,BIO}$-(1-f_E)*$i_{S,XB}$
15				-f_E*($i_{N,XE}$-$i_{N,BIO}$)			(1-f_E)*$i_{S,BIO}$-(1-f_E)*$i_{S,XB}$

Ordinary heterotrophic organisms (OHO) kinetic rate expressions

j	*Rate*
1	$\mu_{OHO} X_{OHO} \frac{S_{VFA}}{S_{VFA}+K_{VFA}} \frac{S_{O_2}}{S_{O_2}+K_{O_2,OHO}} \frac{S_{NH_X}}{S_{NH_X}+K_{NH_X,BIO}} \frac{S_{PO_4}}{S_{PO_4}+K_{PO_4,BIO}}$
2	$\mu_{OHO} X_{OHO} \eta_{OHO,NO_3} \frac{S_{VFA}}{S_{VFA}+K_{VFA,NO_3}} \frac{S_{NO_3}}{S_{NO_3}+K_{NO_3,OHO}} \frac{K_{O_2,OHO,NO_3}}{S_{O_2}+K_{O_2,OHO,NO_3}} \frac{S_{NH_X}}{S_{NH_X}+K_{NH_X,BIO}} \frac{S_{PO_4}}{S_{PO_4}+K_{PO_4,BIO}}$

3	$\mu_{OHO} X_{OHO} \eta_{OHO,NO_2} \frac{S_{VFA}}{S_{VFA}+K_{VFA,NO_2}} \frac{S_{NO_2}}{S_{NO_2}+K_{NO_2,OHO}} \frac{K_{O_2,OHO,NO_2}}{S_{O_2}+K_{O_2,OHO,NO_2}} \frac{Ki_{NO,OHO,NO_2}}{S_{O_2}+Ki_{NO,OHO,NO_2}} \frac{S_{NH_X}}{S_{NH_X}+K_{NH_X,BIO}} \frac{S_{PO_4}}{S_{PO_4}+K_{PO_4,BIO}}$
4	$\mu_{OHO} X_{OHO} \eta_{OHO,N_2O} \frac{S_{VFA}}{S_{VFA}+K_{VFA,NO}} \frac{S_{NO,OHO}}{K_{NO,OHO}+S_{NO,OHO}+\frac{{S_{NO,OHO}}^2}{Ki_{NO,OHO,NO}}} \frac{K_{O_2,OHO,NO}}{S_{O_2}+K_{O_2,OHO,NO}} \frac{S_{NH_X}}{S_{NH_X}+K_{NH_X,BIO}}$
5	$\mu_{OHO} X_{OHO} \eta_{OHO,N_2O} \frac{S_{VFA}}{S_{VFA}+K_{VFA,N_2O}} \frac{S_{N_2O}}{S_{N_2O}+K_{N_2O,OHO}} \frac{K_{O_2,OHO,N_2O}}{S_{O_2}+K_{O_2,OHO,N_2O}} \frac{Ki_{NO,OHO,N_2O}}{S_{O_2}+Ki_{NO,OHO,N_2O}} \frac{S_{NH_X}}{S_{NH_X}+K_{NH_X,BIO}} \frac{S_{PO_4}}{S_{PO_4}+K_{PO_4,BIO}}$
6	$\mu_{OHO} X_{OHO} \frac{S_B}{S_B+K_{SB}} \frac{K_{VFA}}{S_{VFA}+K_{VFA}} \frac{S_{O_2}}{S_{O_2}+K_{O_2,OHO}} \frac{S_{NH_X}}{S_{NH_X}+K_{NH_X,BIO}} \frac{S_{PO_4}}{S_{PO_4}+K_{PO_4,BIO}}$
7	$\mu_{OHO} X_{OHO} \eta_{OHO,NO_3} \frac{S_B}{S_B+K_{SB,NO_3}} \frac{K_{VFA}}{S_{VFA}+K_{VFA}} \frac{S_{NO_3}}{S_{NO_3}+K_{NO_3,OHO}} \frac{K_{O_2,OHO,NO_3}}{S_{O_2}+K_{O_2,OHO,NO_3}} \frac{S_{NH_X}}{S_{NH_X}+K_{NH_X,BIO}} \frac{S_{PO_4}}{S_{PO_4}+K_{PO_4,BIO}}$
8	$\mu_{OHO} X_{OHO} \eta_{OHO,NO_2} \frac{S_B}{S_B+K_{SB,NO_2}} \frac{K_{VFA}}{S_{VFA}+K_{VFA}} \frac{S_{NO_2}}{S_{NO_2}+K_{NO_2,OHO}} \frac{K_{O_2,OHO,NO_2}}{S_{O_2}+K_{O_2,OHO,NO_2}} \frac{Ki_{NO,OHO,NO_2}}{S_{O_2}+Ki_{NO,OHO,NO_2}} \frac{S_{NH_X}}{S_{NH_X}+K_{NH_X,BIO}} \frac{S_{PO_4}}{S_{PO_4}+K$
9	$\mu_{OHO} X_{OHO} \eta_{OHO,NO} \frac{S_B}{S_B+K_{SB,NO}} \frac{K_{VFA}}{S_{VFA}+K_{VFA}} \frac{S_{NO}}{S_{NO_3}+K_{NO,OHO}} \frac{K_{O_2,OHO,NO}}{S_{O_2}+K_{O_2,OHO,NO}} \frac{S_{NH_X}}{S_{NH_X}+K_{NH_X,BIO}} \frac{S_{PO_4}}{S_{PO_4}+K_{PO_4,BIO}}$
10	$\mu_{OHO} X_{OHO} \eta_{OHO,N_2O} \frac{S_B}{S_B+K_{SB,N_2O}} \frac{K_{VFA}}{S_{VFA}+K_{VFA}} \frac{S_{N_2O}}{S_{N_2O}+K_{N_2O,OHO}} \frac{K_{O_2,OHO,N_2O}}{S_{O_2}+K_{O_2,OHO,N_2O}} \frac{Ki_{NO,OHO,N_2O}}{S_{O_2}+Ki_{NO,OHO,N_2O}} \frac{S_{NH_X}}{S_{NH_X}+K_{NH_X,BIO}} \frac{S_{PO_4}}{S_{PO_4}+K$
11	$\mu_{FERM,OHO} X_{OHO} S_{VFA} \frac{S_{VFA}}{S_{VFA}+K_{VFA,FERM} e^{[(K_{VFA}-S_{VFA})]/(\left(-1\times\frac{2}{K_{VFA,FERM}\times Lograng e_{VFA,FERM}}\right)\times\ln\left(\frac{1}{19}\times\left(1+\frac{1}{2}\times\left(K_{VFA,FERM}\frac{Lograng e_{VFA,FERM}}{K_{VFA,FERM}}\right)\right)\right.}} \times \frac{S_B}{S_B+K_{SB,ana}} \frac{K_{O_2,OHO}}{S_{O_2}+K_{O_2,OHO}} \frac{K_{NO_2,OHO}}{S_{NO_2}+K_{NO_2,OHO}} \frac{K_{NO_3,OHO}}{S_{NO_3}+K_{NO_3,OHO}} \frac{S_{NH_X}}{S_{NH_X}+K_{NH_X,BIO}} \frac{S_{PO_4}}{S_{PO_4}+K_{PO_4,BIO}}$
12	$\mu_{FERM,OHO} X_{OHO} (1 - S_{VFA} \frac{S_{VFA}}{S_{VFA}+K_{VFA,FERM} e^{[(K_{VFA}-S_{VFA})]/(\left(-1\times\frac{2}{K_{VFA,FERM}\times Lograng e_{VFA,FERM}}\right)\times\ln\left(\frac{1}{19}\times\left(1+\frac{1}{2}\times\left(K_{VFA,FERM}\frac{Lograng e_{VFA,FERM}}{K_{VFA,FERM}}\right)\right)\right)\right)]}}) \frac{S_B}{S_B+K_{SB,ana}}$

	$\frac{K_{O_2,OHO}}{S_{O_2}+K_{O_2,OHO}}\frac{K_{NO_2,OHO}}{S_{NO_2}+K_{NO_2,OHO}}\frac{K_{NO_3,OHO}}{S_{NO_3}+K_{NO_3,OHO}}\frac{S_{NH_X}}{S_{NH_X}+K_{NH_X,BIO}}\frac{S_{PO_4}}{S_{PO_4}+K_{PO_4,BIO}}$
13	$\mu_{OHO}X_{OHO}\frac{S_{MEOL}}{S_{MEOL}+K_{MEOL,OHO}}\frac{S_{O_2}}{S_{O_2}+K_{O_2,OHO}}\frac{S_{NH_X}}{S_{NH_X}+K_{NH_X,BIO}}\frac{S_{PO_4}}{S_{PO_4}+K_{PO_4,BIO}}$
14	$b_{OHO}X_{OHO}+\left(\frac{S_{O_2}}{S_{O_2}+K_{O_2,OHO}}+\eta_{b,anox}\frac{S_{NO_2}}{S_{NO_2}+K_{NO_2,OHO}}\frac{K_{O_2,OHO}}{S_{O_2}+K_{O_2,OHO}}+\eta_{b,anox}\frac{S_{NO_3}}{S_{NO_3}+K_{NO_3,OHO}}\frac{K_{NO_2,OHO}}{S_{NO_2}+K_{NO_2,OHO}}\frac{K_{O_2,OHO}}{S_{O_2}+K_{O_2,OHO}}\right)$
15	$b_{OHO}X_{OHO}\eta_{b,ana}\frac{K_{NO_2,OHO}}{S_{NO_2}+K_{NO_2,OHO}}\frac{K_{NO_3,OHO}}{S_{NO_3}+K_{NO_3,OHO}}\frac{K_{O_2,OHO}}{S_{O_2}+K_{O_2,OHO}}$

Ammonia-oxidizing bacteria (AOB) kinetics matrix

j	X_{AOB}	S_{NHx}	S_{NH2OH}	S_{NO2}	$S_{NO,AOB}$	S_{N2O}	S_{O2}	S_{SO4}
1		-1	1				$-EEQ_{NH2OH}$	
2	1	$-i_{N,BIO}$	$-1/Y_{AOB}$		$1/Y_{AOB}$		$-(EEQ_{NH2OH,NO}-Y_{AOB})/Y_{AOB}$	$-i_{S,BIO}$
3				1	-1		$-EEQ_{NO,NO2}$	
4			-1	1	-4	4		
5			-1	-1		2		
6	-1	$-f_E*(i_{N,XE}-i_{N,BIO})$						$(1-f_E)*i_{S,BIO}-(1-f_E)*i_{S,XB}$
7	-1	$-f_E*(i_{N,XE}-i_{N,BIO})$						$(1-f_E)*i_{S,BIO}-(1-f_E)*i_{S,XB}$

Ammonia-oxidizing bacteria (AOB) kinetic rate expressions

j	*Rate*
1	$\mu_{AOB}X_{AOB}\frac{S_{O_2}}{S_{O_2}+K_{O_2,AOB}}\frac{S_{NH_X}}{S_{NH_X}+K_{NH_X,AOB}}\frac{S_{NH_X}}{S_{NH_X}+K_{NH_X,NH2OH,AOB}}$
2	$\mu_{AOB}X_{AOB}\frac{S_{O_2}}{S_{O_2}+K_{O_2,NH2OH,AOB}}\frac{S_{NH_X}}{S_{NH_X}+K_{NH_X,AOB}}\frac{S_{NH2OH}}{S_{NH2OH}+K_{NH_X,NH2OH,AOB}}$

j	*Rate*
3	$\mu_{AOB} X_{AOB} \frac{S_{O_2}}{S_{O_2} + K_{O_2,NH2OH,AOB}} \frac{S_{NO}}{S_{NO} + K_{NO,NO2,AOB}}$
4	$\mu_{AOB} X_{AOB} \mu_{AOB,NO,N2O} \frac{S_{NH2OH}}{S_{NH2OH} + K_{NH_X,NH2OH,AOB}} \frac{S_{NO}}{S_{NO} + K_{NO,N2O,AOB}}$
5	$\mu_{AOB} X_{AOB} \mu_{AOB,NO2,N2O} \frac{S_{O_2}}{S_{O_2} + K_{O_2,NH2OH,AOB}} \frac{S_{HNO_2}}{S_{HNO_2} + K_{NH_X,NH2OH,AOB}} \frac{Ki_{O_2,AOB}}{S_{O_2} + Ki_{O_2,AOB}}$
6	$b_{AOB} X_{AOB} (\frac{S_{O_2}}{S_{O_2}+K_{O_2,AOB}} + \eta_{b,anox} \frac{S_{NO_x}}{S_{NO_x}+K_{NO_x,AOB}} \frac{K_{O_2,AOB}}{S_{O_2}+K_{O_2,AOB}})$
7	$b_{AOB} X_{AOB} (\eta_{b,ana} \frac{K_{NO_x,AOB}}{S_{NO_x}+K_{NO_x,AOB}} \frac{K_{O_2,AOB}}{S_{O_2}+K_{O_2,AOB}} + m_{tox,ana})$

Nitrite-oxidizing bacteria (NOB) kinetic matrix

j	X_{NOB}	S_{NHx}	S_{NO3}	S_{NO2}	S_{O2}	S_{SO4}
1	1	$-i_{N,BIO}$	$1/Y_{NOB}$	$-1/Y_{NOB}$	$-(EEQ_{NO2,NO3}-Y_{NOB})/Y_{NOB}$	$-i_{S,BIO}$
2	-1	$-f_E*(i_{N,XE}-i_{N,BIO})$				$(1-f_E)*i_{S,BIO}-(1-f_E)*i_{S,XB}$
3	-1	$-f_E*(i_{N,XE}-i_{N,BIO})$				$(1-f_E)*i_{S,BIO}-(1-f_E)*i_{S,XB}$

Nitrite-oxidizing bacteria (NOB) kinetic rate expressions

j	*Rate*
1	$\mu_{NOB} X_{NOB} \frac{S_{NO_2}}{S_{NO_2} + K_{NO_2,NOB}} \frac{S_{O_2}}{S_{O_2} + K_{O_2,NOB}} \frac{S_{NH_X}}{S_{NH_X} + K_{NH_X,BIO}} \frac{S_{PO_4}}{S_{PO_4} + K_{PO_4,BIO}}$
2	$b_{NOB} X_{NOB} (\frac{S_{O_2}}{S_{O_2}+K_{O_2,NOB}} + \eta_{b,anox} \frac{S_{NO_x}}{S_{NO_x}+K_{NO_x,NOB}} \frac{K_{O_2,NOB}}{S_{O_2}+K_{O_2,NOB}})$
3	$b_{NOB} X_{NOB} (\eta_{b,ana} \frac{K_{NO_x,NOB}}{S_{NO_x}+K_{NO_x,NOB}} \frac{K_{O_2,NOB}}{S_{O_2}+K_{O_2,NOB}} + m_{tox,ana})$

Methane oxidizing bacteria (MOB) kinetic matrix

j	S_{NHx}	$X_{N,B}$	S_{PO4}	$X_{P,B}$	S_{O2}	S_{CH4}	S_{CO2}	S_{SO4}	X_{MOB}
1	$-i_{N,BIO}$		$-i_{P,BIO}$		$-(1-Y_{MOB})/Y_{MOB}$	$-1/Y_{MOB}$	$i_{CIT,CH4}/Y_{MOB}-i_{CIT,BIO}$	$-i_{S,BIO}$	1

2	$-f_E*(i_{N,XE}-i_{N,BIO})$	$(1-f_E)*i_{N,BIO}$	$(1-f_E)*i_{P,BIO}$	$(1-f_E)*(i_{CIT,BIO}-i_{CIT,SB})$	$(1-f_E)*i_{S,BIO}-(1-f_E)*i_{S,XB}$	-1

Methane oxidizing bacteria (MOB) kinetic rate expressions

j	*Rate*
1	$\mu_{MOB} X_{NMOB} \frac{S_{O_2}}{S_{O_2} + K_{O_2,MOB}} \frac{S_{CH_4}}{S_{CH_4} + K_{CH_4,MOB}}$
2	$b_{MOB} \cdot X_{MOB}$

1. Key model parameters

	Ordinary heterotrophic organism kinetics (OHO)	**Type(Kinetic)**	
Symbol	Name	Default	Unit
μ_{OHO}	Maximum specific growth rate of OHOs	4.0	d^{-1}
$\mu_{FERM,OHO}$	Fermentation growth rate of OHOs	0.3	d^{-1}
b_{OHO}	Decay rate of OHOs	0.62	d^{-1}
$\eta_{OHO,NO3}$	Reduction factor for anoxic growth of OHOs on NO_3	0.28	unitless
$\eta_{OHO,NO2}$	Reduction factor for anoxic growth of OHOs on NO_2	0.16	unitless
$\eta_{OHO,NO}$	Reduction factor for anoxic growth of OHOs on NO	0.35	unitless
$\eta_{OHO,N2O}$	Reduction factor for anoxic growth of OHOs on N2O	0.35	unitless
$K_{SB,AS}$	Half-saturation of readily biodegradable substrate for OHOs (AS)	5.0	g COD.m^{-3}
$K_{SB,NO3,AS}$	Half-saturation of readily biodegradable substrate for OHOs on NO_3 (AS)	5.0	g COD.m^{-3}
$K_{SB,NO2,AS}$	Half-saturation of readily biodegradable substrate for OHOs on NO_2 (AS)	5.0	g COD.m^{-3}
$K_{SB,NO,AS}$	Half-saturation of readily biodegradable substrate for OHOs on NO (AS)	5.0	g COD.m^{-3}
$K_{SB,N2O,AS}$	Half-saturation of readily biodegradable substrate for OHOs on N2O (AS)	5.0	g COD.m^{-3}
$K_{O2,OHO,AS}$	Half-saturation of O_2 for OHOs (AS)	0.15	g O_2.m^{-3}
$K_{O2,OHO,NO3,AS}$	Half-saturation of O_2 for OHOs on NO_3 (AS)	0.15	g O_2.m^{-3}
$K_{O2,OHO,NO2,AS}$	Half-saturation of O_2 for OHOs on NO_2 (AS)	0.15	g O_2.m^{-3}
$K_{O2,OHO,NO,AS}$	Half-saturation of O_2 for OHOs on NO (AS)	0.15	g O_2.m^{-3}

$K_{O2,OHO,N2O,AS}$	Half-saturation of O_2 for OHOs on N2O (AS)	0.15	g O_2.m^{-3}
$K_{VFA,AS}$	Half-saturation of VFA for OHOs (AS)	0.5	g COD.m^{-3}
$K_{VFA,NO3,AS}$	Half-saturation of VFA for OHOs on NO_3 (AS)	0.5	g COD.m^{-3}
$K_{VFA,NO2,AS}$	Half-saturation of VFA for OHOs on NO_2 (AS)	0.5	g COD.m^{-3}
$K_{VFA,NO,AS}$	Half-saturation of VFA for OHOs on NO (AS)	0.5	g COD.m^{-3}
$K_{VFA,N2O,AS}$	Half-saturation of VFA for OHOs on N2O (AS)	0.5	g COD.m^{-3}
$K_{MEOL,OHO,AS}$	Half-saturation of methanol for OHOs (AS)	0.1	g COD.m^{-3}
$K_{NO3,OHO,AS}$	Half-saturation of NO_3 for OHOs (AS)	0.20	g N.m^{-3}
$K_{NO2,OHO,AS}$	Half-saturation of NO_2 for OHOs (AS)	0.20	g N.m^{-3}
$K_{NO,OHO,AS}$	Half-saturation of NO for OHOs (AS)	0.05	g N.m^{-3}
$K_{N2O,OHO,AS}$	Half-saturation of N_2O for OHOs (AS)	0.05	g N.m^{-3}
$Ki_{NO,OHO,NO2,AS}$	Half-inhibition of NO for OHOs denitrification of NO_2 (AS)	0.50	g N.m^{-3}
$Ki_{NO,OHO,NO,AS}$	Half-inhibition of NO for OHOs denitrification of NO (AS)	0.30	g N.m^{-3}
$Ki_{NO,OHO,N2O,AS}$	Half-inhibition of NO for OHOs denitrification of N_2O (AS)	0.08	g N.m^{-3}
$K_{VFA,FERM,AS}$	Half-saturation of VFA in fermentation of OHOs (AS)	50.0	g COD.m^{-3}
$Lograngе_{VFA,FERM,AS}$	Effective range of logistic switch for VFA fermentation by OHOs (AS)	0.012	unitless
$K_{SB,ana,AS}$	Half-saturation of readily biodegradable substrate in fermentation by OHOs (AS)	5.0	g COD.m-3
$K_{SB,ana,DIG}$	Half-saturation of readily biodegradable substrate in fermentation by OHOs in digester (AS)	350.0	g COD.m-3

Aerobic ammonia oxidizer kinetics (AOB) **Type(Kinetic)**

Symbol	Name	Default	Unit
μ_{AOB}	Maximum specific growth rate of AOBs	0.9	d^{-1}
$\eta_{AOB,NO,N2O}$	Reduction factor for NO reduction to N2O by AOBs (NN pathway)	0.0015	unitless
$\eta_{AOB,NO2,N2O}$	Reduction factor for HNO2 reduction to N2O by AOBs (ND pathway)	0.2500	unitless
b_{AOB}	Decay rate of AOBs	0.17	d^{-1}
$K_{CO2,AOB,AS}$	Half-saturation of CO_2 for AOBs (AS)	12.0	g TIC.m^{-3}
$Lograngе_{CO2,AOB,AS}$	Effective range of CO_2 logistic switch for AOBs (AS)	2.00	unitless

$K_{CO2,AOB,pH,AS}$	Half-saturation of bicarbonate for AOBs (AS)	0.001	mol $[HCO_3^-].L^{-1}$
$Lograng e_{CO2,AOB,pH,AS}$	Effective range of bicarbonate logistic switch for AOBs (AS)	1.00	unitless
$K_{O2,NHx,AOB,AS}$	Half-saturation of O_2 for NHx oxydation by AOBs (AS)	0.25	g $O_2.m^{-3}$
$K_{O2,NH2OH,AOB,AS}$	Half-saturation of O_2 for NH2OH oxydation by AOBs (AS)	0.15	g $O_2.m^{-3}$
$K_{NHx,AOB,AS}$	Half-saturation of NH_x for AOBs (AS)	0.01	g $N.m^{-3}$
$K_{NHx,NH2OH,AOB,AS}$	Half-saturation of NH_x to NH2OH for AOBs (AS)	0.7	g $N.m^{-3}$
$K_{NH2OH,AOB,AS}$	Half-saturation of NH_2OH for AOBs (AS)	0.9000	g $N.m^{-3}$
$K_{NOx,AOB,AS}$	Half-saturation of NO_x (anoxic conditions) for AOBs (AS)	0.0300	g $N.m^{-3}$
$K_{HNO2,AOB,AS}$	Half-saturation of HNO_2 for AOBs (AS)	0.0040	g $N.m^{-3}$
$K_{NO,NO2,AOB,AS}$	Half-saturation of NO to NO_2 for AOBs (AS)	0.0003	g $N.m^{-3}$
$K_{NO,N2O,AOB,AS}$	Half-saturation of NO to N_2O for AOBs (AS)	0.0080	g $N.m^{-3}$
$Ki_{O2,AOB,AS}$	Half-inhibition of O_2 for N_2O production by AOBs (AS)	0.8	g $O_2.m^{-3}$
$K_{O2,AOB,AS}$	Half-saturation of O_2 for AOBs (AS)	0.3	g $O_2.m^{-3}$

Nitrite oxidizer kinetics (NOB) **Type(Kinetic)**

Symbol	Name	Default	Unit
μ_{NOB}	Maximum specific growth rate of NOBs	0.65	d^{-1}
b_{NOB}	Decay rate of NOBs	0.15	d^{-1}
$K_{NO2,NOB,AS}$	Half-saturation of NO_2 for NOBs (AS)	0.10	g $N.m^{-3}$
$K_{CO2,NOB,AS}$	Half-saturation of CO_2 for NOBs (AS)	1.00	g $CO_2.m^{-3}$
$Lograng e_{CO2,NOB,AS}$	Effective range of CO_2 logistic switch for NOBs (AS)	2.00	unitless
$K_{CO2,NOB,pH,AS}$	Half-saturation of bicarbonate for NOBs (AS)	1.00E-10	mol $[HCO_3^-].L^{-1}$
$Lograng e_{CO2,NOB,pH,AS}$	Effective range of bicarbonate logistic switch for NOBs (AS)	2.00	unitless
$K_{O2,NOB,AS}$	Half-saturation of O_2 for NOBs (AS)	0.25	g $O_2.m^{-3}$

$K_{NOx,NOB,AS}$	Half-saturation of NO_x (anoxic conditions) for NOBs (AS)	0.03	g $N.m^{-3}$

Methane oxidizing bacteria kinetics (MOB) **Type(Kinetic)**

Symbol	Name	Default	Unit
μ_{MOB}	Maximum specific growth rate of MOBs	3.7	d^{-1}
b_{MOB}	Decay rate of MOBs	0.55	d^{-1}
$K_{O2,MOB}$	Half-saturation of O_2 for MOB	0.21	g O2.m-3
$K_{CH4,MOB}$	Half-saturation of CH4 for MOB	1.79	g COD.m-3
	Temperature dependency		
Symbol	Name		
$\theta_{\mu,OHO}$	Arrhenius coefficient for OHO growth		
$\theta_{FERM,OHO}$	Arrhenius coefficient for fermentation (OHO)		
$\theta_{b,OHO}$	Arrhenius coefficient for OHO decay		
$\theta_{\mu,AOB}$	Arrhenius coefficient for AOB growth		
$\theta_{b,AOB}$	Arrhenius coefficient for AOB decay		
$\theta_{\mu,NOB}$	Arrhenius coefficient for NOB growth		
$\theta_{b,NOB}$	Arrhenius coefficient for NOB decay		
$\theta_{\mu,MOB}$	Arrhenius coefficient for MOB growth		
$\theta_{b,MOB}$	Arrhenius coefficient for MOB decay		
T_{base}	Arrhenius base temperature		

Stoichiometric yields **Type(Stoichiometric)**

Symbol	Name	Default	Unit
$Y_{OHO,VFA,ox}$	Yield of OHOs on VFA under aerobic conditions	0.60	g X_{OHO}.g S_{VFA}^{-1}
$Y_{OHO,VFA,anox}$	Yield of OHOs on VFA under anoxic conditions	0.45	g X_{OHO}.g S_{VFA}^{-1}
$Y_{OHO,SB,ox}$	Yield of OHOs on readily biodegradable substrate under aerobic conditions	0.67	g X_{OHO}.g S_B^{-1}

$Y_{OHO,SB,anox}$	Yield of OHOs on readily biodegradable substrate under anoxic conditions	0.54	g X_{OHO}.g S_B^{-1}
$Y_{OHO,SB,ana}$	Yield of OHOs on readily biodegradable substrate under anaerobic conditions	0.10	g X_{OHO}.g S_B^{-1}
$Y_{OHO,H2,ana,high}$	Yield of H2 production in fermentation with high VFA concentration (OHO)	0.35	g S_{H2}.g S_B^{-1}
$Y_{OHO,H2,ana,low}$	Yield of H2 production in fermentation with low VFA concentration (OHO)	0.1	g S_{H2}.g S_B^{-1}
$Y_{OHO,SMEOL,ox}$	Yield of OHOs on methanol under aerobic conditions	0.40	g X_{OHO}.g S_{MEOL}^{-1}
Y_{AOB}	Yield of AOBs on NH_x	0.15	g X_{AOB}.g S_{NHx}^{-1}
Y_{NOB}	Yield of NOBs on NO_2	0.09	g X_{NOB}.g S_{NO2}^{-1}
Y_{MOB}	Yield of MOB	0.12	g X_{MOB}.g S_{CH4}^{-1}